

# INTERNAL WAVES

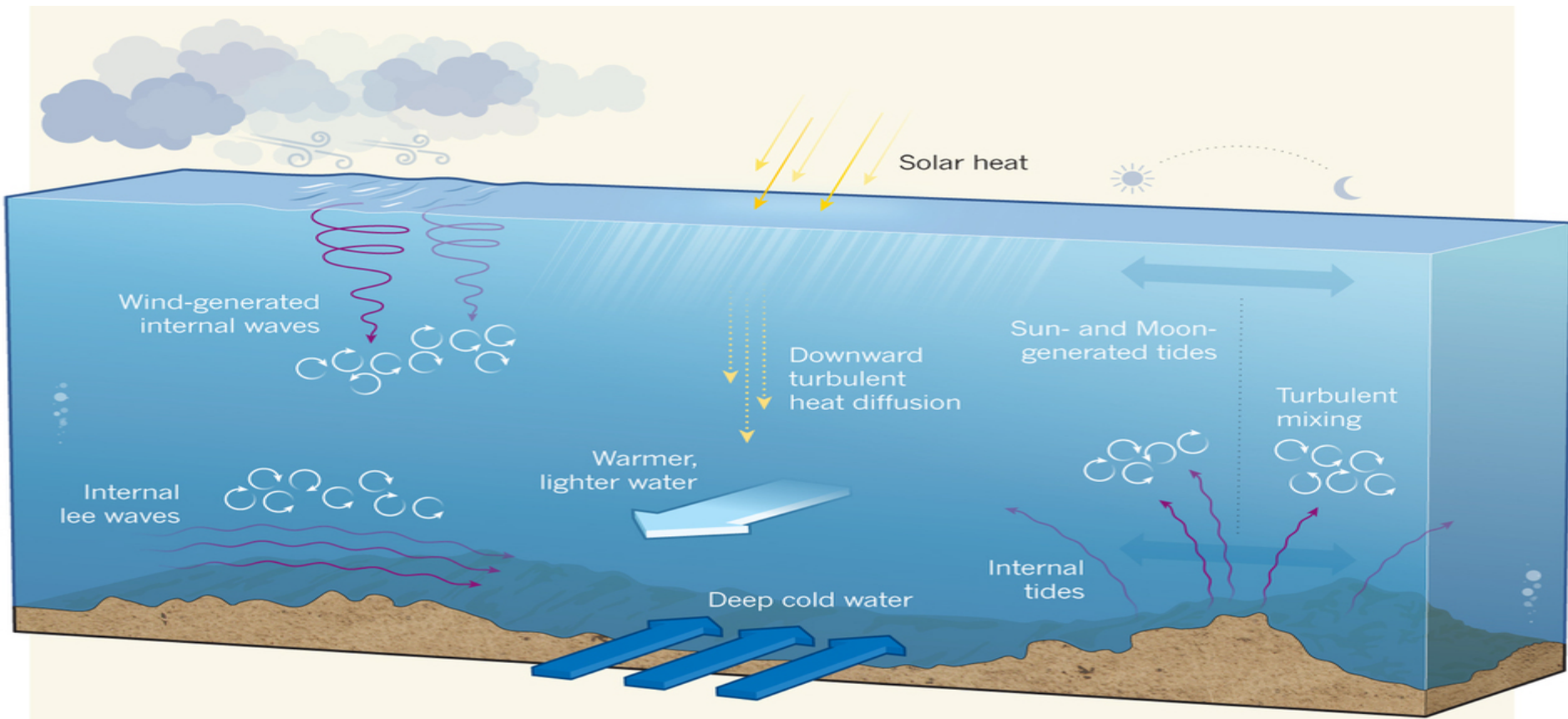
---

## 3. GENERATION AND DISSIPATION

- **1.3.1 : Generation of Internal waves**
  - Internal tides
  - Lee waves
  - Near-Inertial waves
- **1.3.2 : Propagation and dissipation of internal waves**
-

# 1. Internal waves generation

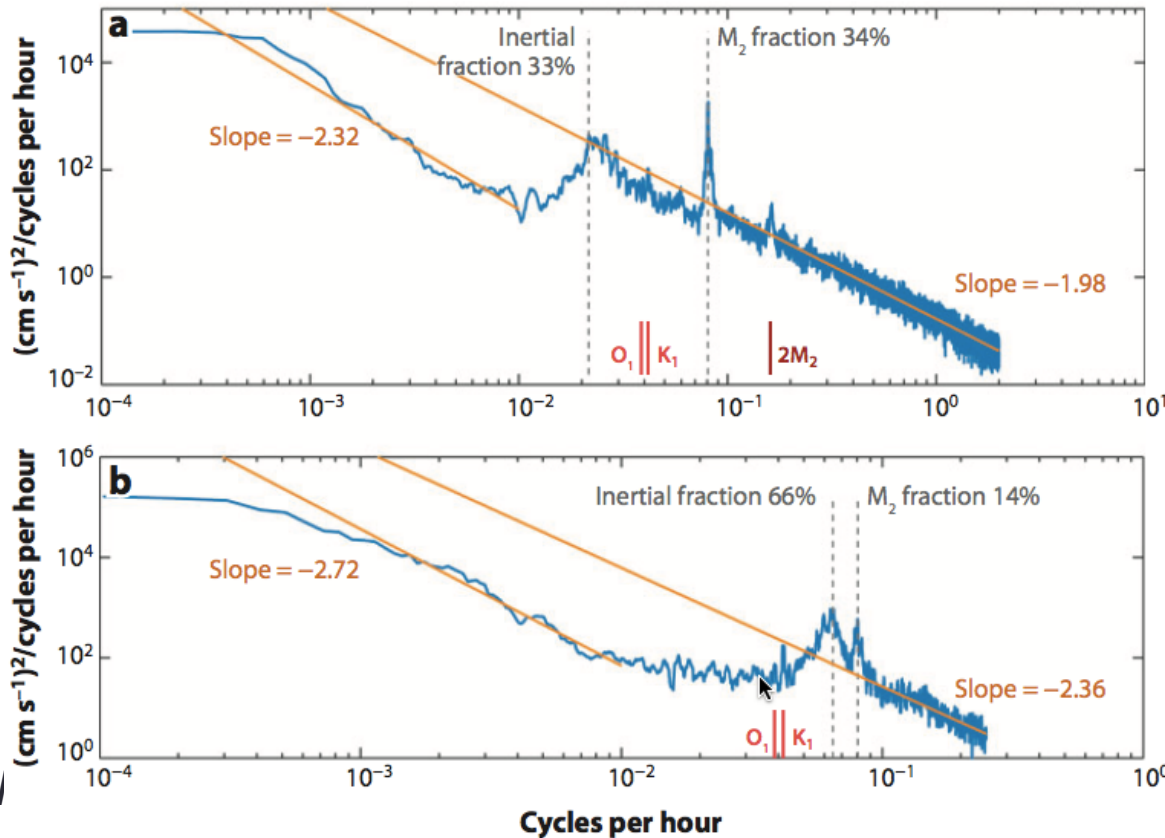
- Mechanisms:



From Mackinnon 2013

# 1. Internal waves generation

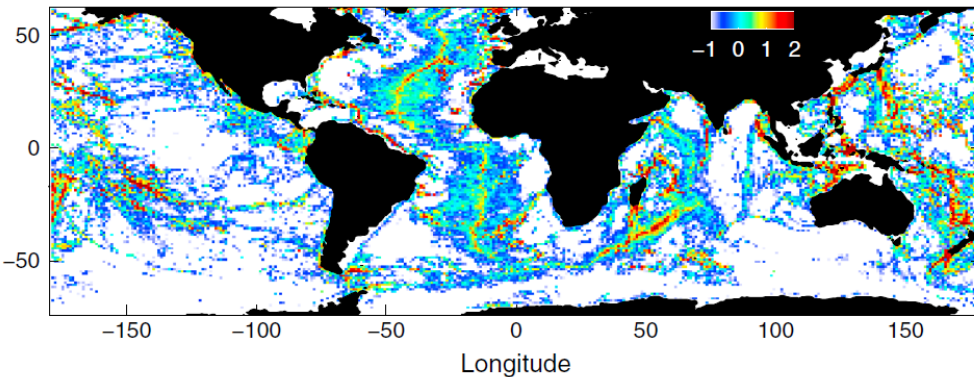
- Winds generate mostly near-inertial waves (frequency close to  $f$ )
- Barotropic tides generate internal tides at the frequency of tides



(a) Kinetic energy estimate for an instrument in the western North Atlantic near  $15^\circ\text{N}$  at 500 m. (b) Power density spectral estimate from a record at 1000 m at  $50.7^\circ\text{S}$ ,  $143^\circ\text{W}$ , south of Tasmania in the Southern Ocean

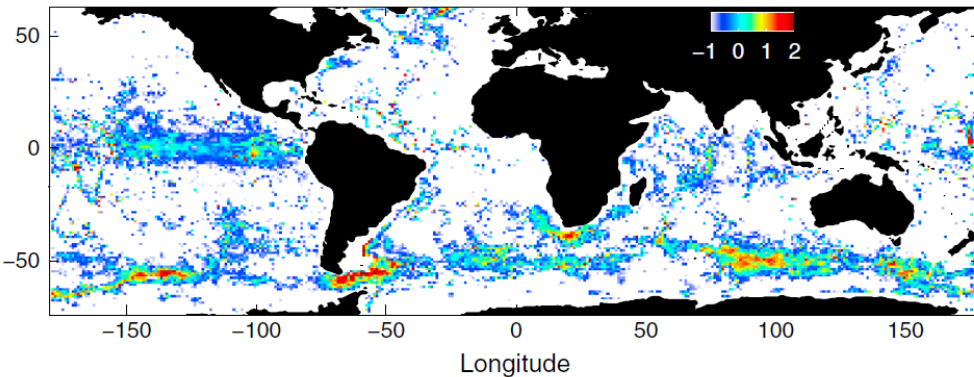
# 1. Internal waves generation

Latitude



Internal tides (1 TW)

Latitude



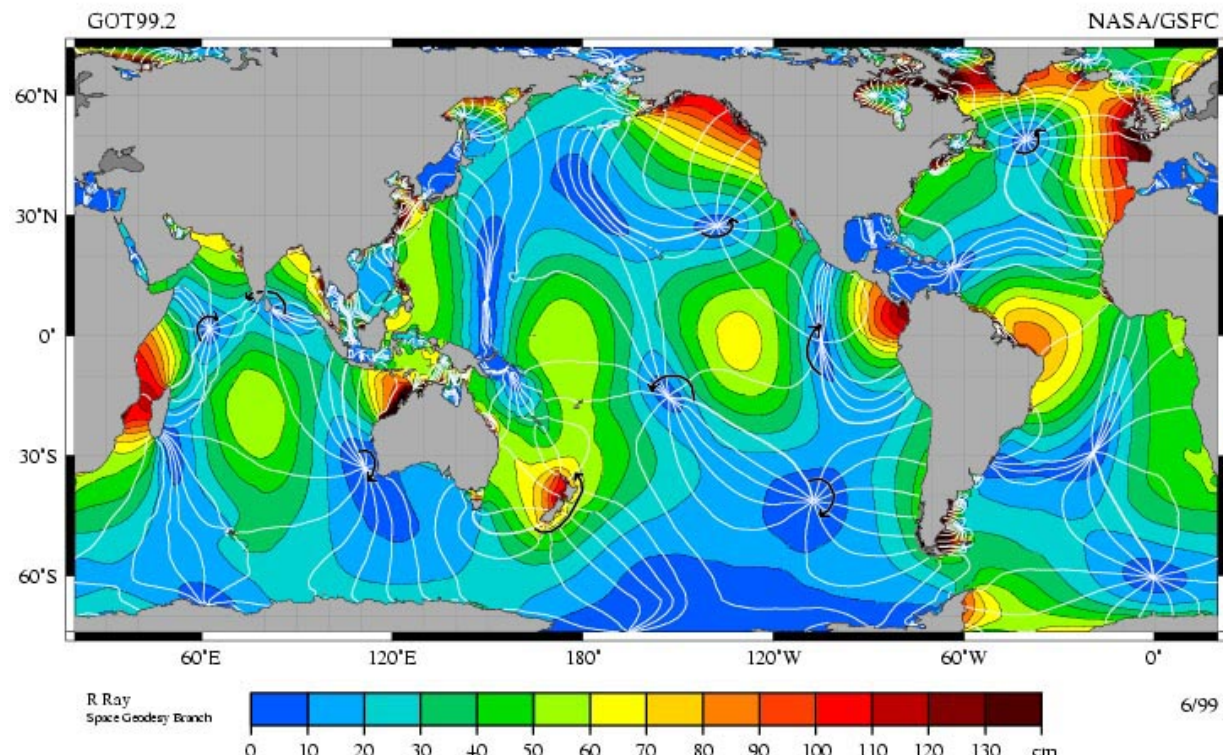
Lee waves (0.2 TW)

Energy input  $E(x,y)$   
 $\log(\text{mW/m}^2)$

[Nikurashin & Ferrari, 2013]

# 1.1 Generation of internal tides

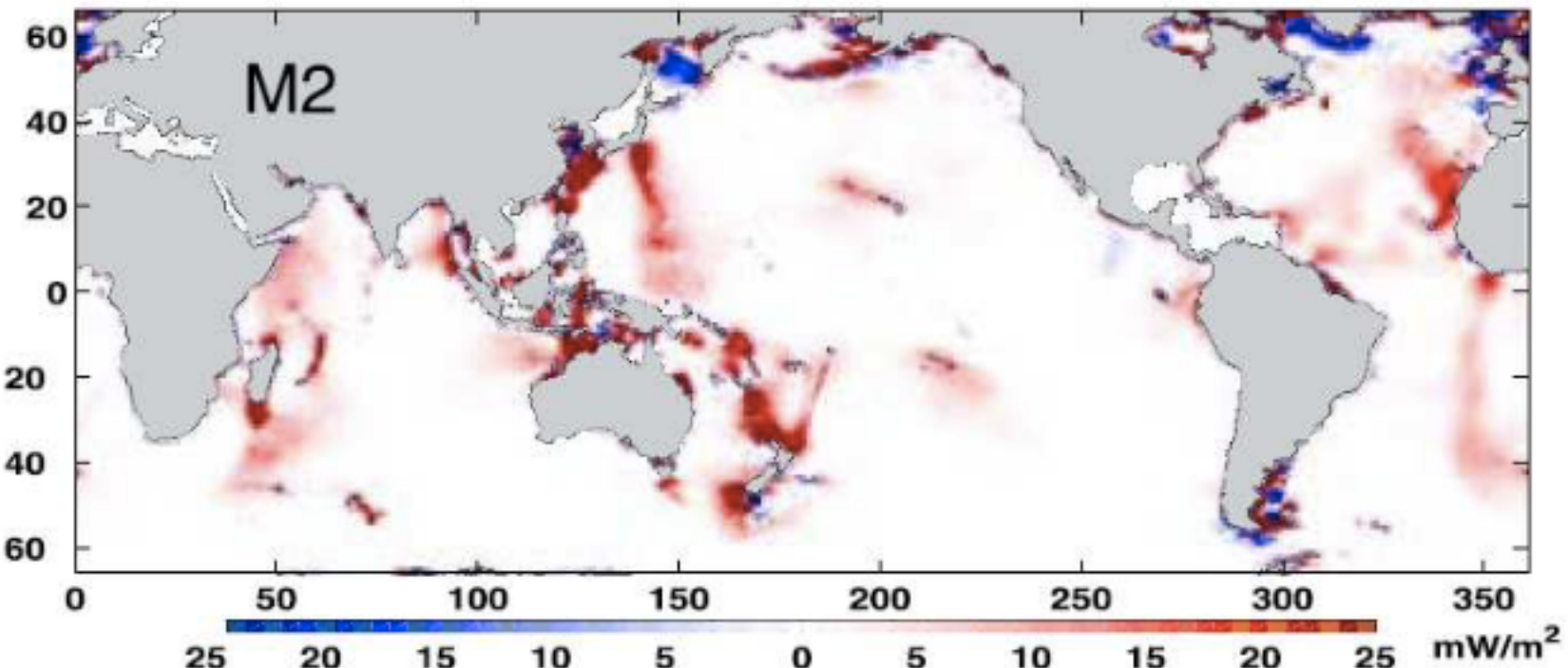
- Barotropic tides



The *M2* tidal constituent. Amplitude is indicated by color, and the white lines are cotidal differing by 1 hour. The colors indicate where tides are most extreme (highest highs, lowest lows), with blues being least extreme.

# 1.1 Generation of internal tides

- Barotropic tides generate internal tides at the frequency of tides



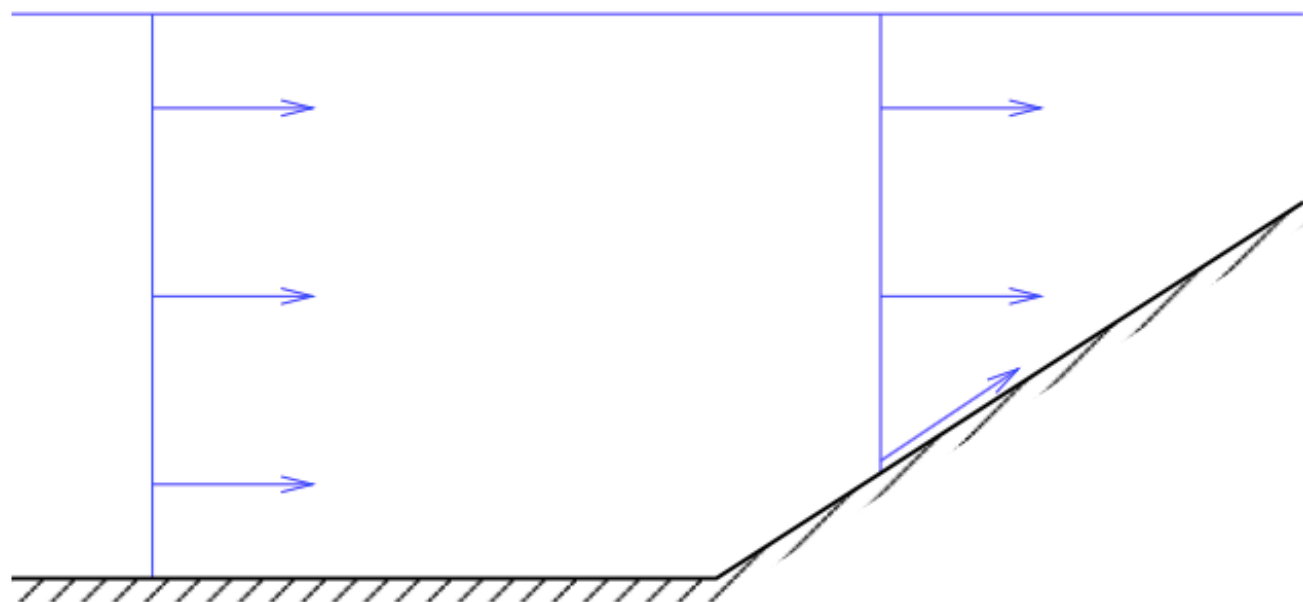
Regions where dissipation of the semi-diurnal lunar barotropic tide (M2) occurs, determined using data from satellite altimetry. There is a clear correspondence with bottom topography; noticeable dissipation occurs over, for example, the Mid-Atlantic Ridge and the Hawaiian Ridge.

## 1.1 Generation of internal tides

- Generation of Internal Tide on a Slope:

*A barotropic velocity profile impinging on a sloping boundary. On the boundary, the velocity vector can only have a component tangential to it and hence over the slope, the velocity profile is no longer barotropic.*

*Energy must go into generating internal waves, and propagate away along characteristics*



## 1.1 Generation of internal tides

- Starting from:  $\frac{\partial^2}{\partial t^2} \nabla^2 w + (\vec{f} \cdot \nabla)^2 w + N^2 \nabla_h^2 w = 0.$

- We can restrict to the u-z plane and define a streamfunction:

$$u = \dot{\Psi}_z \text{ and } w = -\dot{\Psi}_x,$$

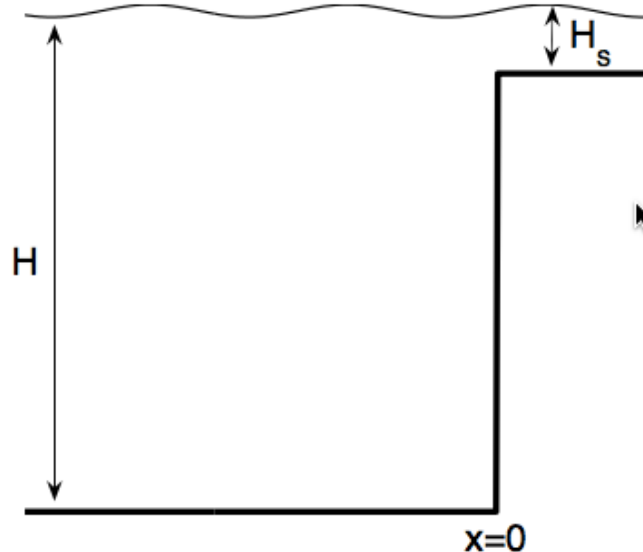
- Such that  $\nabla^2 \Psi_{tt} + f^2 \Psi_{zz} + N^2 \Psi_{xx} = 0.$

- To impose the prescribed barotropic tide field, we use the boundary conditions:

$$\Psi = 0 \quad \text{at } z = 0; \quad \Psi = Q_0 \exp(-i\omega t) \quad \text{at } z = -h(x),$$

## 1.1 Generation of internal tides

- Step-topography:



- The solution is:

$$\Psi = \begin{cases} -\frac{zQ_0}{H} \exp(-i\omega t) + \sum_n a_n \sin\left(\frac{n\pi z}{H}\right) \exp i(-k_n x - \omega t) & \text{for } x < 0 \\ -\frac{zQ_0}{H_s} \exp(-i\omega t) + \sum_n a_{s,n} \sin\left(\frac{n\pi z}{H_s}\right) \exp i(k_{s,n} x - \omega t) & \text{for } x > 0 \end{cases}$$

$$k_{(s,)n} = \frac{n\pi}{H_{(s)}} \left( \frac{\omega^2 - f^2}{N^2 - \omega^2} \right)^{1/2}, \quad n = 1, 2, 3, \dots.$$

## 1.1 Generation of internal tides

- To find the coefficient we match solutions and their derivative ( $w$ ) at  $x=0$ :

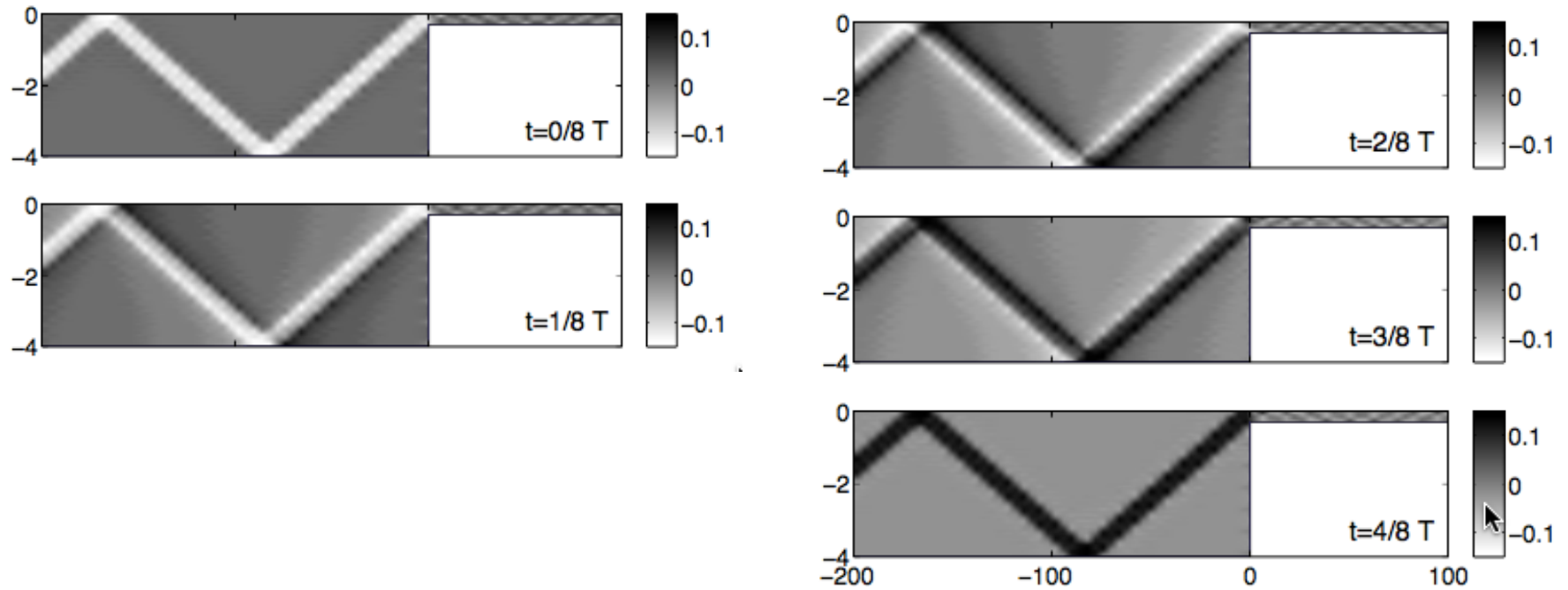
$$-\frac{zQ_0}{H} + \sum_n a_n \sin\left(\frac{n\pi z}{H}\right) = \begin{cases} Q_0 & \text{for } -H < z < -H_s \\ -\frac{zQ_0}{H_s} + \sum_n a_{s,n} \sin\left(\frac{n\pi z}{H_s}\right) & \text{for } -H_s < z < 0. \end{cases}$$

- Which gives:

$$a_m = -\frac{2Q_0}{\alpha(m\pi)^2} \sin(m\pi\alpha) + \frac{2\alpha}{\pi} \sin(m\pi\alpha) \sum_n \frac{n(-1)^n}{(m\alpha)^2 - n^2} a_{s,n}.$$

$$a_{s,m} = -\frac{2\alpha(-1)^m}{\pi} \sum_n \frac{n \sin(n\pi\alpha)}{(n\alpha)^2 - m^2} a_n,$$

## 1.1 Generation of internal tides

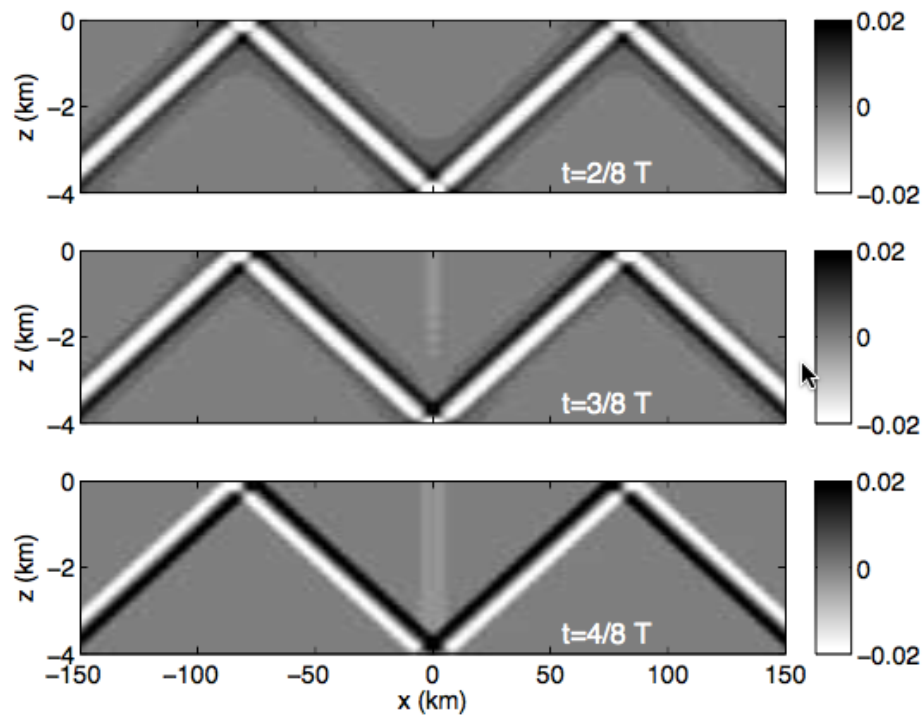
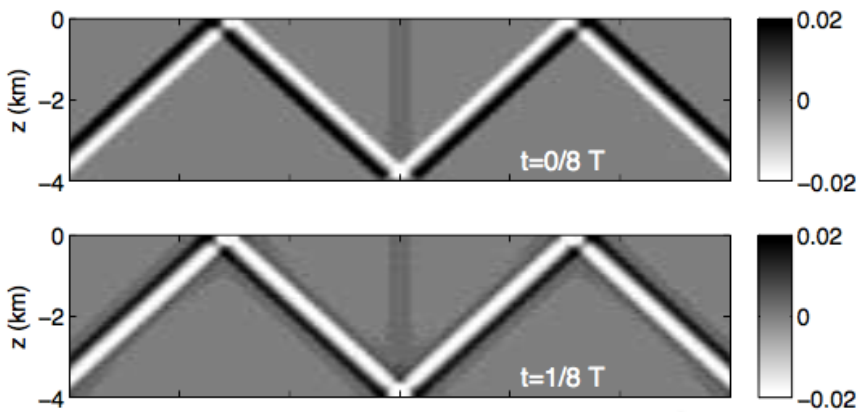
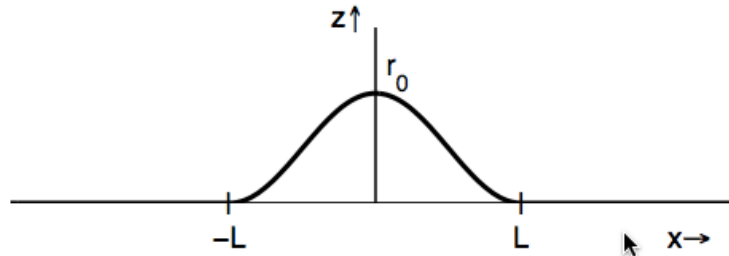


**See Gerkema.pdf**

Internal-tide generation over a steep continental slope: the horizontal baroclinic velocity (in  $\text{m s}^{-1}$ ) at five instances during half a tidal period.

# 1.1 Generation of internal tides

- Infinitesimal seamount:  
(cst N)

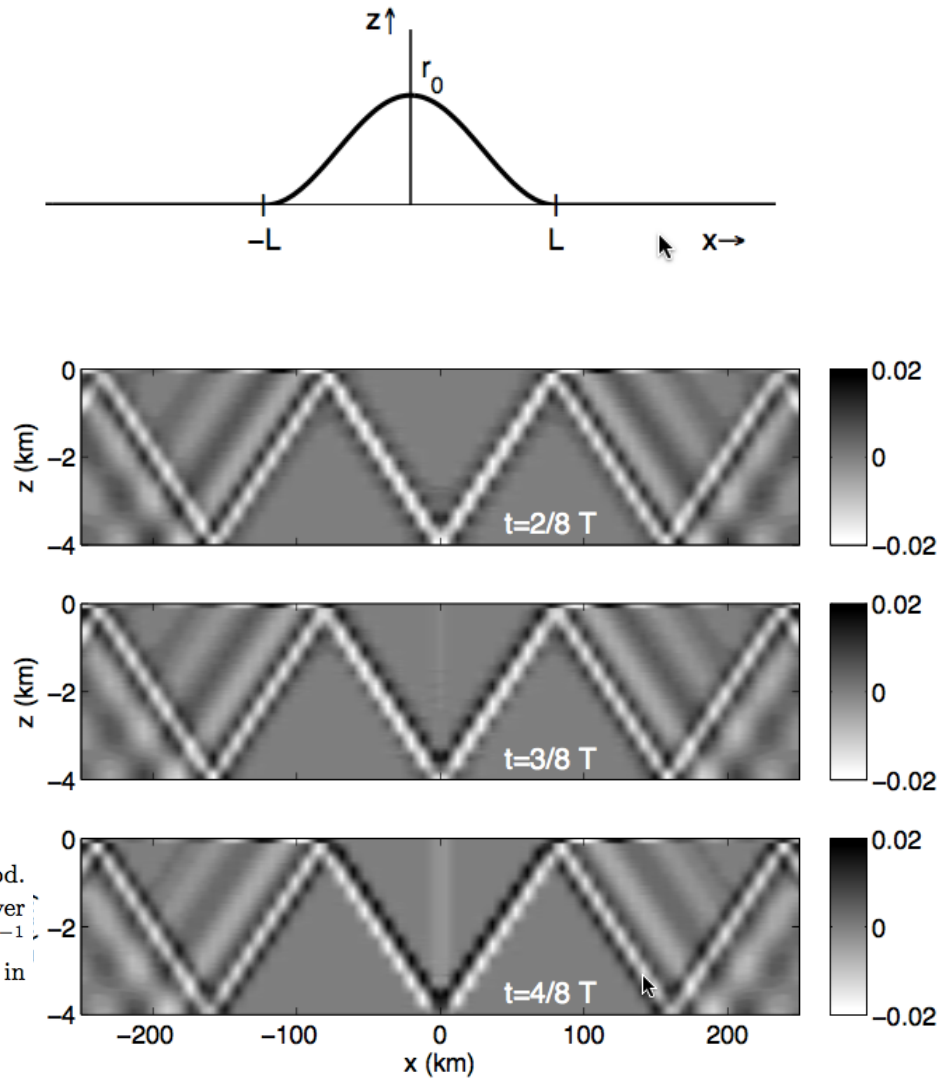
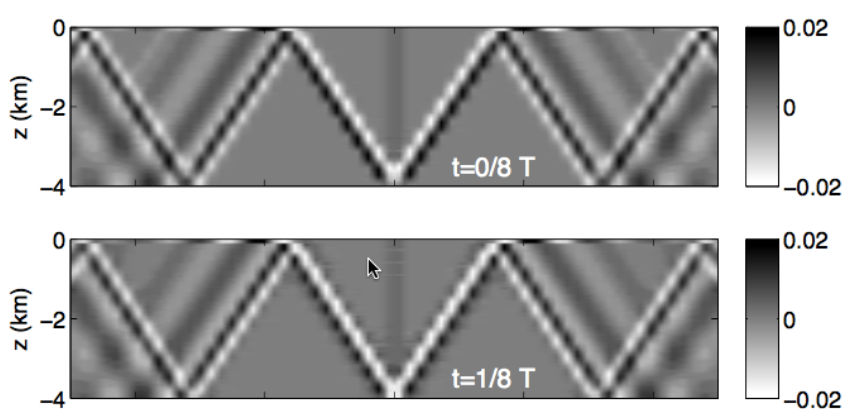


the horizontal baroclinic velocity  $u$  (in  $\text{m s}^{-1}$ ) at five instances during half a tidal period. Parameter values are:  $N = 2 \times 10^{-3}$ ,  $f = 1.0 \times 10^{-4}$  (latitude  $\phi = 45^\circ\text{N}$ ),  $\omega = 1.4052 \times 10^{-4} \text{ rad s}^{-1}$  ( $M_2$  tidal frequency);  $H = 4000 \text{ m}$ ,  $r_0 = 500 \text{ m}$ ,  $L = 10 \text{ km}$ , and  $Q_0 = 100 \text{ m}^2 \text{s}^{-1}$ ; 25 modes are included.

# 1.1 Generation of internal tides

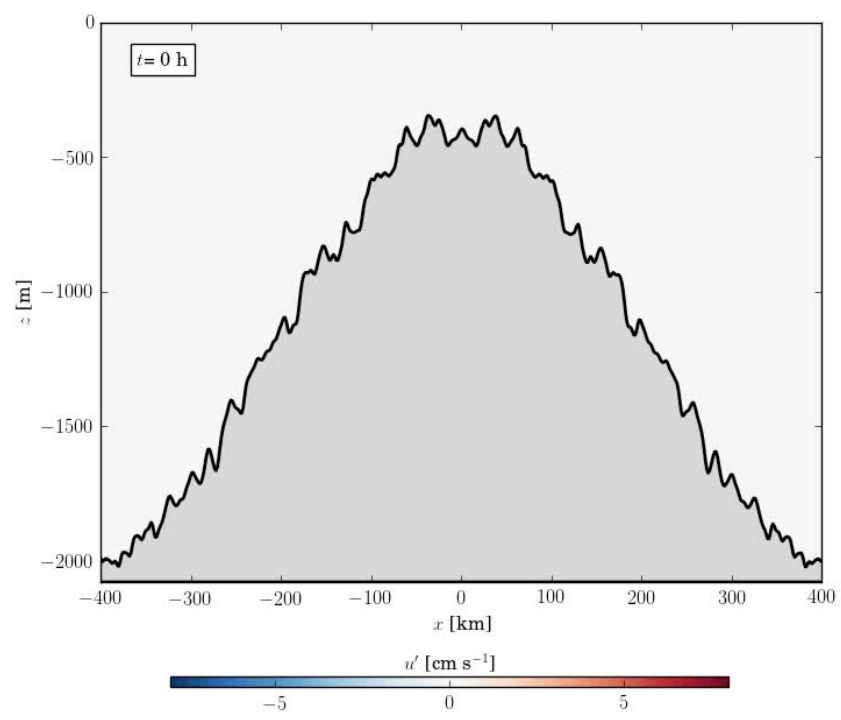
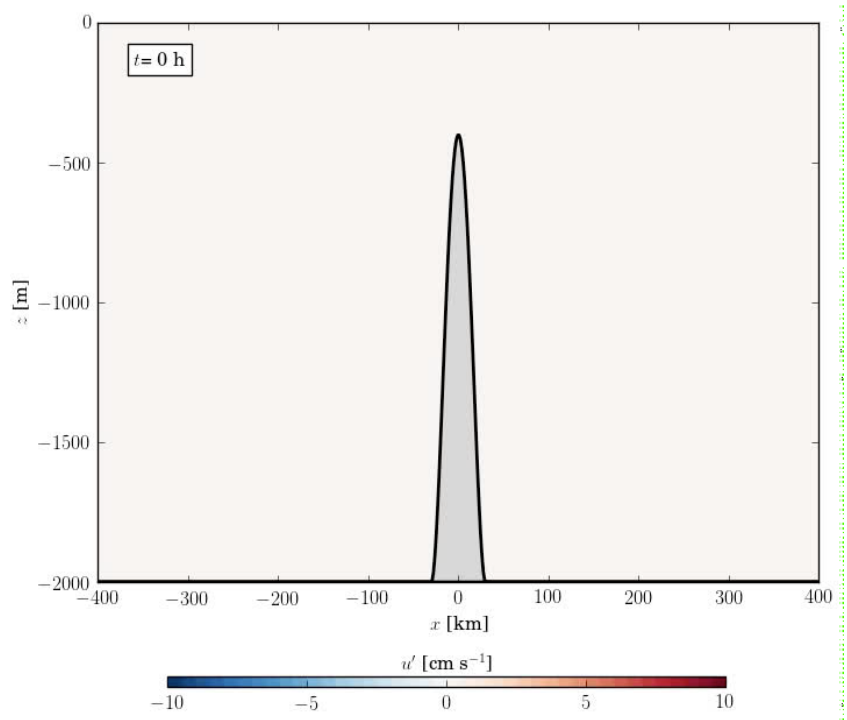
- Infinitesimal seamount:  
(+ a thermocline)

$$N^2(z) = \begin{cases} 0 & -d < z < 0 \\ g'/\epsilon & -d - \epsilon < z < -d \\ N_c^2 & -H < z < -d - \epsilon \end{cases} \quad \begin{matrix} \text{(mixed layer)} \\ \text{(thermocline)} \\ \text{(abyss),} \end{matrix}$$



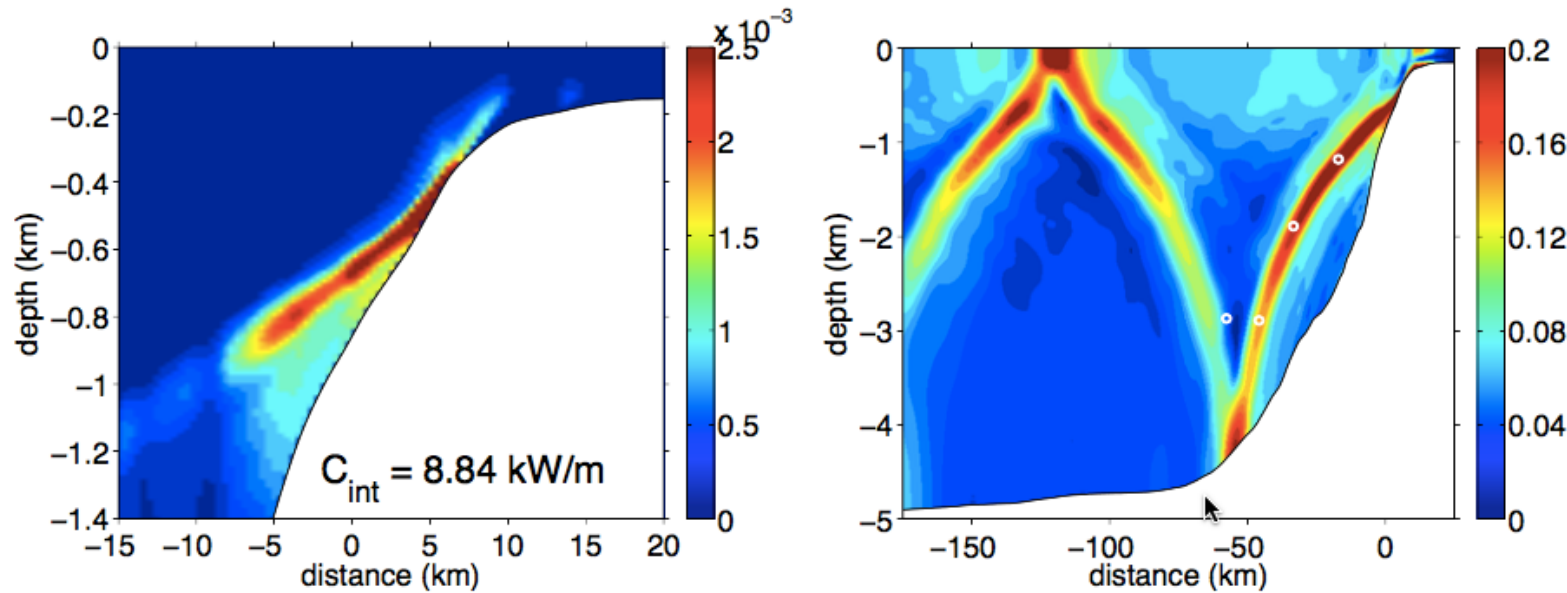
horizontal baroclinic velocity  $u$  (in  $\text{m s}^{-1}$ ) at five instances during half a tidal period. Here the stratification of Figure 5.11 is used (for  $\epsilon \rightarrow 0$ ), with  $d = 100 \text{ m}$  (mixed-layer thickness),  $g' = 0.005 \text{ m s}^{-2}$  (strength of the thermocline), and  $N_c = 2 \times 10^{-3} \text{ rad s}^{-1}$  (abyssal stratification). The remaining parameters ( $H$ ,  $f$ ,  $\omega$ ,  $r_0$ ,  $L$  and  $Q_0$ ) are as in the previous figure; here, too, 25 modes are used.

# 1.1 Generation of internal tides



Generation of internal tides [C. Vic and I. Salaün]

## 1.1 Generation of internal tides



Results from a numerical model, here applied to the Bay of Biscay. Left: The spatial distribution tidally-averaged conversion rate,  $C = -\rho_* \langle bW \rangle$ , in W/m<sup>3</sup>; Right: The internal tide emanating from the continental slope, here depicted in terms of the amplitude of the cross-slope velocity  $u$ , in m/s.

# 1.1 Generation of internal tides

Mechanism by New et Pingree (1991, JPO, 1992, Deep sea).

Internal beams are excited where the slope is equal to the critical angle:

$$\tan \theta = \pm \left( \frac{\omega^2 - f^2}{N^2 - \omega^2} \right)^{1/2}$$

One ray goes toward the coast (difficult to see because of mixing).

A second ray goes downward, is reflected at the bottom, and hit the surface about 150 km from the coast.

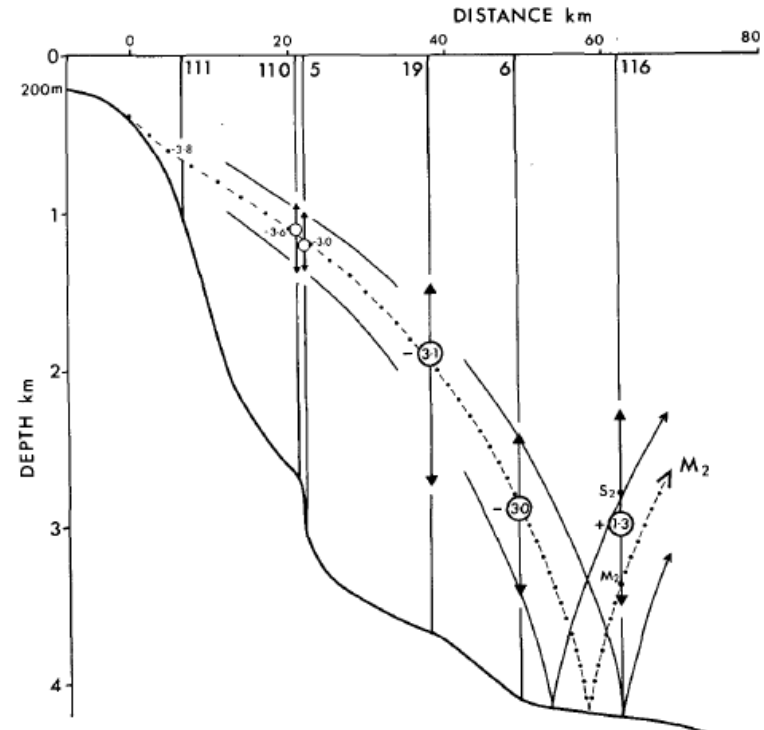


FIG. 9. Diagram showing the theoretical ray path (chained line) for a beam of internal tidal energy at the  $M_2$  tidal frequency emanating from the critical depth (385 m) on the upper slopes and reflecting off the Biscay abyssal plain at a depth of about 4200 m, 58 km from the critical point. Also shown is a summary of the internal tidal oscillations obtained during the RRS *Challenger* cruises in 1988 (CH 31/88) and 1987 (CH 18/87). Vertical lines represent mooring and CTD station positions and are identified with numbers. CTD stations 5 and 6 and mooring 116 are from the 1988 cruise, whereas moorings 110 and 111 and CTD 19 were obtained in 1987. The depth of the maximum amplitude of the internal tidal oscillation found at each station is plotted as an open circle and the range where the amplitude is more than 70% of the maximum value is indicated by the arrows. Two further rays are shown (solid lines) passing through the 70% limits near mooring 110. The phase of the maximum upward displacement is given (within the circles) in hours with respect to HWP. A ray at the  $M_2$  tidal frequency would intersect mooring 116 at the depth marked  $M_2$ ;  $S_2$  is the corresponding point for a ray at the  $S_2$  tidal frequency. The topography is depicted by the bold line and is critical at 385 m; the horizontal distance scale is measured from the critical point.

# 1.1 Generation of internal tides

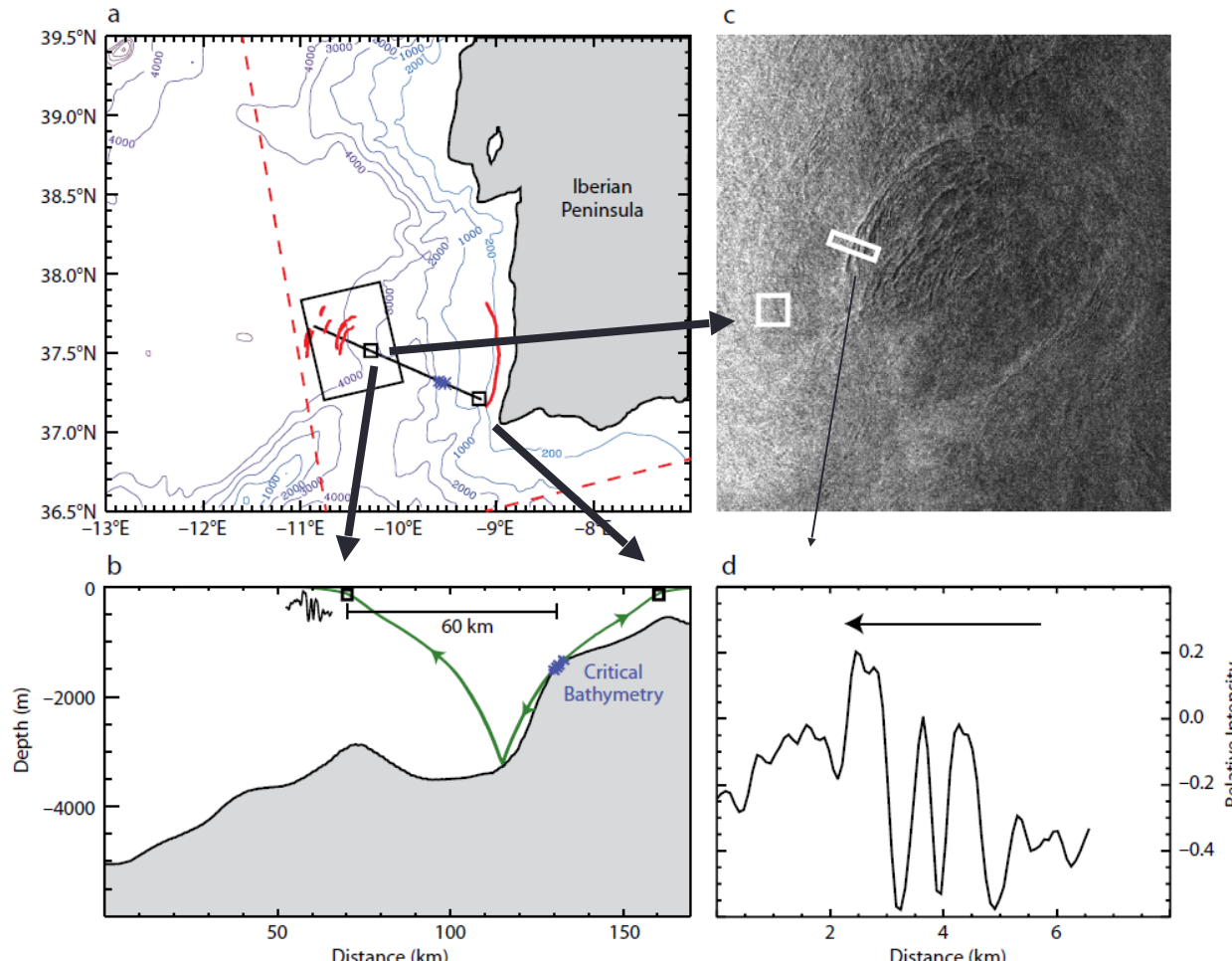
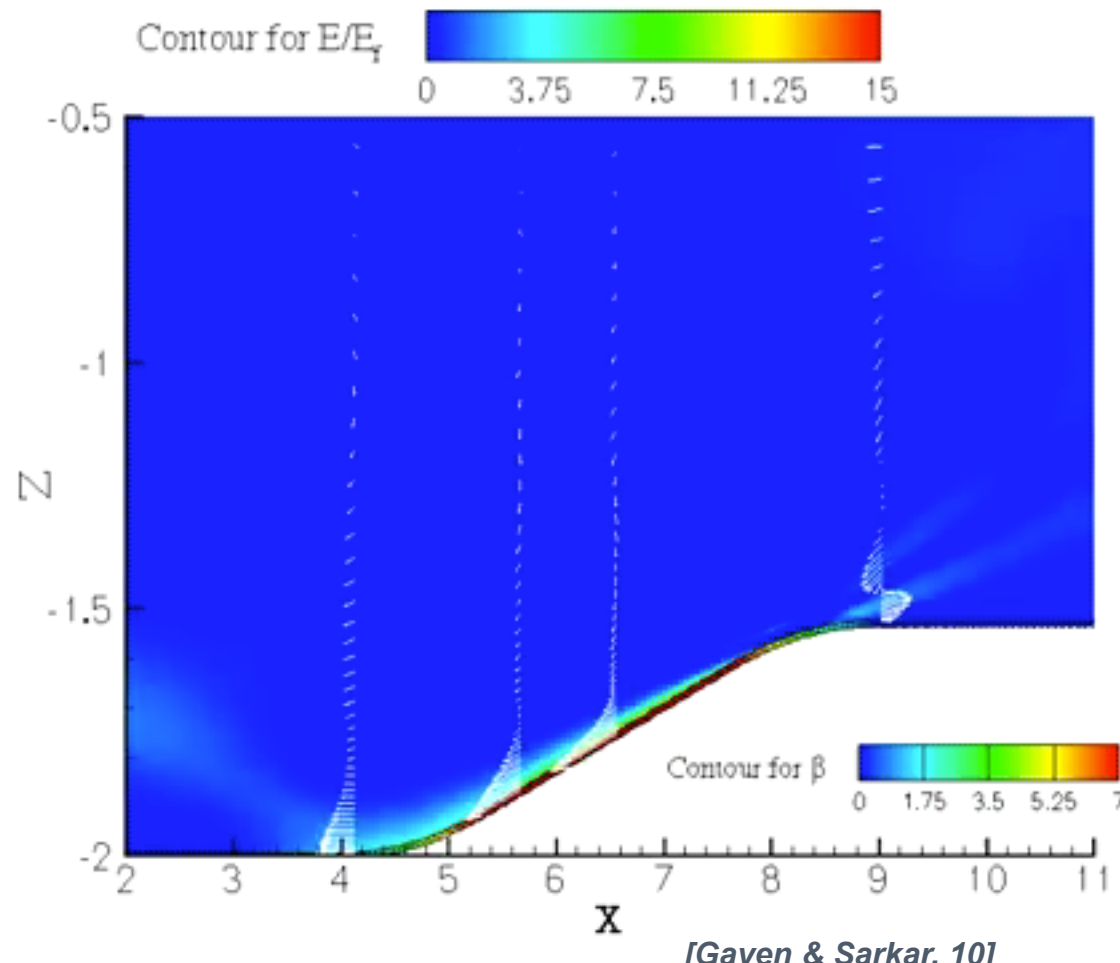


Figure 5. (a) Map of area southwest of the Iberian Peninsula with internal solitary wave crests marked in red based on one Envisat Advanced Synthetic Aperture Radar (ASAR) image in Wide-Swath Mode dated August 4, 2004 (22:27 UTC). (b) Ray-tracing diagram showing internal tide ray paths (in green; emanating from critical topography, in blue) along the black line in part (a). The small black squares in part (a) show where the ray path crosses the near-surface thermocline (taken at a depth of 50 m), and are also marked in part (b). (c) Full-resolution detail of a nonlinear internal wave train observed to propagate toward the west-northwest and believed to be generated by the tidal beam in part (b). (d) Radar backscatter profile showing the wavelength cross section of a nonlinear internal wave train generated by the tidal beam. The narrow rectangle in part (c) represents the cross section from which part (d) was obtained. The square in part (c) is a background backscatter reference used to normalize the radar profile in part (d). Zero in part (d) represents the average unperturbed backscatter of the SAR image in part (c).

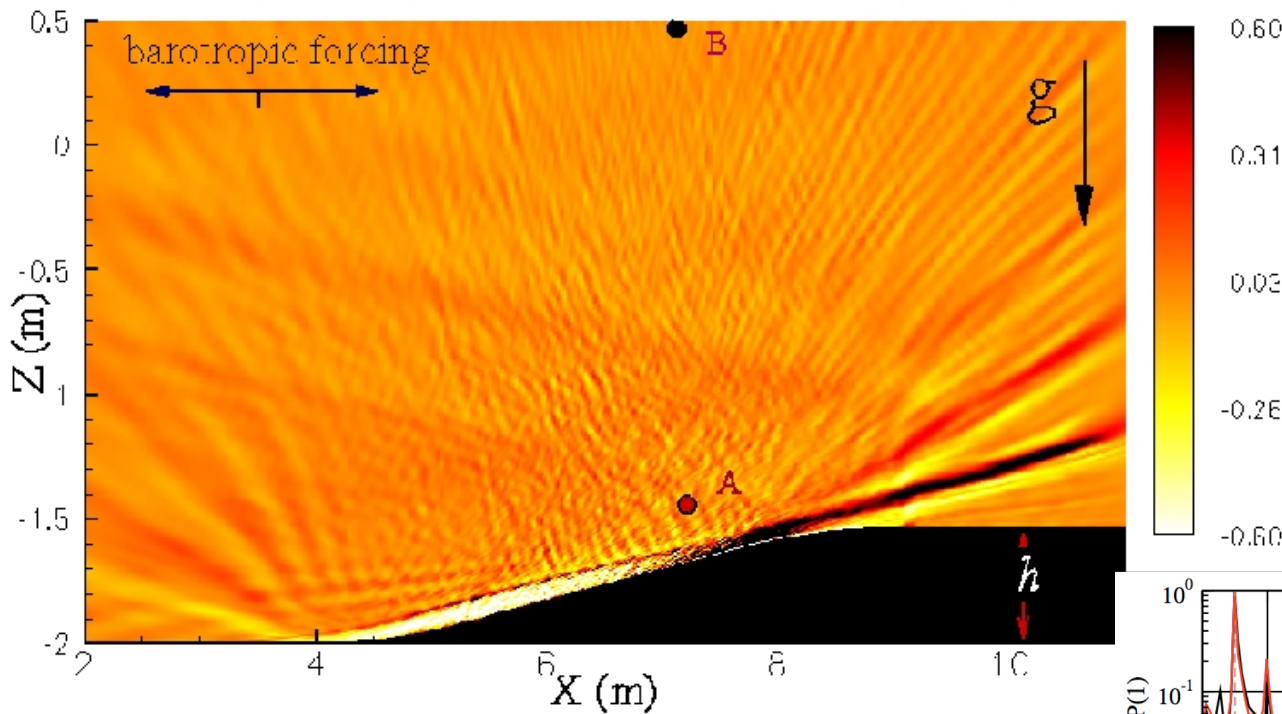
## 1.1 Generation of internal tides

- Generation of Internal Tide on a Critical Slope:

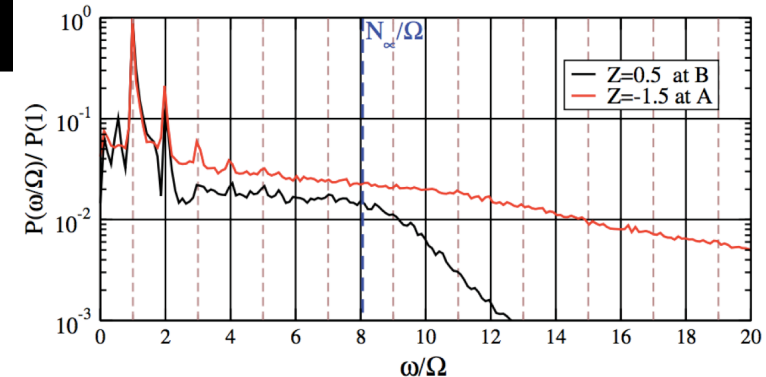


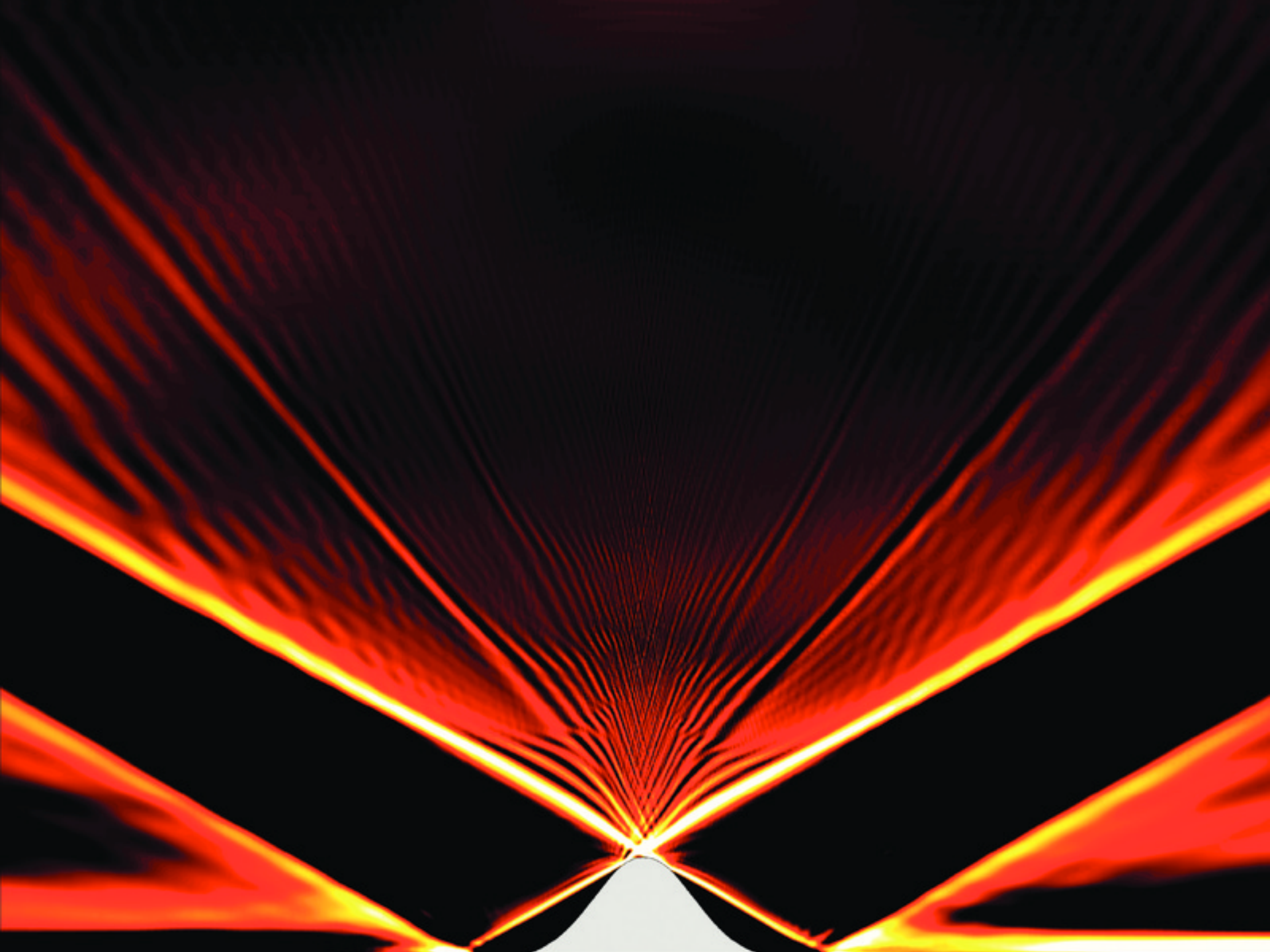
# 1.1 Generation of internal tides

- Generation of Internal Tide on a Critical Slope:



Internal wave field from DNS visualized by a slice of  $dw/dz$  field in  $x$ - $z$  plane [Gayen & Sarkar, 10]



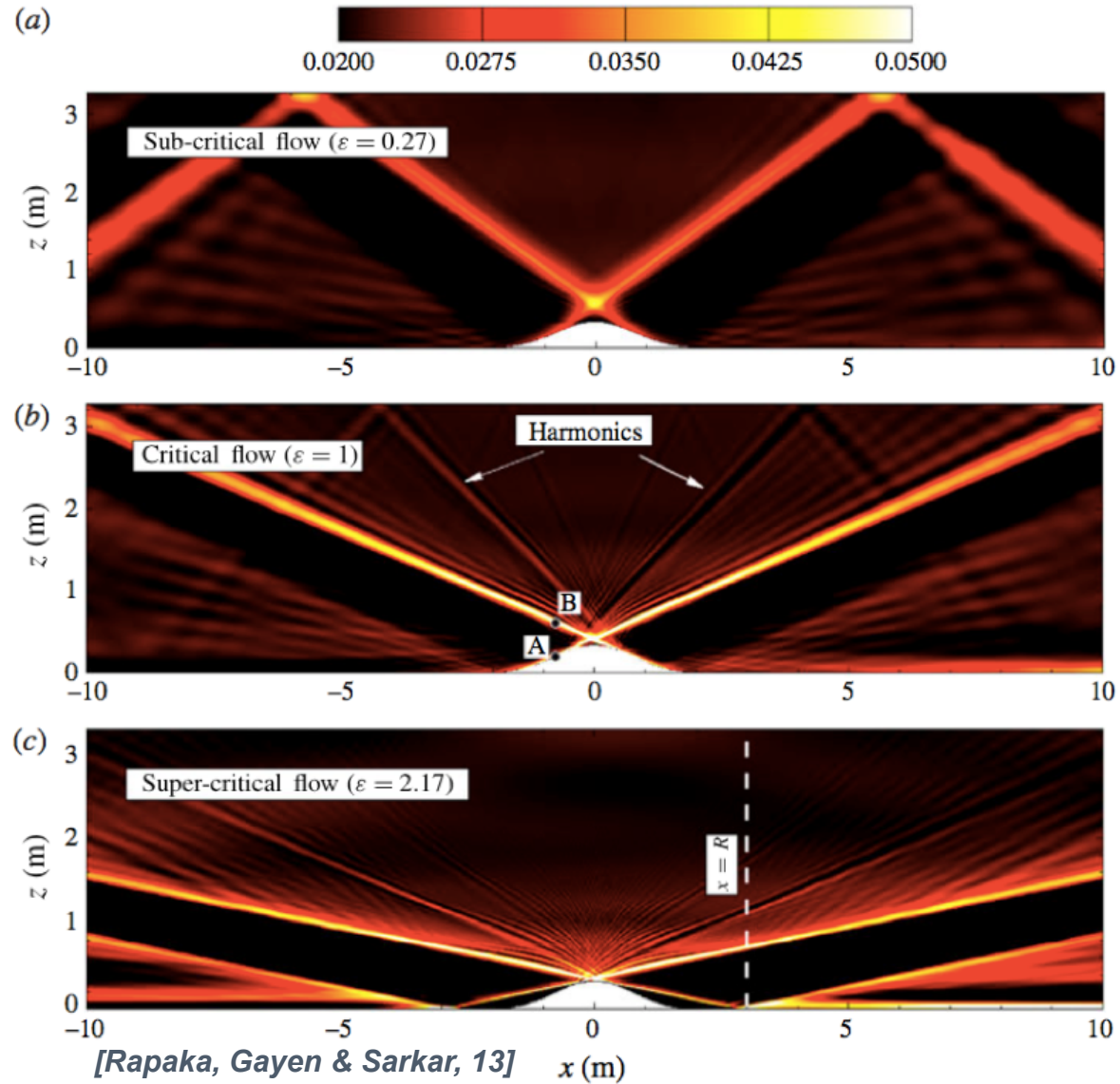
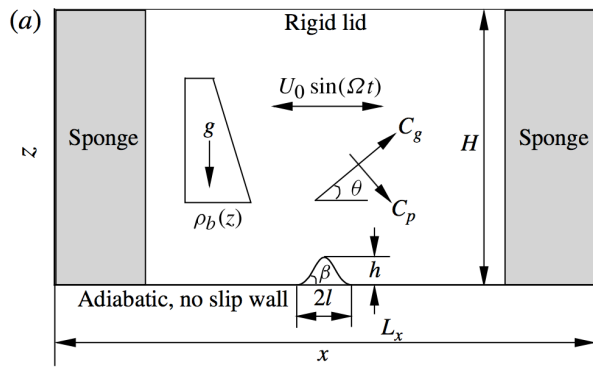


# 1.1 Generation of internal tides

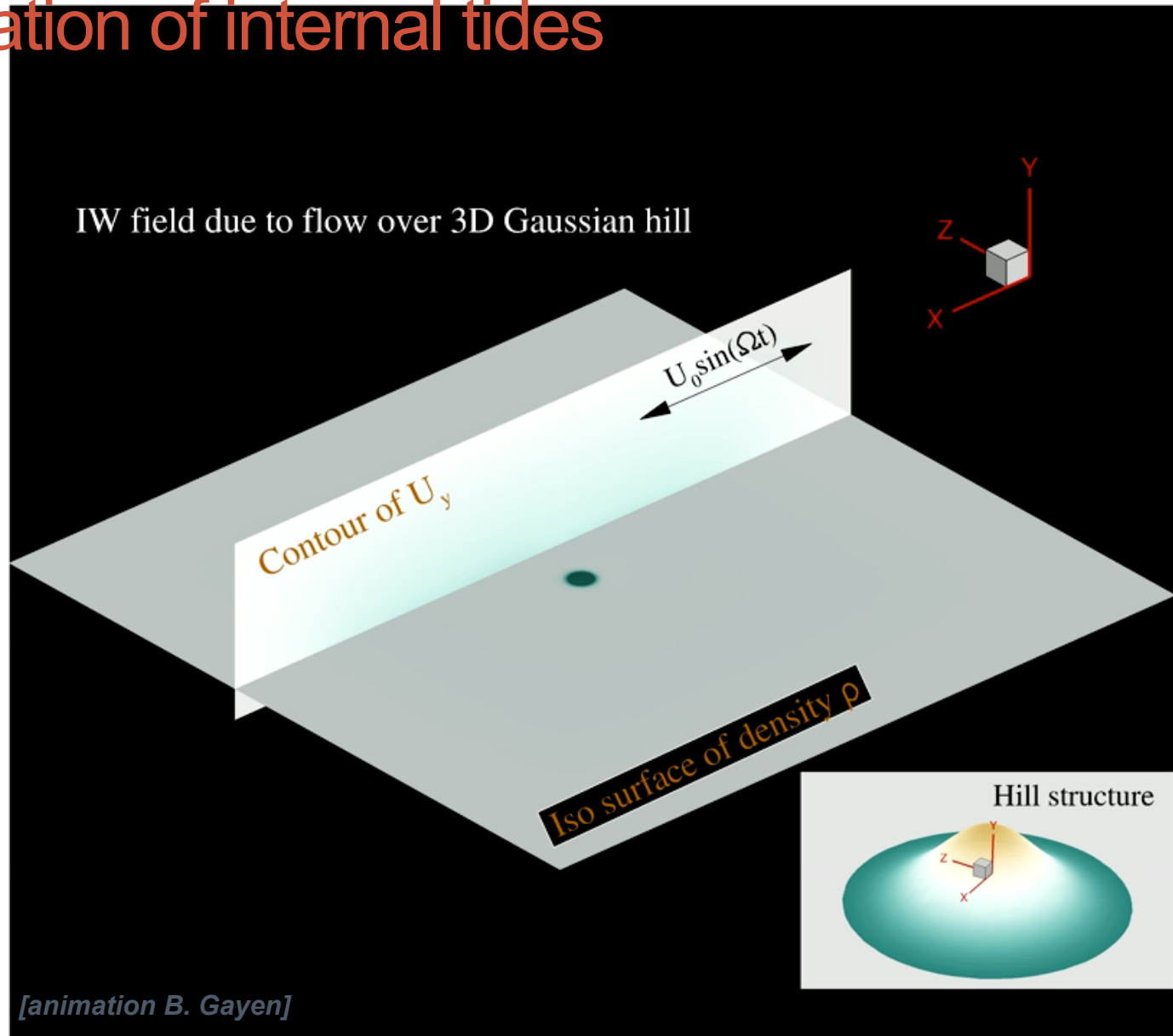
- Criticality of the slope
  - example with a ridge

$$\epsilon = \frac{\tan\beta}{\tan\theta}$$

$$\tan\theta = \sqrt{\frac{\omega^2 - f^2}{N^2 - \omega^2}}$$



## 1.1 Generation of internal tides



# 1.1 Generation of internal tides

## The Shaping of Continental Slopes by Internal Tides

D. A. Cacchione,<sup>1</sup> L. F. Pratson,<sup>2</sup> A. S. Ogston<sup>3</sup>

The angles of energy propagation of semidiurnal internal tides may determine the average gradient of continental slopes in ocean basins ( $\sim 2$  to 4 degrees). Intensification of near-bottom water velocities and bottom shear stresses caused by reflection of semi-diurnal internal tides affects sedimentation patterns and bottom gradients, as indicated by recent studies of continental slopes off northern California and New Jersey. Estimates of bottom shear velocities caused by semi-diurnal internal tides are high enough to inhibit deposition of fine-grained sediment onto the slopes.

Science 26 Apr 2002:  
Vol. 296, Issue 5568, pp. 724-727  
DOI: 10.1126/science.1069803

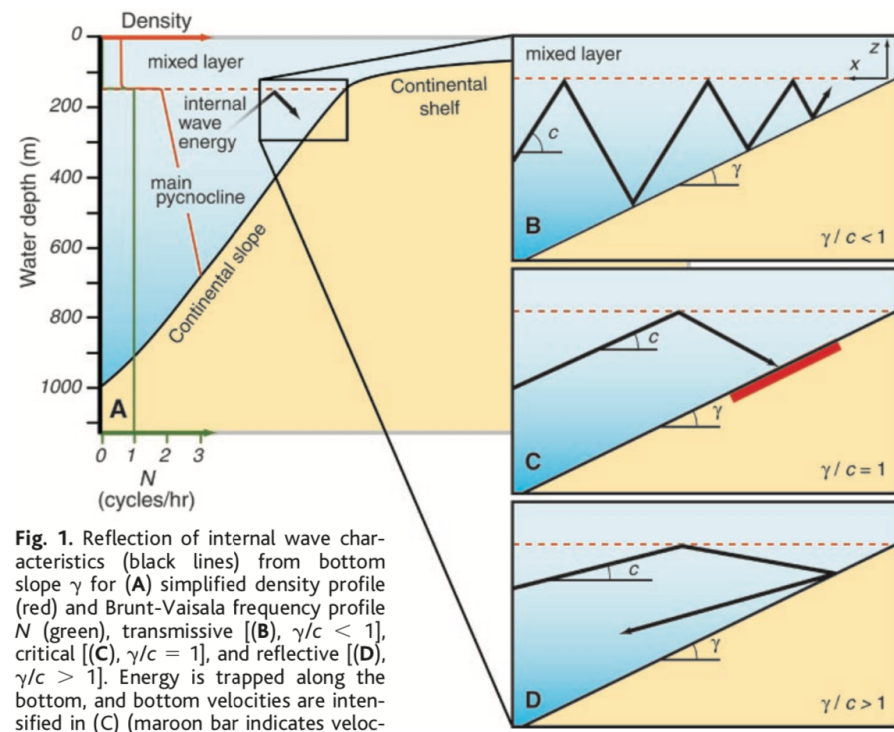
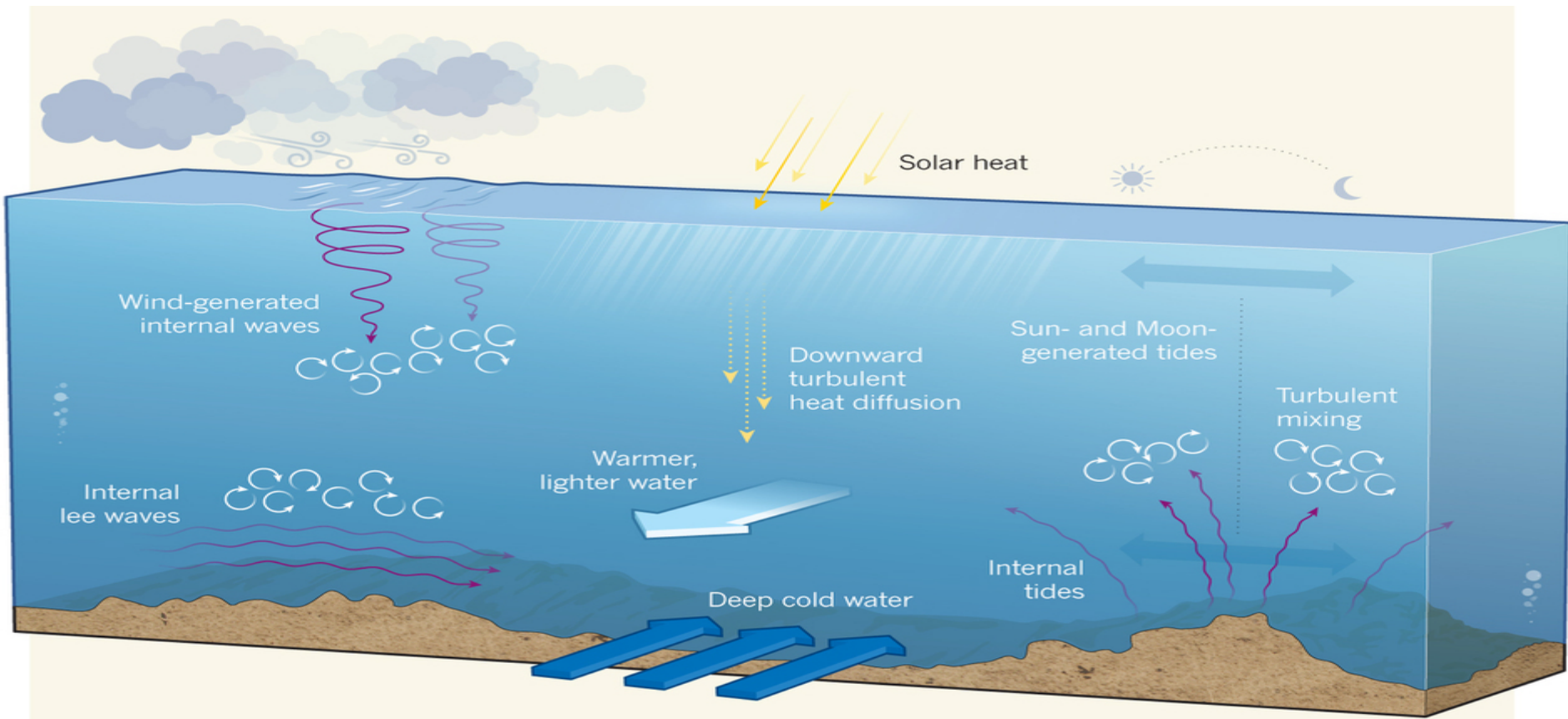


Fig. 1. Reflection of internal wave characteristics (black lines) from bottom slope  $\gamma$  for (A) simplified density profile (red) and Brunt-Vaisala frequency profile  $N$  (green), transmissive [(B),  $\gamma/c < 1$ ], critical [(C),  $\gamma/c = 1$ ], and reflective [(D),  $\gamma/c > 1$ ]. Energy is trapped along the bottom, and bottom velocities are intensified in (C) (maroon bar indicates velocity intensification); bottom velocities also increase upslope in (B) (10).

# 1. Internal waves generation

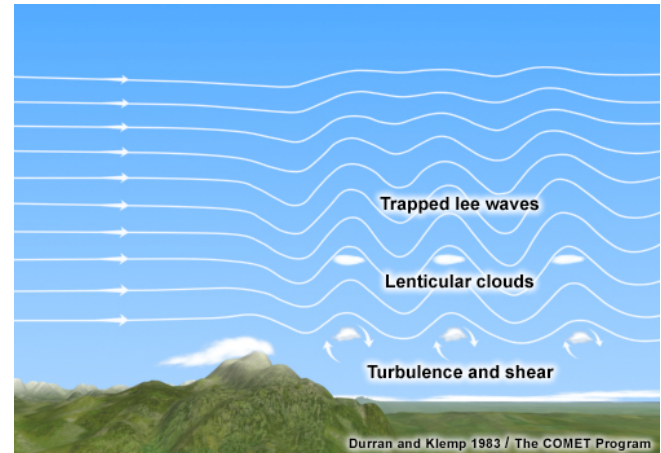
- Mechanisms:



From Mackinnon 2013

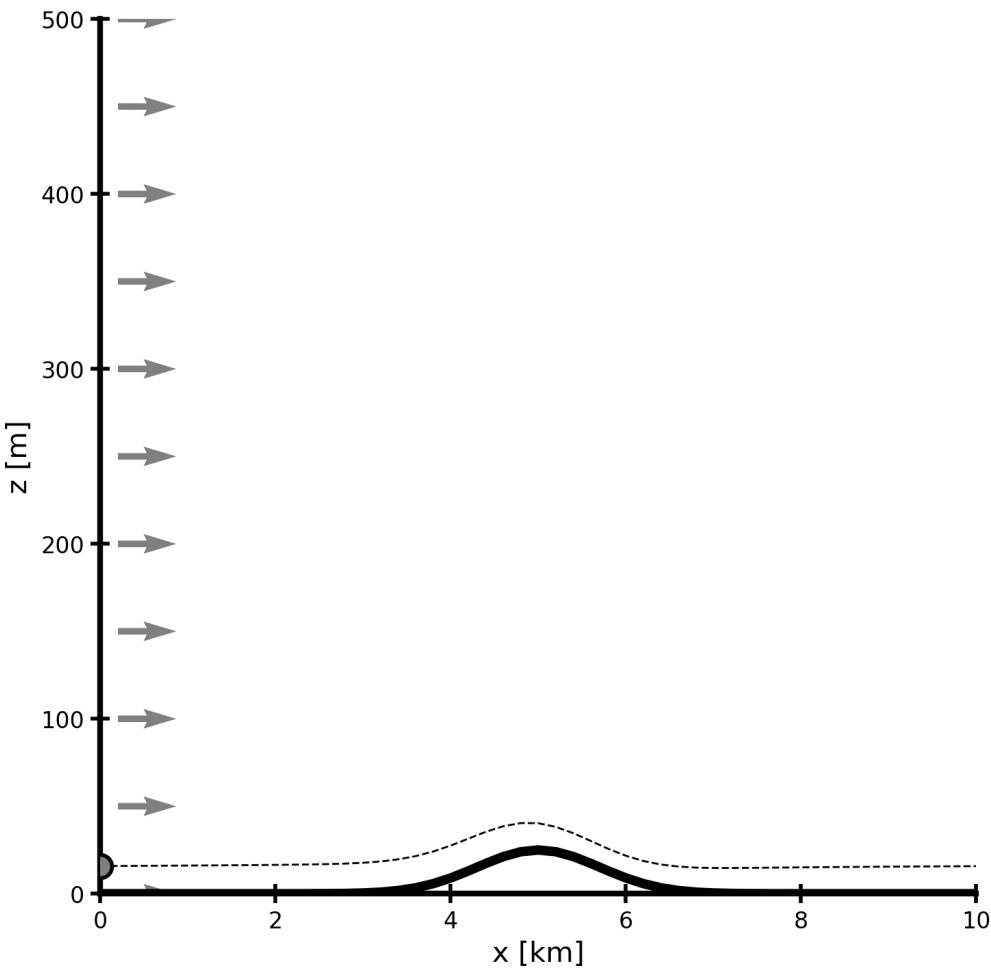
## 1.2 Generation of Lee waves

- **Lee waves** (or mountain waves) can be seen in ocean and atmosphere



Modis, 23/11/2009 - South Atlantic – Sandwich Islands  
The lower atmosphere is drier – Downwind of the islands the waves are seen when the air goes up, condensate and form clouds

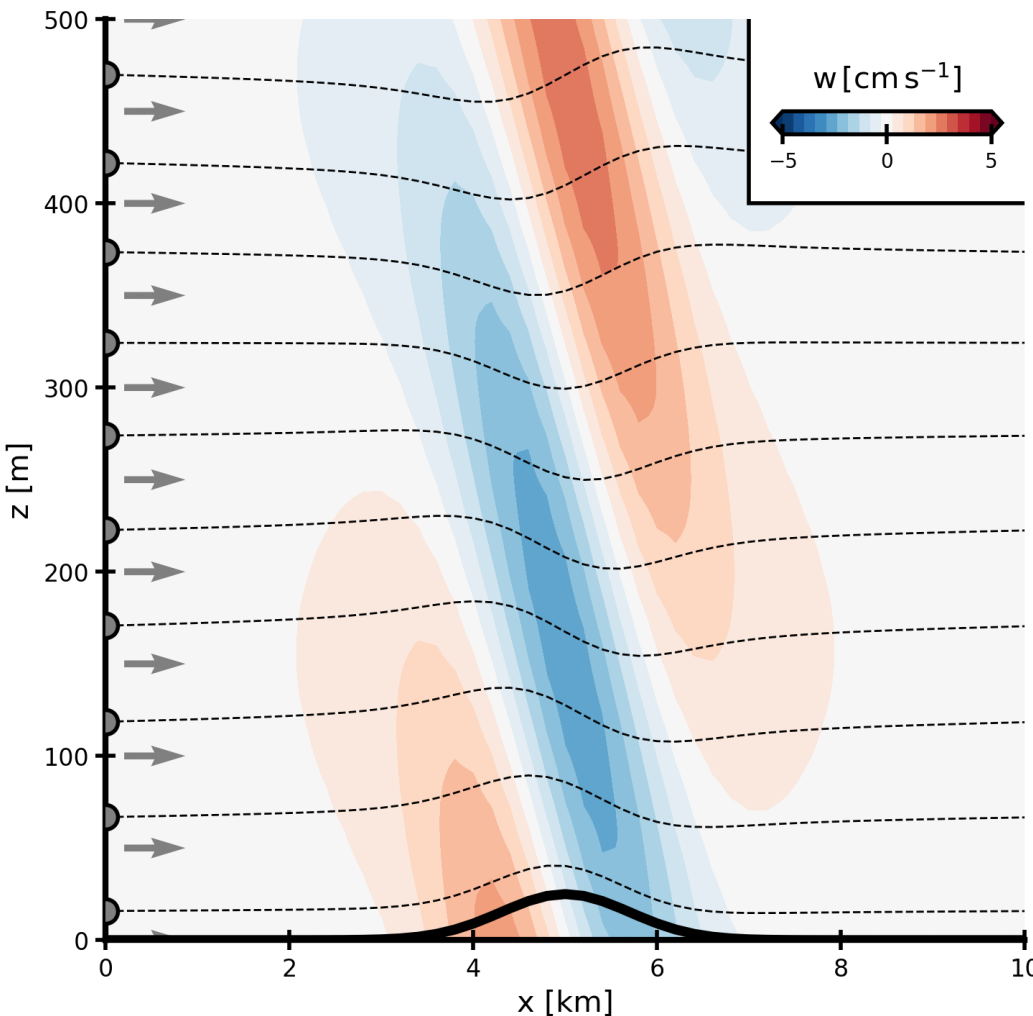
## 1.2 Generation of Lee waves



Ingredients for the propagation of a lee wave :

- ✓ A current...
- ✓ ...flowing over a topography

## 1.2 Generation of Lee waves

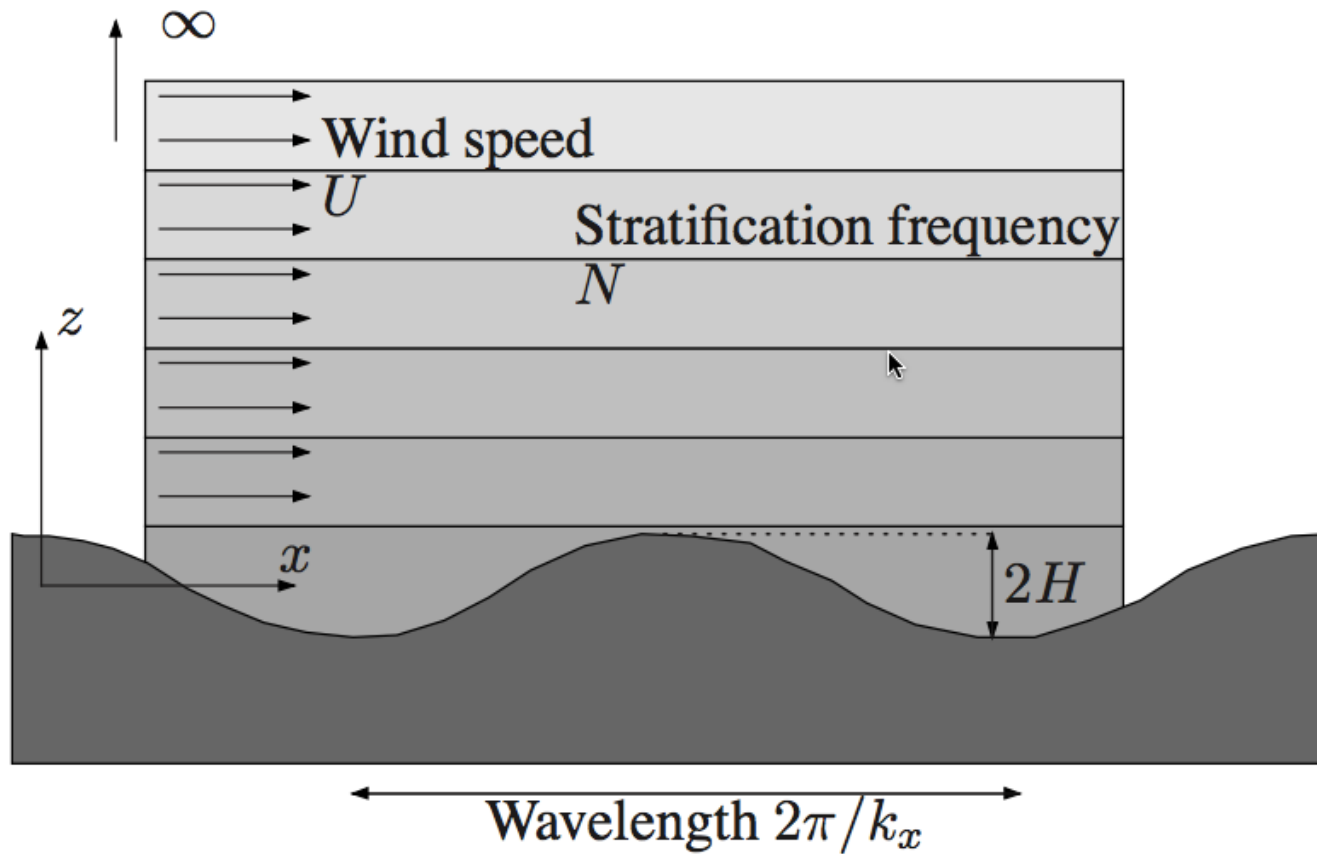


Ingredients for the propagation of a lee wave :

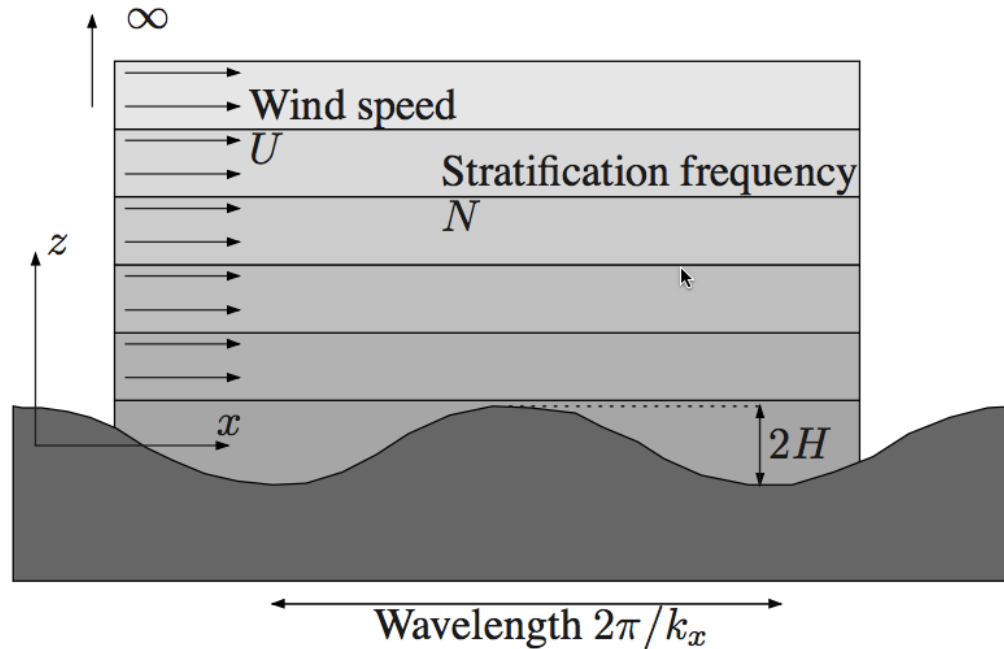
- ✓ A current...
  - ✓ ...flowing over a topography
  - ✓ A stratification
- *Propagation of an internal wave forced by the topography*

## 1.2 Generation of Lee waves

- Internal waves generated at horizontal boundary:



## 1.2 Generation of Lee waves



- Topography (*in the frame moving at constant speed  $U$* ):

$$z = H \sin[k_x(x + Ut)]$$

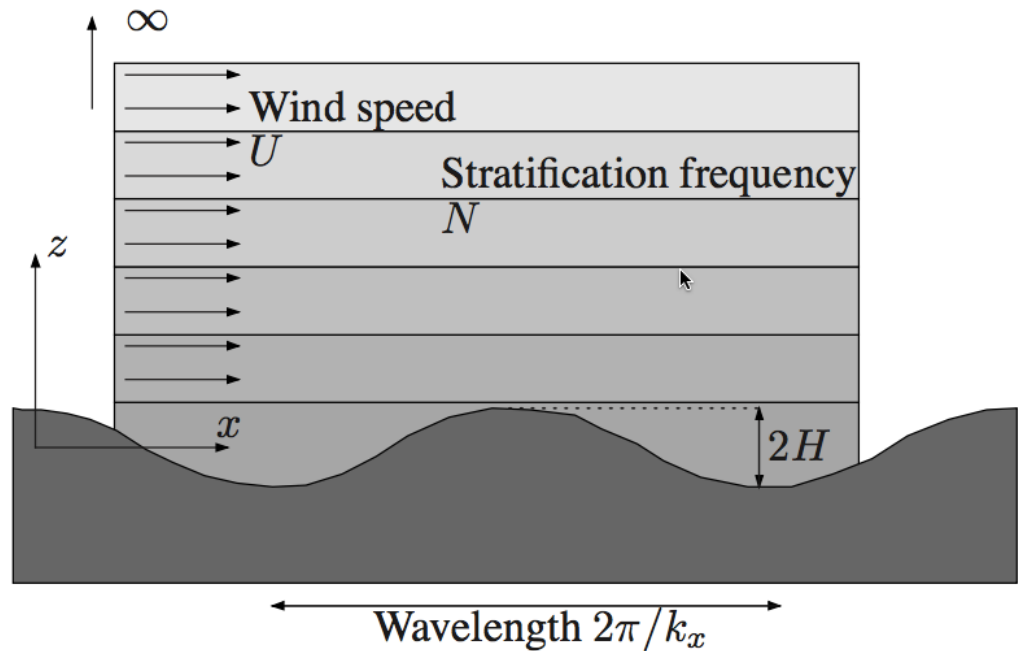
- Frequency of the motion:

$$\omega = -k_x U$$

## 1.2 Generation of Lee waves

$$z = H \sin[k_x(x + Ut)]$$

$$\omega = -k_x U$$



- Activity: Solve the equation for linear internal waves without rotation ( $f=0$ ) in the  $x=z$  plane (assuming  $H \ll U/N$ ).
  1. Write the bottom boundary condition for the vertical velocity  $w$
  2. Solve for a solution in the form  $w = w_0 \exp(i(k_x x + k_z z - \omega t))$

## 1.2 Generation of Lee waves

- Case 1 = **Radiating waves**

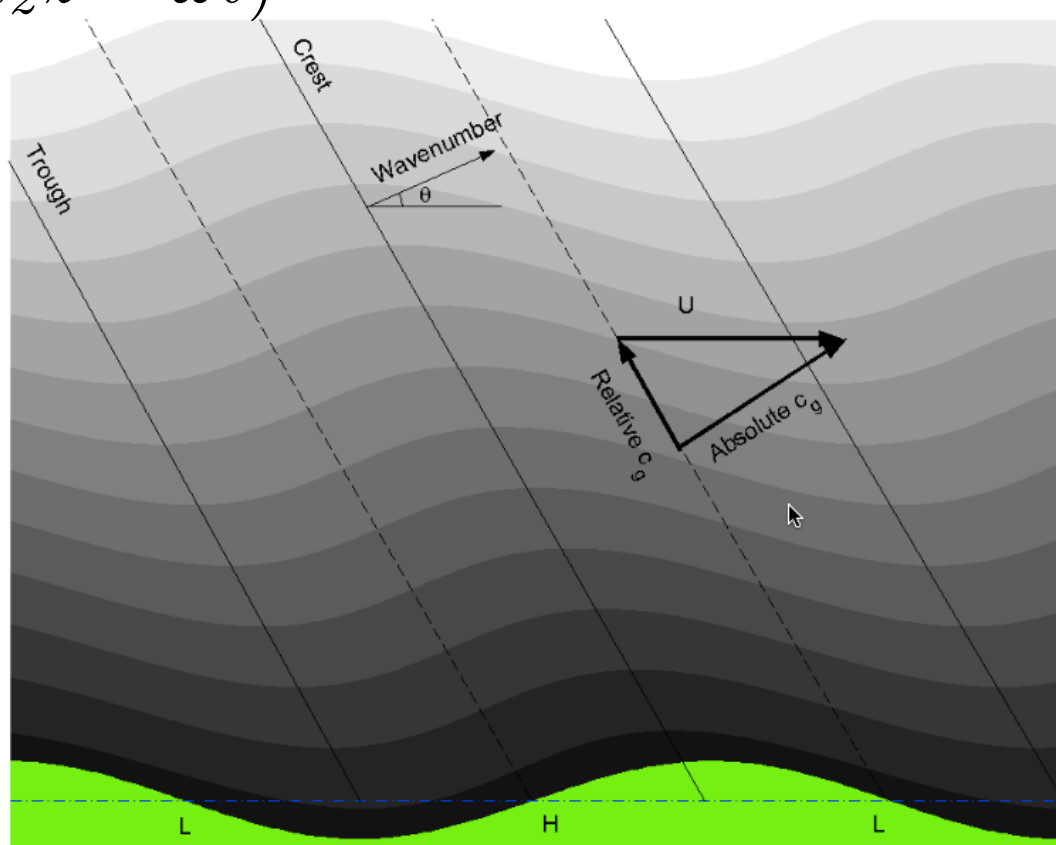
$$\frac{N}{U} > k_x \quad k_z = \pm \sqrt{\frac{N^2}{U^2} - k_x^2}$$

$$w = k_x U H \cos(k_x x + k_z z - \omega t)$$

Angle between wave fronts and vertical:  
 $\cos\theta = \frac{k_x U}{N}$

Group velocity in the vertical:

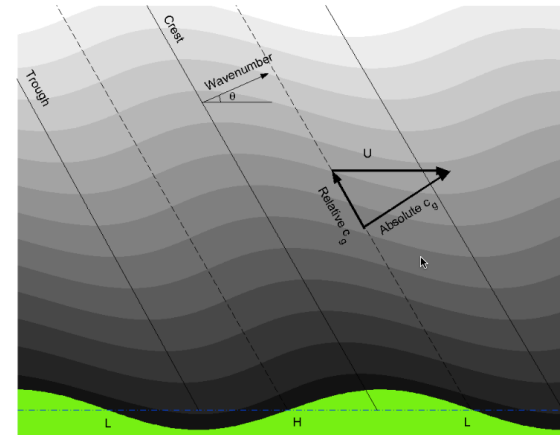
$$c_{gz} = \frac{\partial \omega}{\partial k_z} = \frac{k_x k_z}{k^2} U$$



## 1.2 Generation of Lee waves

- Case 1 = Radiating waves

$$\frac{N}{U} > k_x$$



- Drag force:  $\rho_0 \bar{u} \bar{w}|_{z=0} = -\frac{1}{2} \rho_0 k_k k_z U^2 H^2$

The terrain exerts a drag force on the flowing air mass.

- Energy flux:  $\mathbf{F}' = \overline{p' \mathbf{u}} = E \mathbf{c}_g$

In the vertical  $F'_z = \frac{1}{2} k_x \rho_0 H^2 U^2 \sqrt{N^2 - U^2 k_x^2}$

Continual upward propagation of energy. Supply of energy from the ground to upper levels where it will be absorbed.

## 1.2 Generation of Lee waves

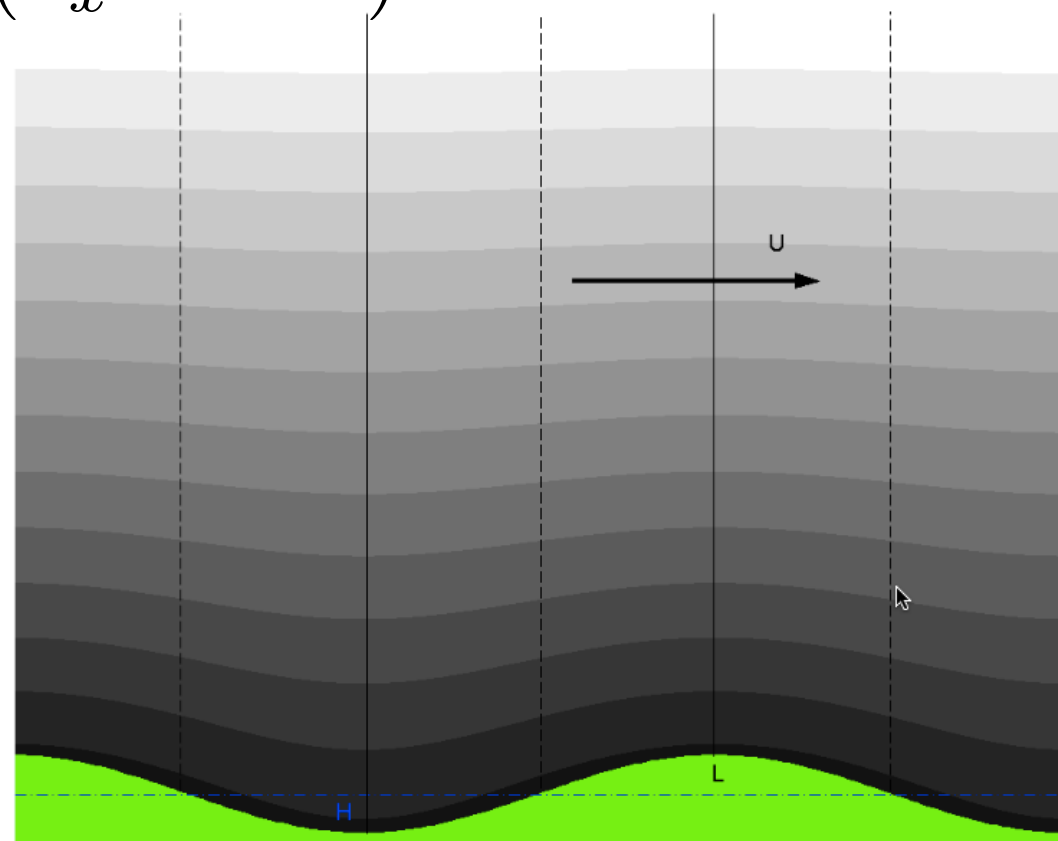
- Case 2 = Trapped waves

$$\frac{N}{U} < k_x \quad \gamma = \sqrt{k_x^2 - \frac{N^2}{U^2}}$$

$$w = k_x U H e^{-\gamma z} \cos(k_x x - \omega t)$$

The solution now contains exponential functions in  $z$ .

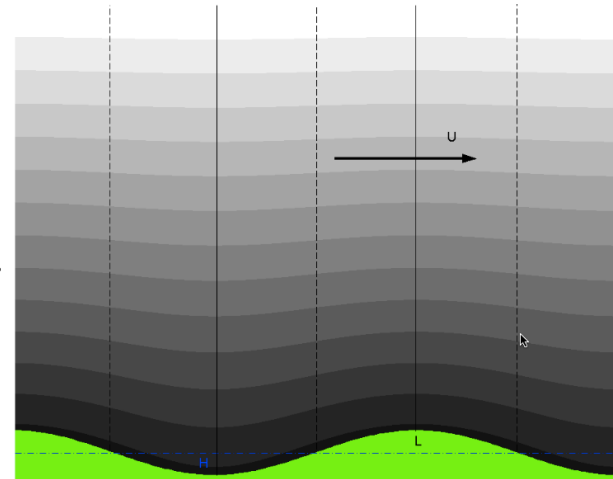
Density surfaces undulate at the same wavelength as the terrain, but the amplitude decays with height.



## 1.2 Generation of Lee waves

- Case 2 = Trapped waves

$$\frac{N}{U} > k_x$$



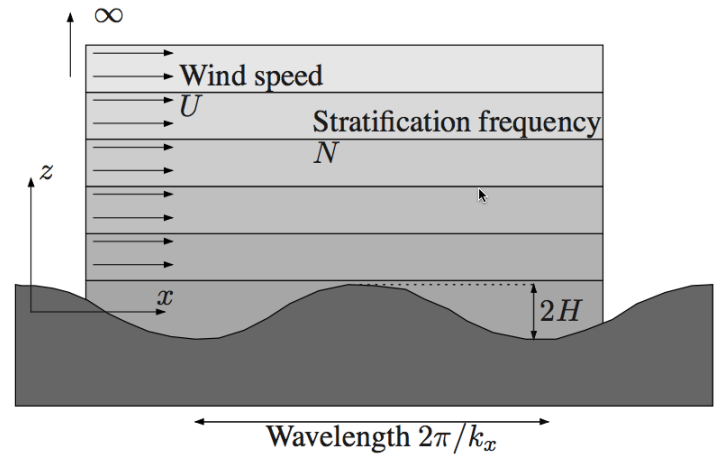
- Drag force:  $\rho_0 \overline{uw}|_{z=0} = 0$

u and w in quadrature = **No Drag**

- Energy flux:  $\mathbf{F}' = \overline{p' \mathbf{u}} = E \mathbf{c}_g$

p and w in quadrature = **no vertical energy flux**

## 1.2 Generation of Lee waves



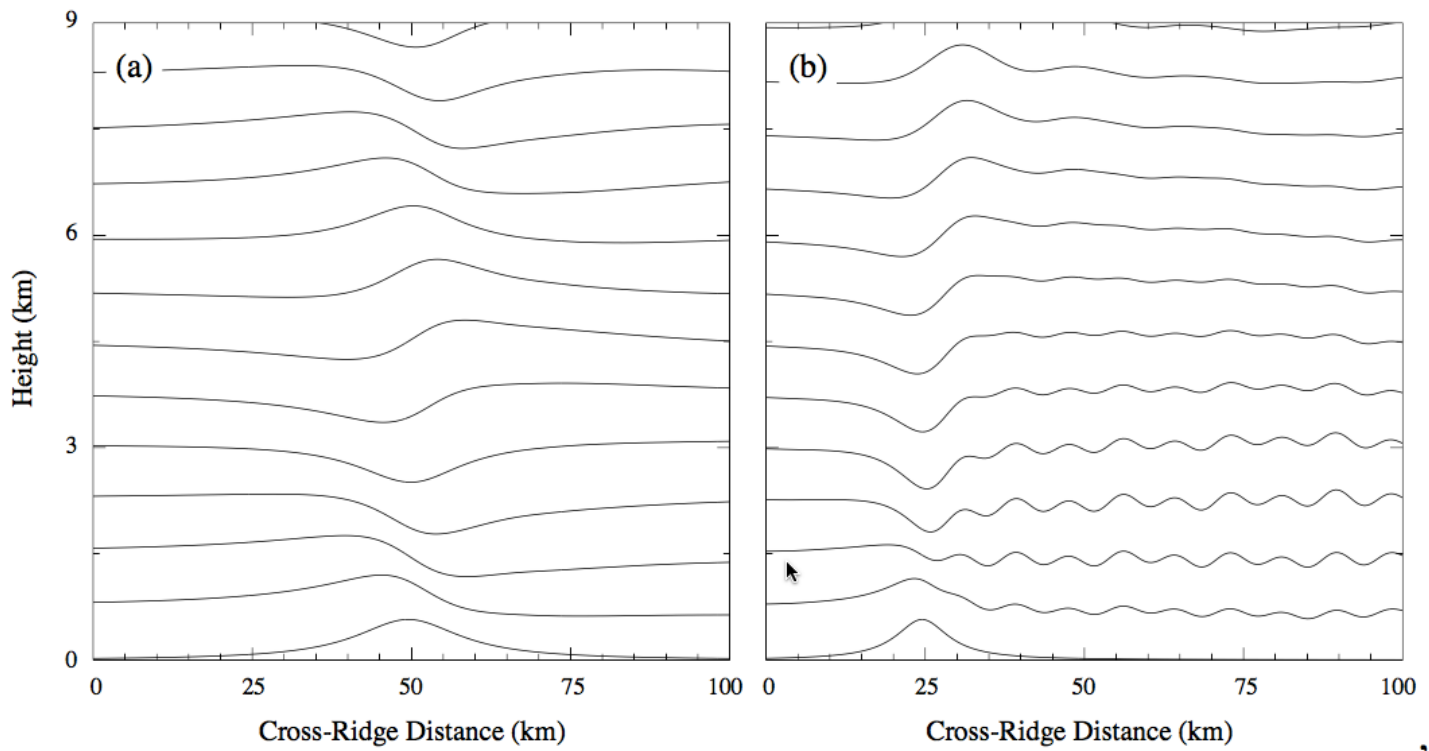
- **Effect of the rotation**

The vertical wave number becomes:  $k_z^2 = k_x^2 \frac{N^2 - \omega^2}{\omega^2 - f^2} = k_x^2 \frac{N^2 - U^2 k_x^2}{U^2 k_x^2 - f^2}$

The upward energy flux is  $F'_z = \frac{1}{2} k_x \rho_0 H^2 U^2 \sqrt{N^2 - U^2 k_x^2} \left( 1 - \frac{f^2}{U^2 k_x^2} \right)$

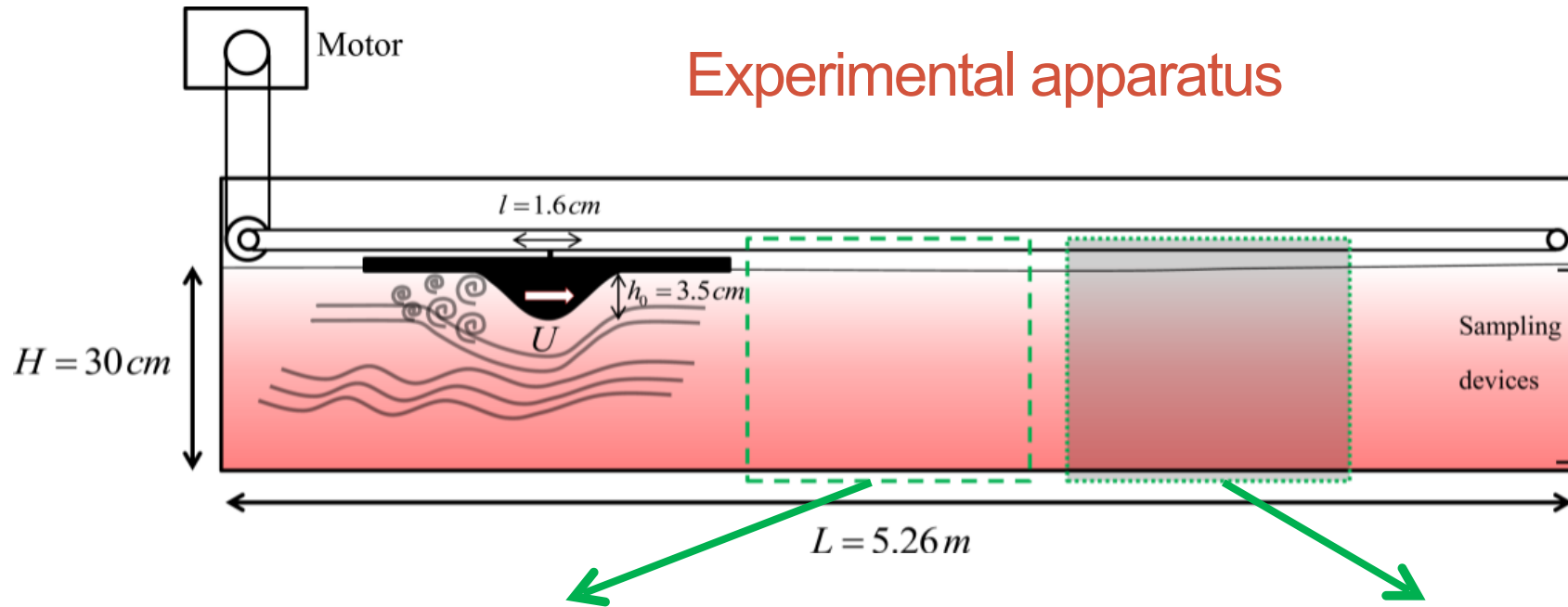
## 1.2 Generation of Lee waves

- General topography

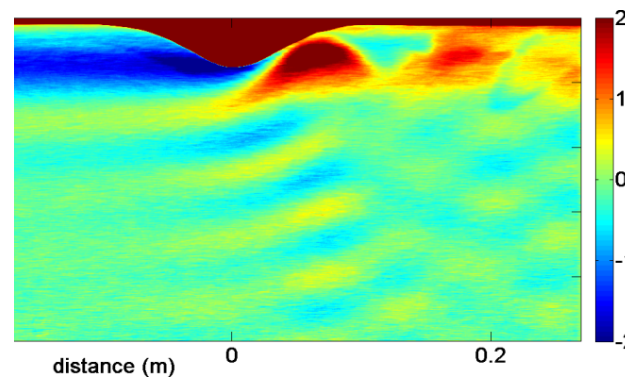
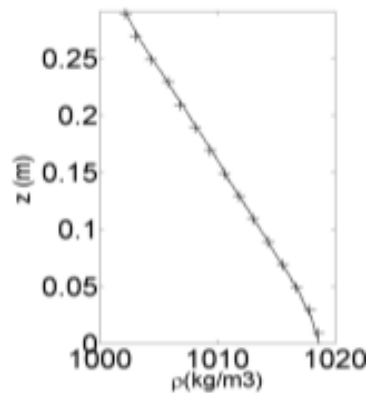


Streamlines in steady airflow over an isolated ridge as predicted by linear theory

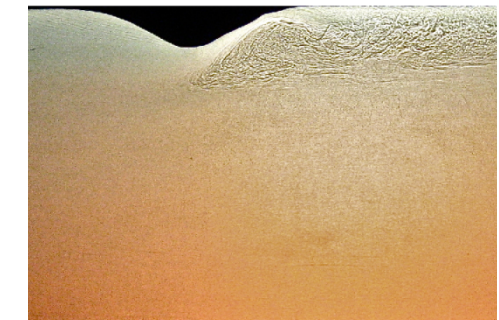
# 1.2 Generation of Lee waves - Experiments



**Light attenuation technique**  
High resolution density measurements

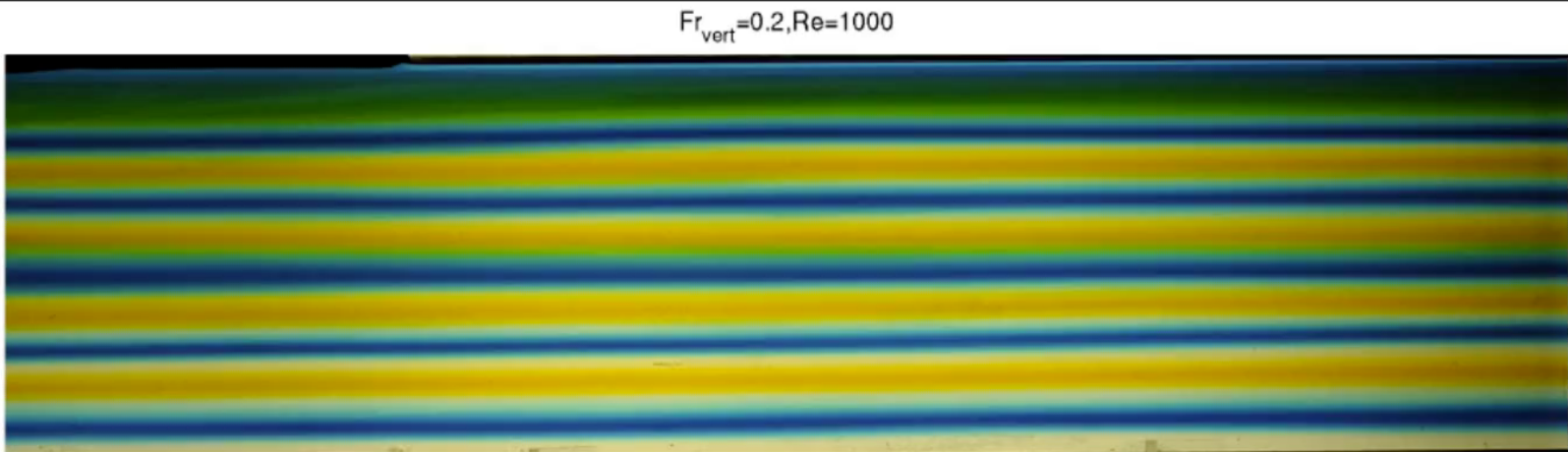


**Shadowgraph pictures**  
Direct observation of mixing



[Y. Dossmann]

## 1.2. Generation of Lee waves - Experiments

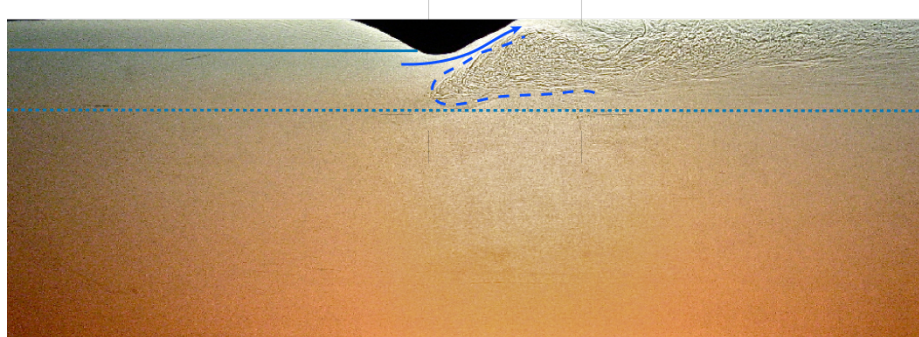


Froude number : Flow regime

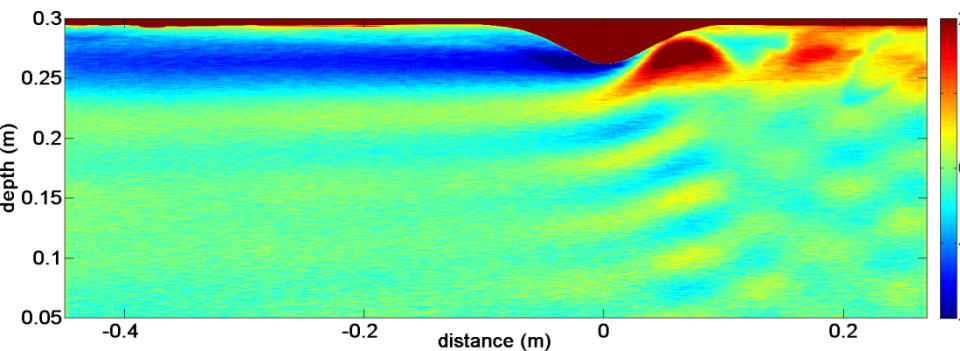
Reynolds number : Turbulence regime

## 1.2. Generation of Lee waves - Experiments

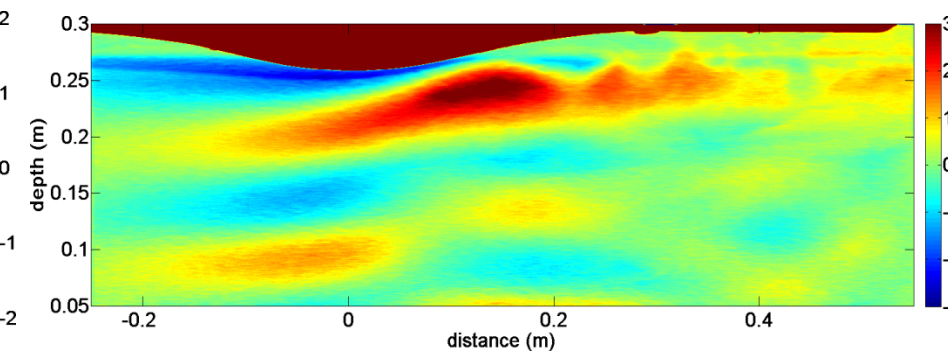
Fr=0.2; Re=500



Fr=0.4; Re=1700



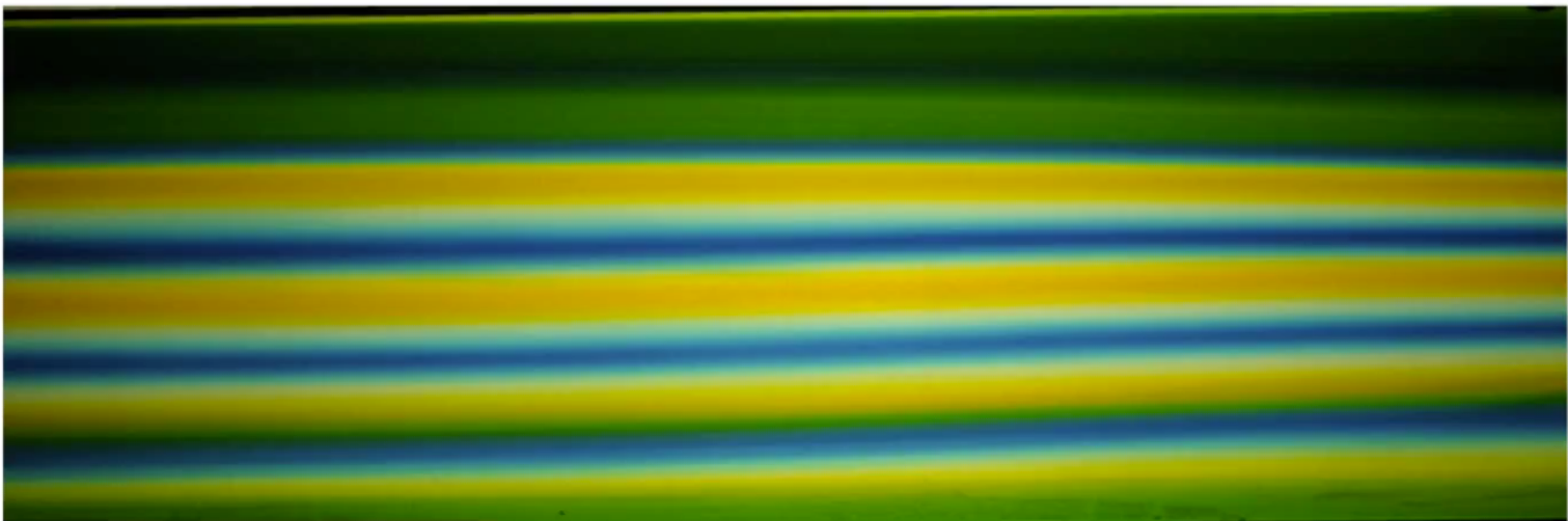
Density anomaly ( $\text{kg}/\text{m}^3$ )



Density anomaly ( $\text{kg}/\text{m}^3$ )

## 1.2. Generation of Lee waves - Experiments

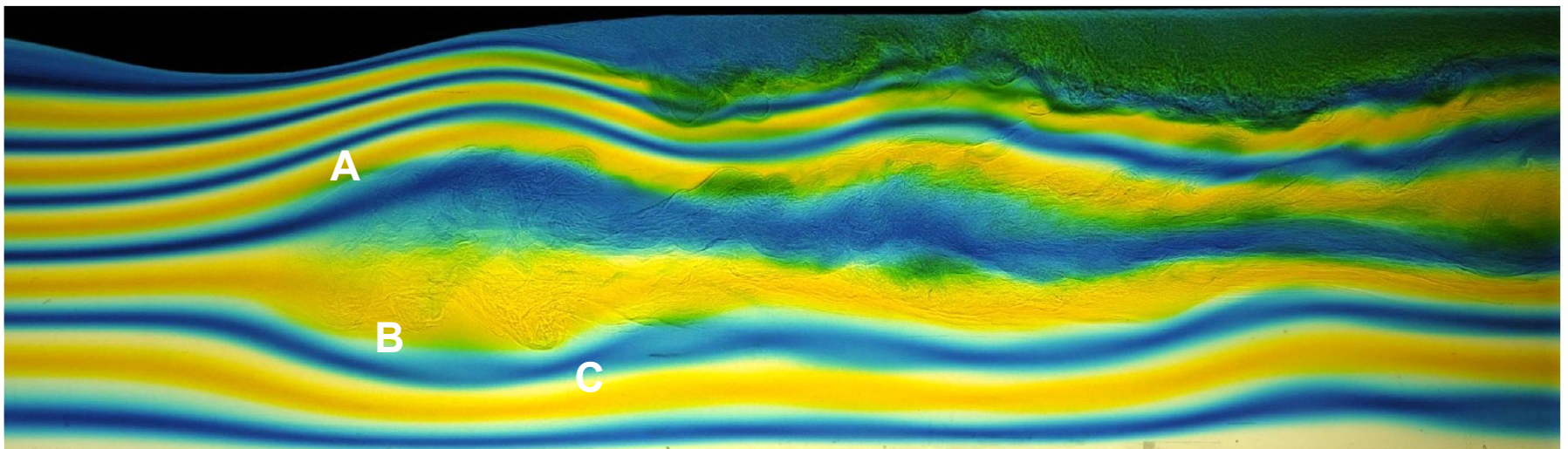
$Fr_{vert} = 1, Re = 5000$



[Y. Dossmann]

## 1.2. Generation of Lee waves - Experiments

$Fr=1$  ;  $Re=3500$

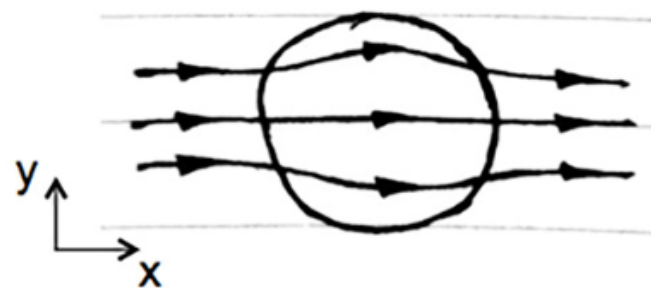
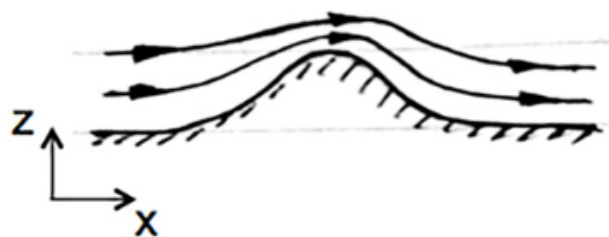
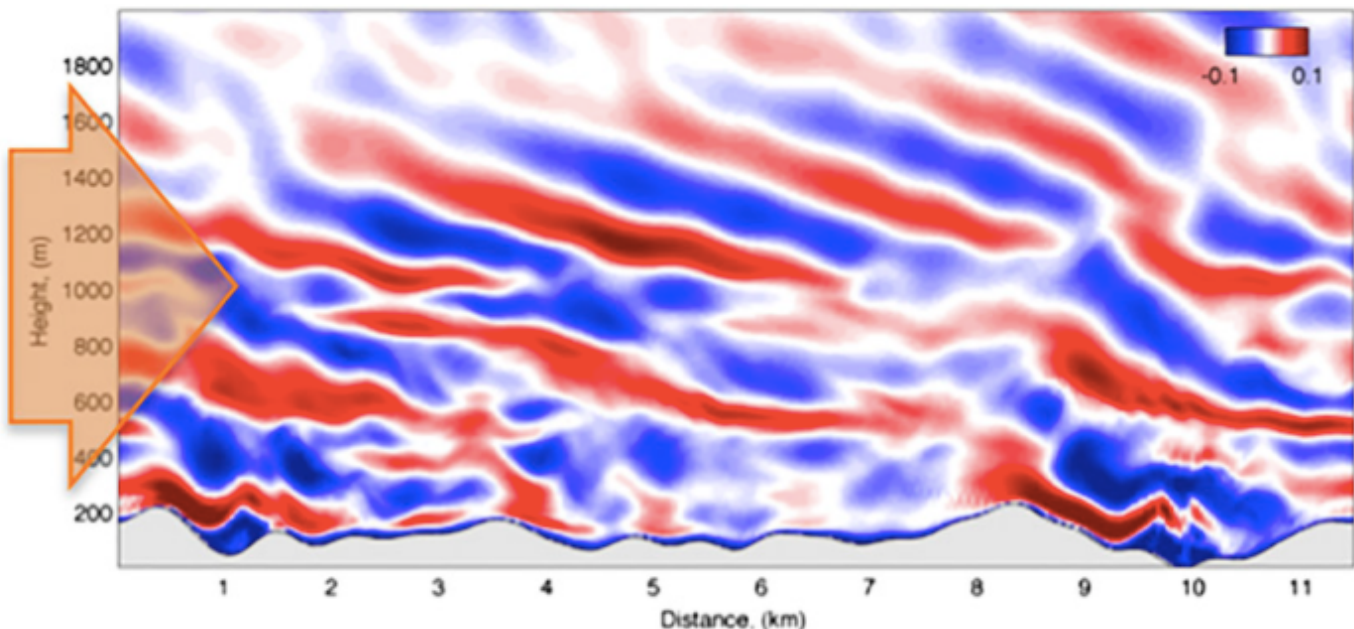


- A: Unstable Lee waves
- B: Narrow accelerating jet
- C: Periodic turbulent patches

[Y. Dossmann]

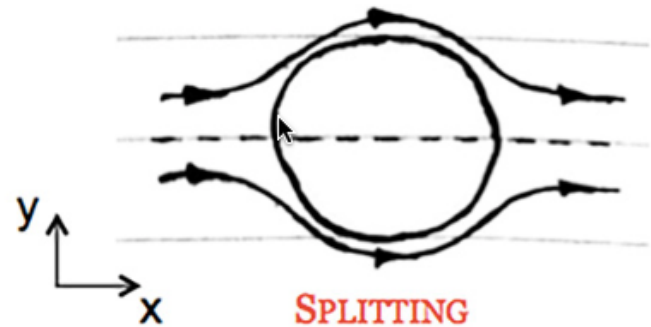
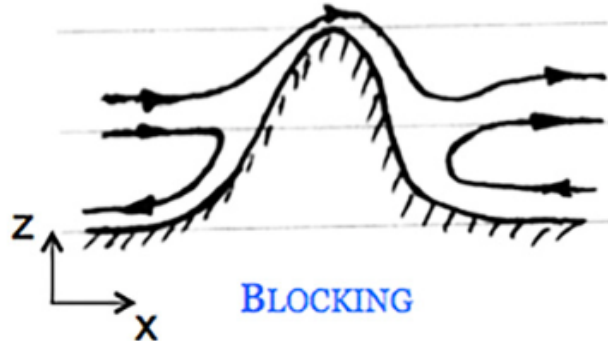
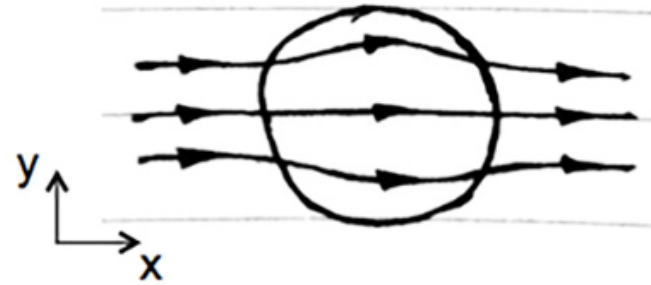
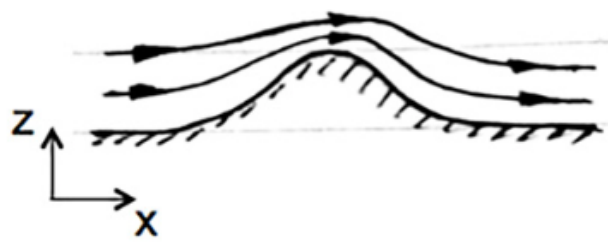
## 1.2. Generation of Lee waves

Limitation of the  
2d linear theory:



## 1.2. Generation of Lee waves

Limitation of the 2d theory

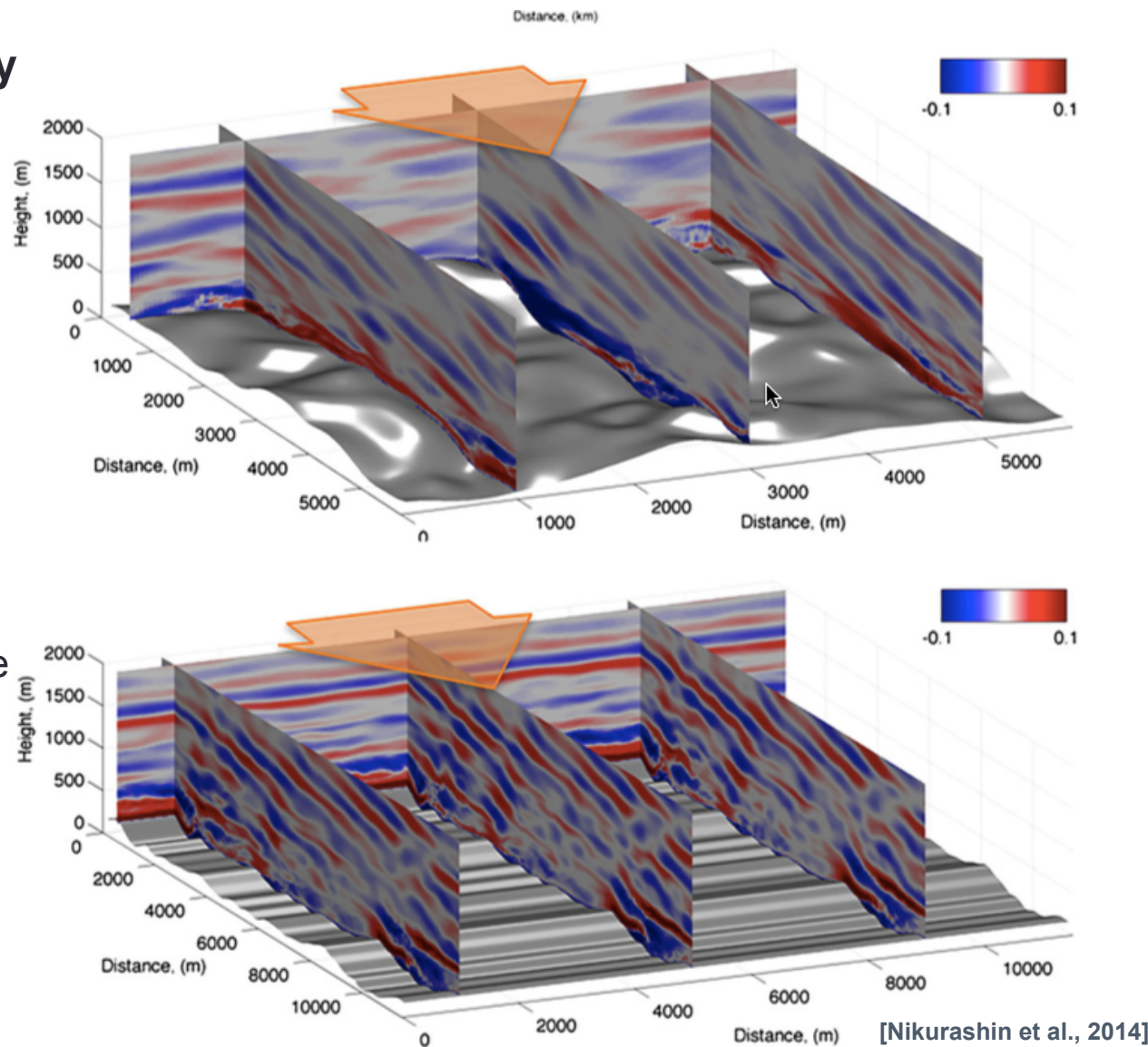


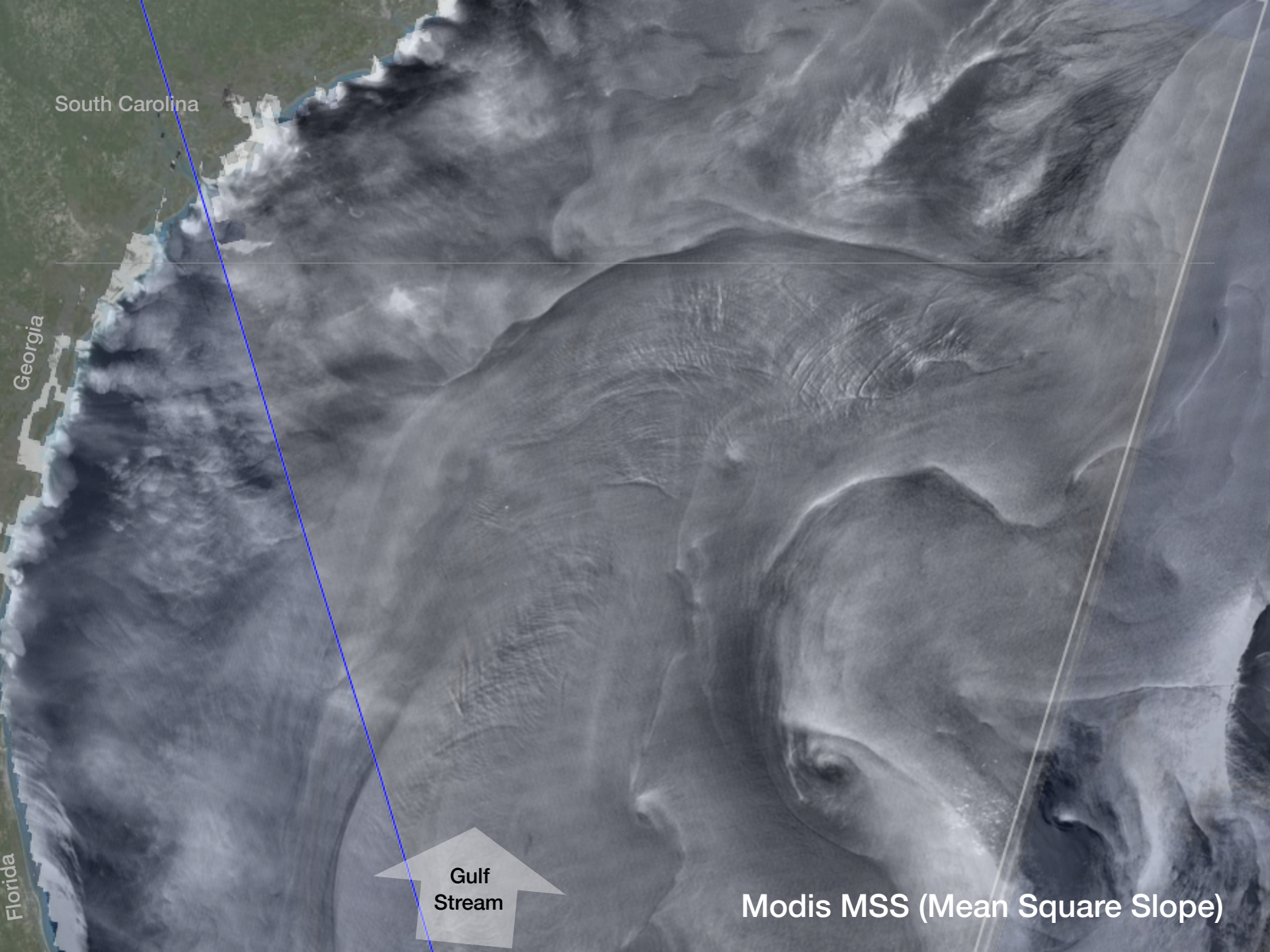
## 1.2. Generation of Lee waves

### Limitation of the 2d theory

Internal wave generation at 3D, finite bottom topography is reduced compared to the two-dimensional case.

The reduction is primarily associated with finite-amplitude bottom topography effects that suppress vertical motions and thus reduce the amplitude of the internal waves radiated from topography.

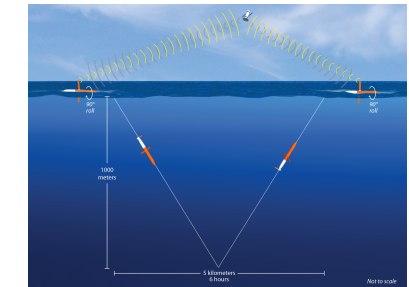




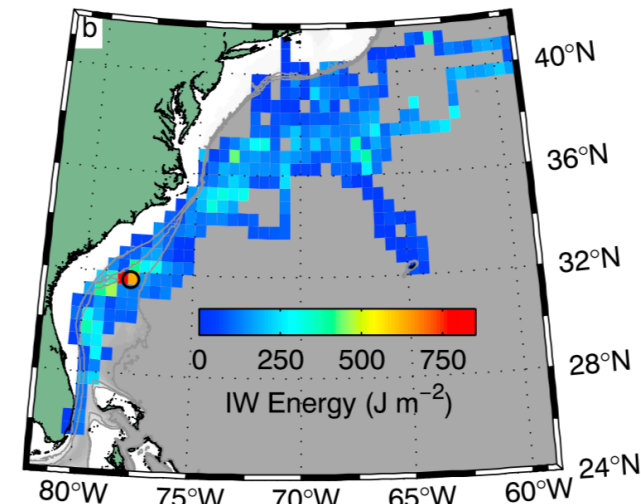
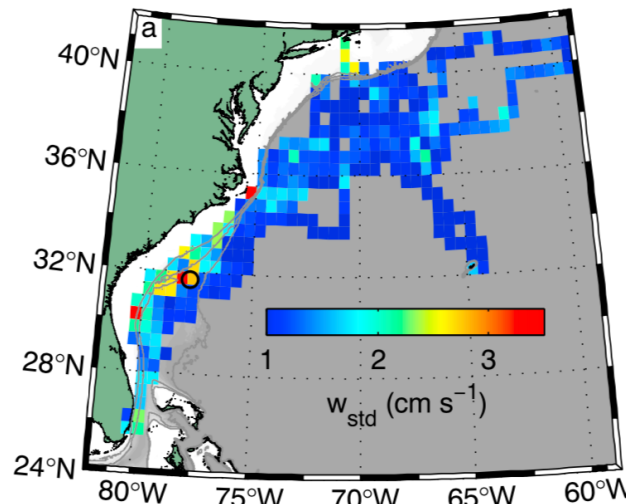
## 1.2. Generation of Lee waves - Real example

internal wave activity in the GS

- Internal waves with vertical velocities exceeding  $0.1 \text{ m s}^{-1}$  are found over the Charleston Bump.



Glider data

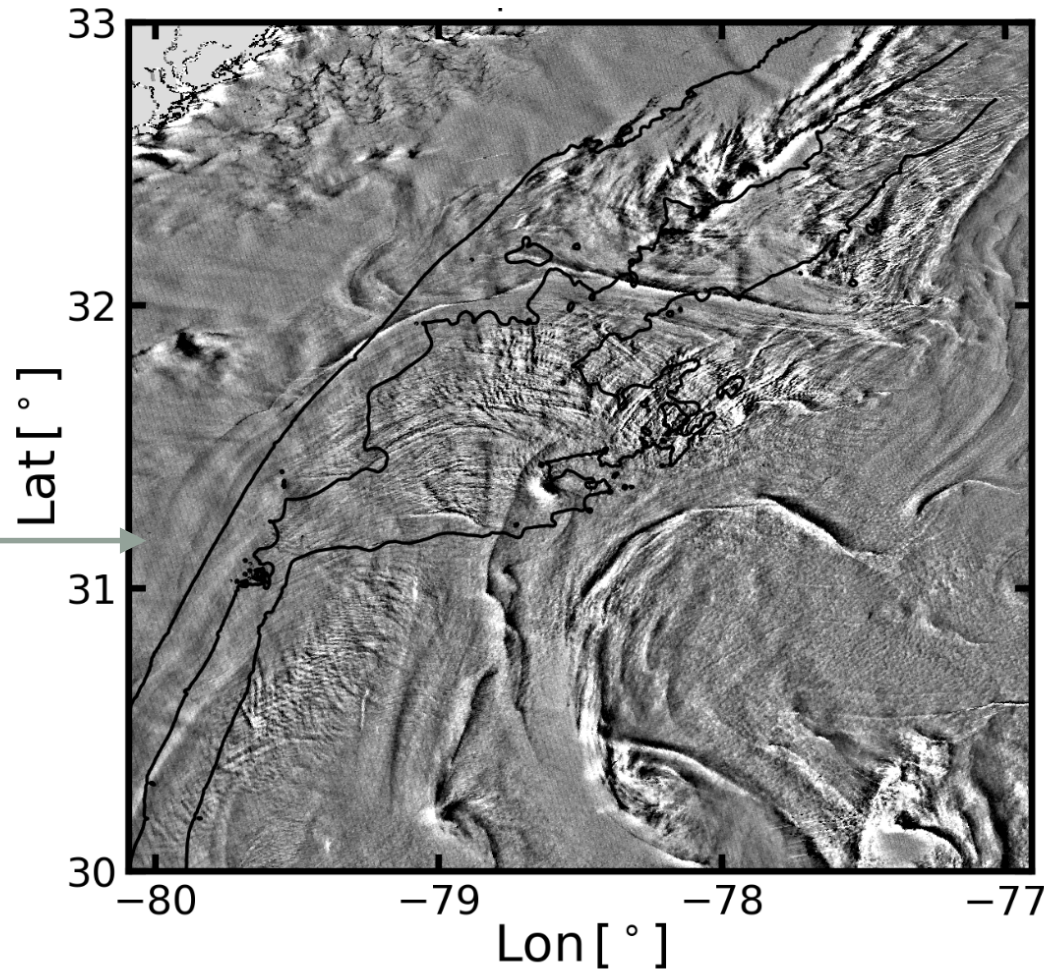
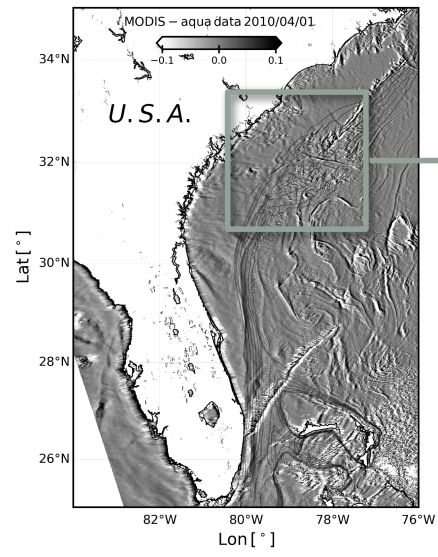


(a) Standard deviations of vertical velocities from individual glider dives averaged in  $0.5^\circ \times 0.5^\circ$  boxes. (b) Vertically integrated internal wave energy [Todd, 17]

## 1.2. Generation of Lee waves - Real example

### Observations of Lee Waves in the Gulf Stream

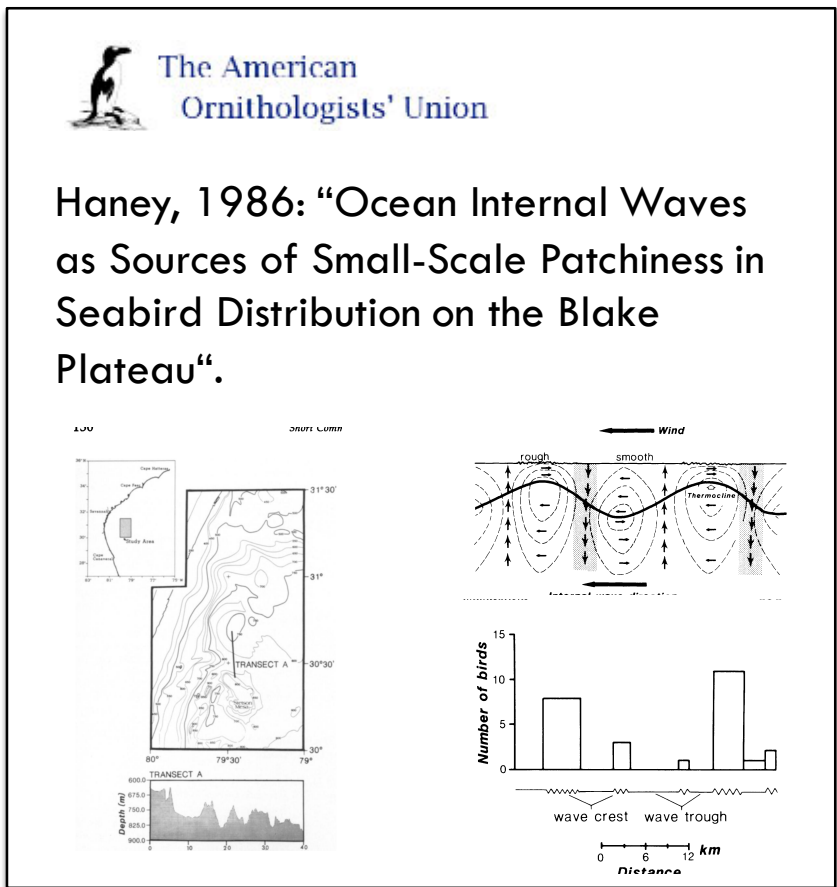
- Internal waves can be observed using synthetic aperture radars (SAR) or Sun-glitter images through their surface roughness signature.



## 1.2. Generation of Lee waves - Real example

### Observations of Lee Waves in the Gulf Stream

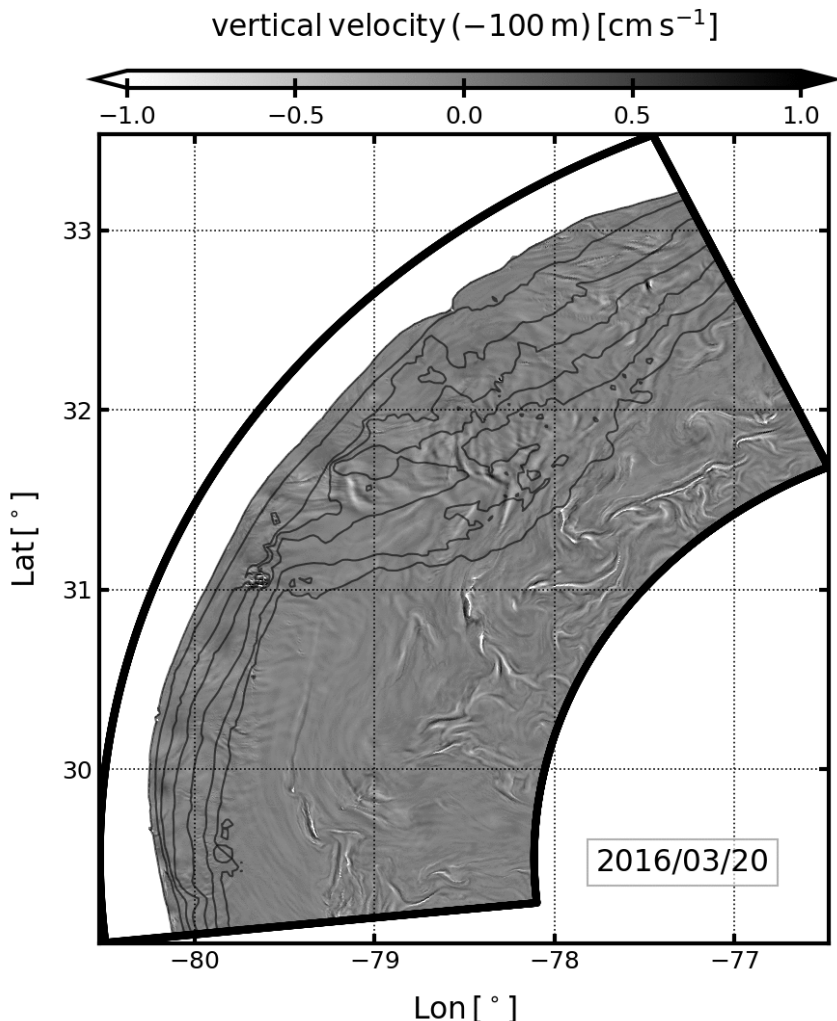
- They were also previously inferred from patchiness in seabirds distribution:



## 1.2. Generation of Lee waves - Real example

### Simulation of the Gulf Stream

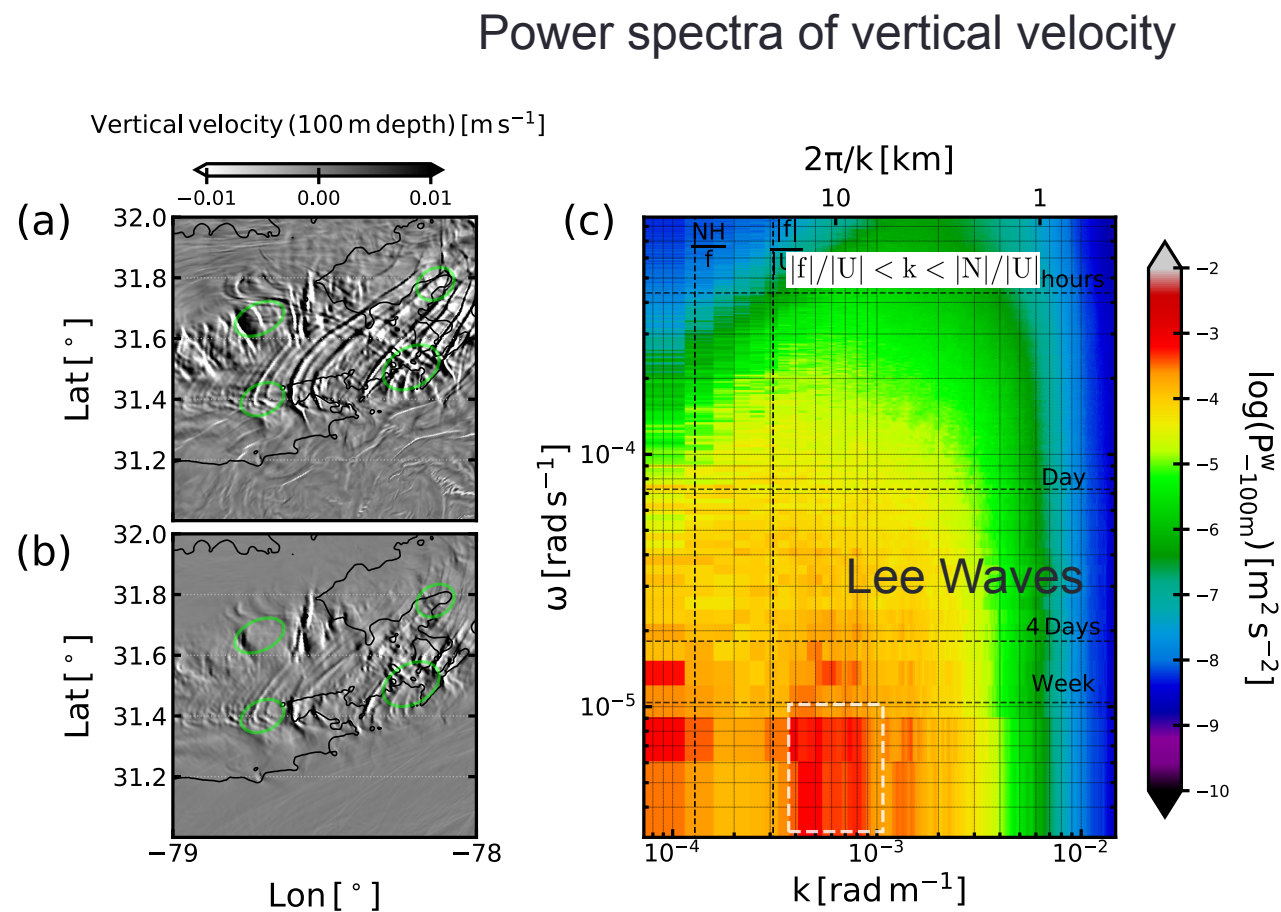
- We performed a ROMS/CROCO nest  $dx = 200$  m,
- $Nx \times Ny \times Nz = 1024 \times 2048 \times 128$
- Climatological forcings (monthly winds, no tides)
- 



# 1.2. Generation of Lee waves - Real example

## Lee Waves in the Gulf Stream

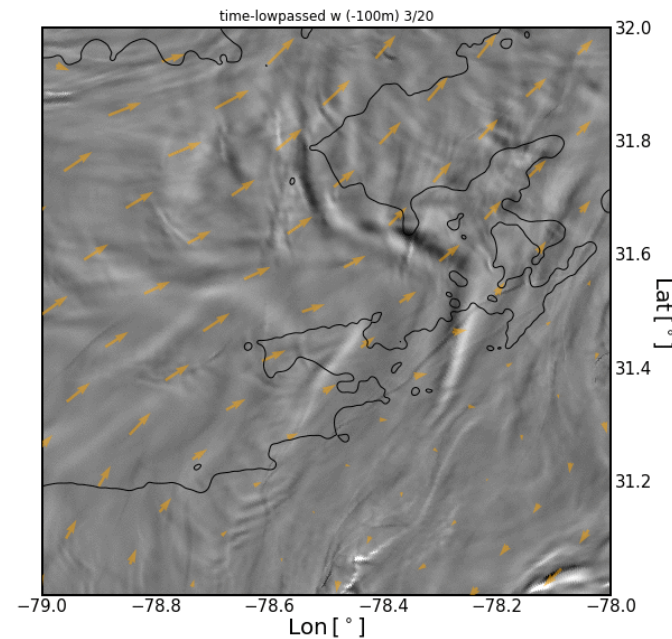
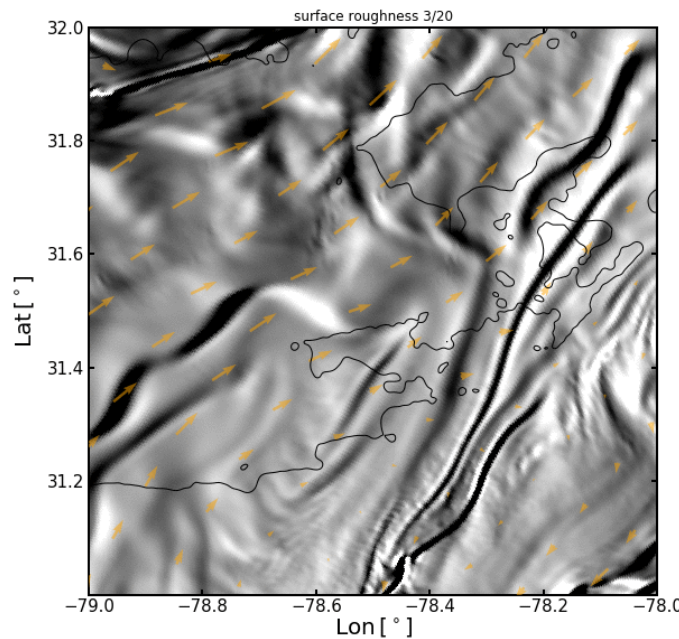
- We can isolate patterns related to Lee Waves by looking at time-low passed vertical velocities below the thermocline:



## 1.2. Generation of Lee waves - Real example

### Lee Waves in the Gulf Stream

- We can isolate patterns related to Lee Waves by looking at time-low passed vertical velocities below the thermocline:



# 1.2. Generation of Lee waves - Real example

## Comparison of Lee Waves with linear theory

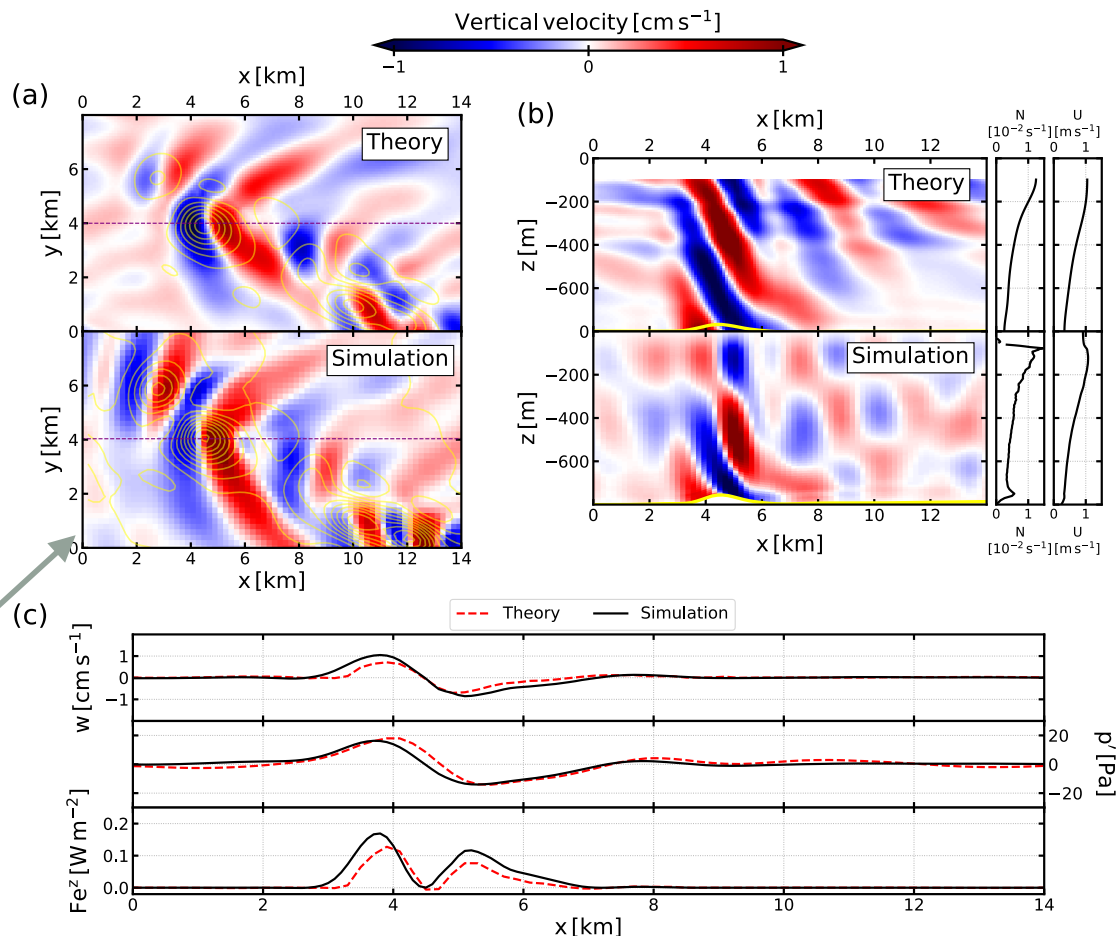
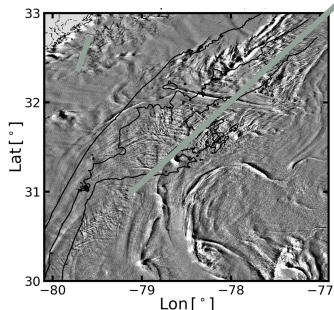
- 3D theoretical prediction of hydrostatic lee waves is obtained by numerically solving:

$$\partial_{zz} \tilde{\eta}(k, m, z) + n^2 \tilde{\eta}(k, m, z) = 0$$

- under the WKBJ approximation with the dispersion relation:

$$n^2(k, m, z) = k^{-2}(k^2 + m^2) \left( \frac{N^2}{U^2} + \frac{\partial_{zz} U}{U} \right)$$

- and radiation condition at the top of the domain and a Dirichlet condition at the bottom.



# 1.2. Generation of Lee waves - Real example

## Energy dissipation due to Lee Waves

- A significant amount of energy ( $O(1)$  GW) is being dissipated in the interior of the fluid by the lee waves, including at locations where these waves may exhibit nonlinearities.

- The lee wave energy flux ( $Fe^z = p'w$ ) computed using analytical formulation of Nikurashin and Ferrari (2011):

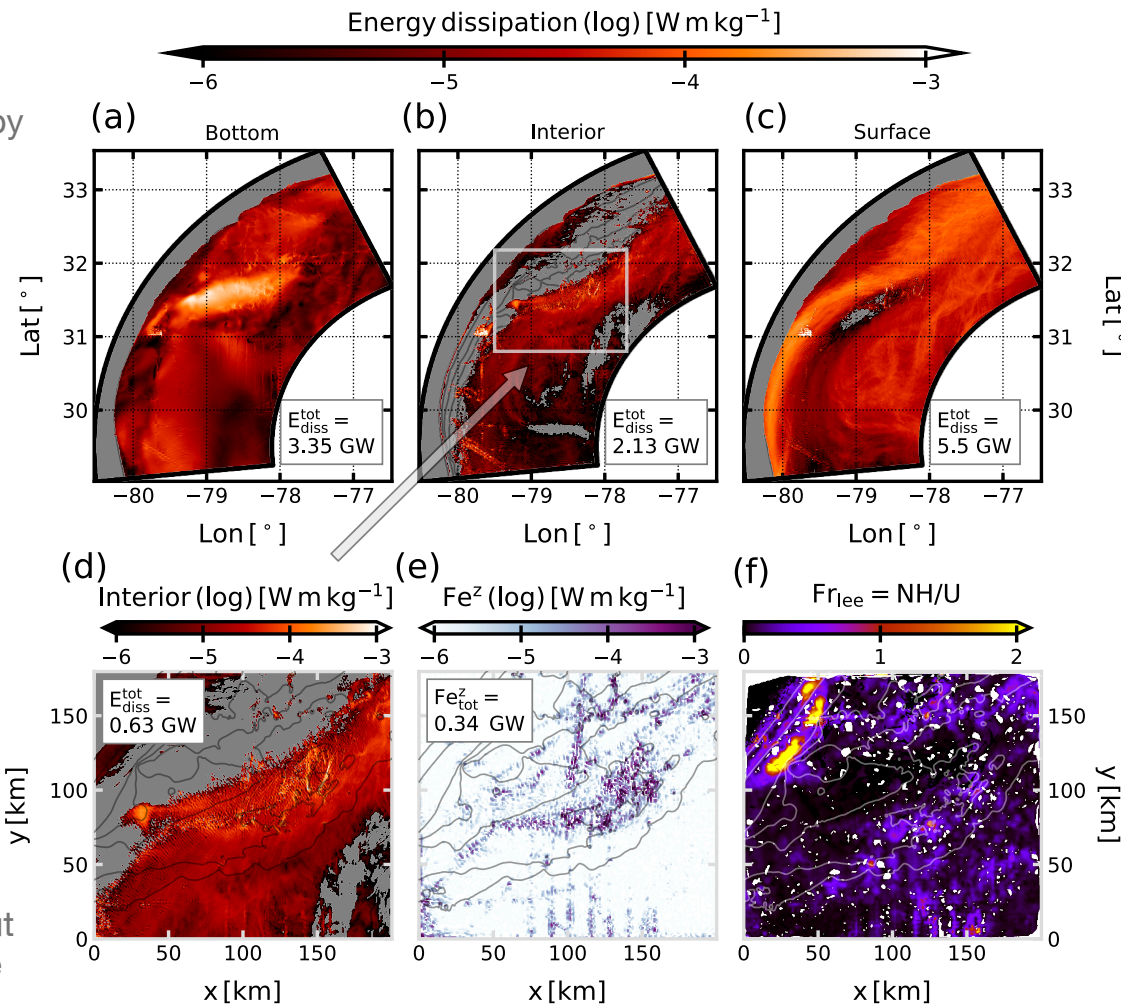
$$E = \frac{\rho_0 |\mathbf{U}|}{2\pi} \int_{|f|/|\mathbf{U}|}^{N/|\mathbf{U}|} P_*(k) \sqrt{N^2 - |\mathbf{U}|^2 k^2} \sqrt{|\mathbf{U}|^2 k^2 - f^2} dk,$$

- yields a total conversion of  $O(0.3)$  GW.

- The wave drag can be computed as:

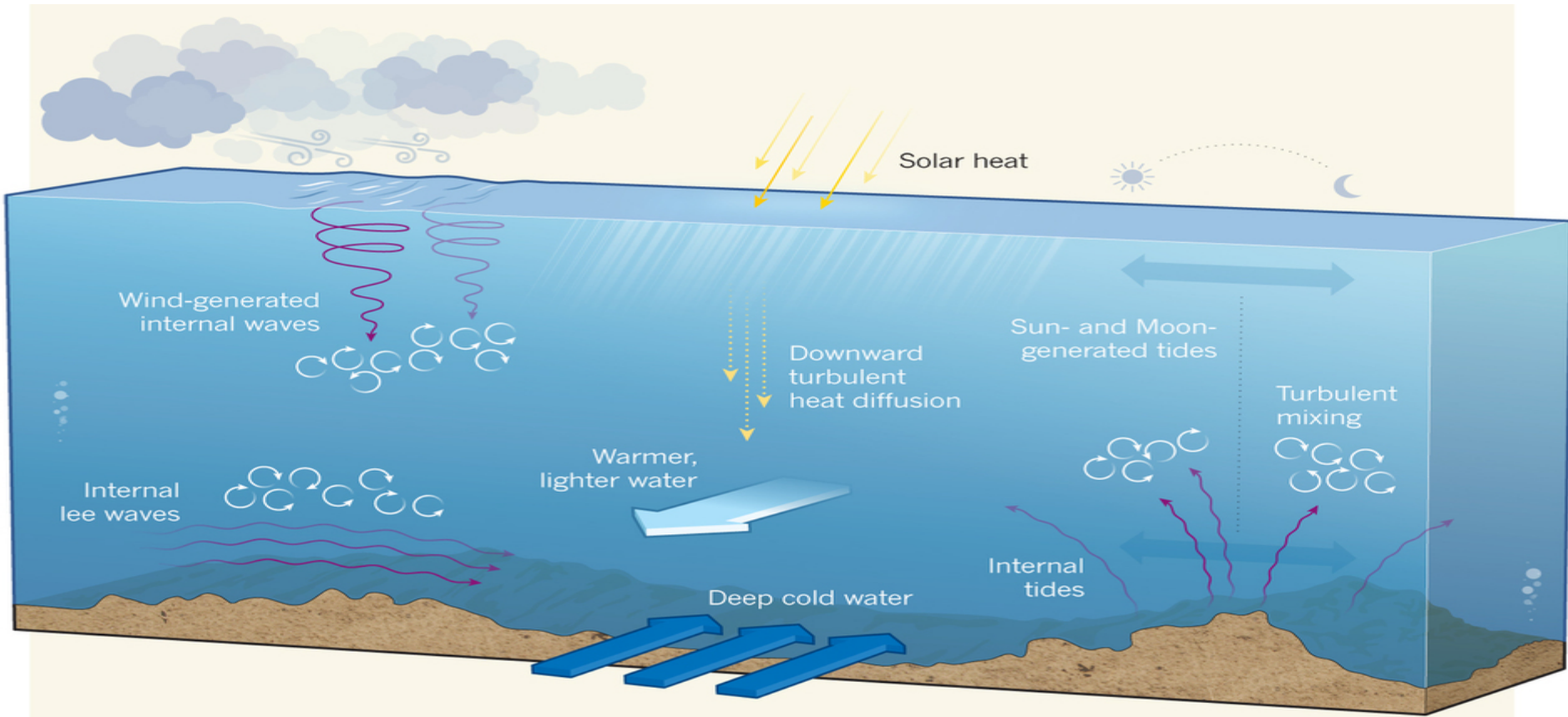
$$\text{Form Drag} = \rho_0 \sqrt{(u'w)^2 + (v'w)^2}$$

- It amounts to  $O(1)$  GN and represents about 20% of the form drag exerted by the whole Charleston Bump.



# 1. Internal waves generation

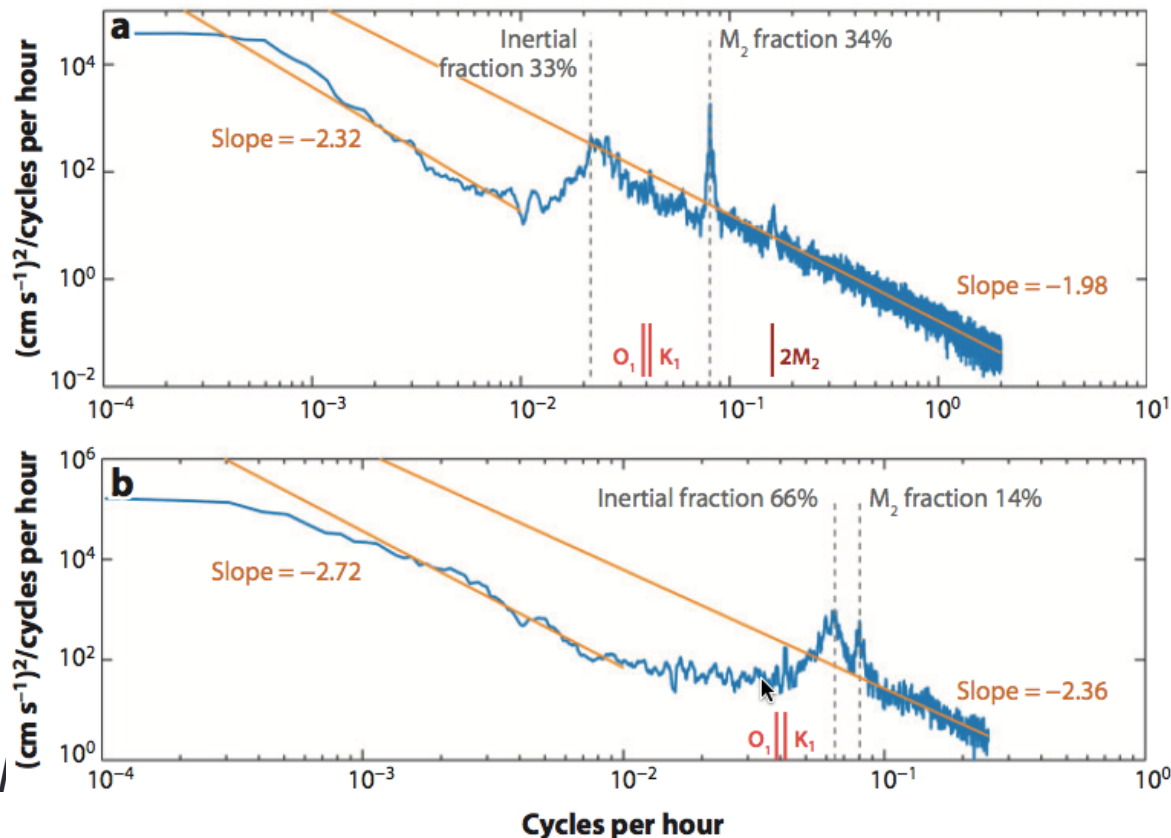
- Mechanisms:



From Mackinnon 2013

# 1. Internal waves generation

- Winds generate mostly near-inertial waves (frequency close to  $f$ )
  - = The near-inertial peak contains about half the kinetic energy in the internal wave spectrum



(a) Kinetic energy estimate for an instrument in the western North Atlantic near  $15^\circ\text{N}$  at 500 m. (b) Power density spectral estimate from a record at 1000 m at  $50.7^\circ\text{S}$ ,  $143^\circ\text{W}$ , south of Tasmania in the Southern Ocean

## 1.3. Generation of Near-Inertial waves (NIW)

- Near-inertial frequencies are associated primarily with atmospheric forcing.
- The ocean selects near-inertial frequencies for amplification because the aspect ratio of the forcing is exceedingly small.
  - Storms tends to have horizontal scales of  $O(100-1000 \text{ km})$
  - The ocean mixed layer is typically no deeper than 100 m
  - Storms move rapidly so that the ocean does not have time to adjust
-

## 1.3. Generation of Near-Inertial waves (NIW)

- We can integrate the linearized hydrostatic Boussinesq equations on the *f*-plane over the mixed layer (Horizontal gradients and vertical velocities can be neglected at the lowest order):

$$\frac{\partial u}{\partial t} = -\frac{1}{\rho_0} \frac{\partial p}{\partial x} + fv + \frac{1}{\rho_0} \frac{\partial}{\partial z} \tau_x,$$

$$\frac{\partial v}{\partial t} = -\frac{1}{\rho_0} \frac{\partial p}{\partial y} - fu + \frac{1}{\rho_0} \frac{\partial}{\partial z} \tau_y,$$

$$\frac{\partial p}{\partial z} = -g\rho',$$

$$\frac{\partial}{\partial z} \mathbf{u} = 0,$$

$$\frac{\partial \rho'}{\partial t} = \frac{\rho_0}{g} N^2 w,$$



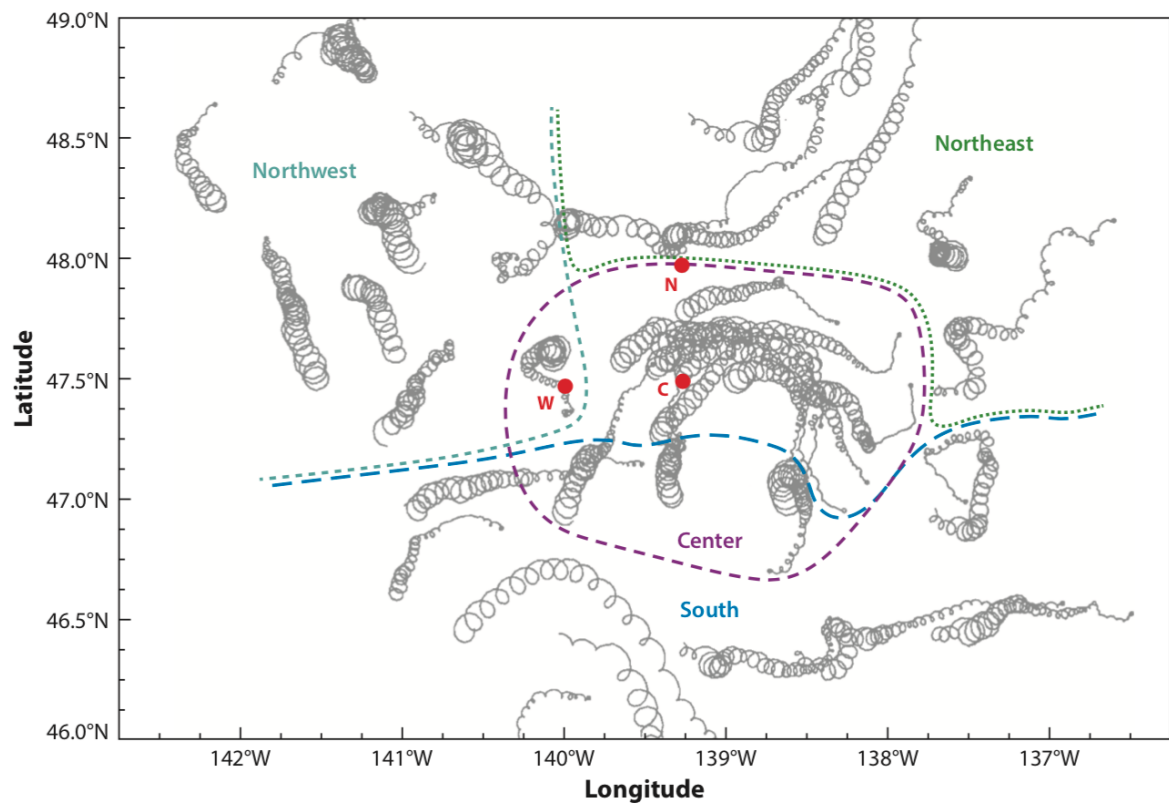
$$\frac{\partial U}{\partial t} = +fV + \frac{1}{\rho_0} \frac{\partial}{\partial z} T_x,$$

$$\frac{\partial V}{\partial t} = -fU + \frac{1}{\rho_0} \frac{\partial}{\partial z} T_y,$$

- Solutions are the sum of a steady Ekman transport to the right of the wind and anticyclonic circular motions at the local inertial frequency, *f*

## 1.3. Generation of Near-Inertial waves (NIW)

- NIW are recognizable by their characteristic circularly polarized velocities



Twenty-five days of surface drifter trajectories after a storm in the eastern north Pacific. The drifters trajectories represent a combination of decaying inertial motions (circular oscillations) and weak geostrophic flow (the time-averaged drift). [D'Asaro et al, 1995]

## 1.3. Generation of Near-Inertial waves (NIW)

- Dispersion relation for internal waves:

$$\omega^2 = \frac{N^2 k^2 + f^2 m^2}{k^2 + m^2}$$

•

## 1.3. Generation of Near-Inertial waves (NIW)

- Dispersion relation for internal waves:

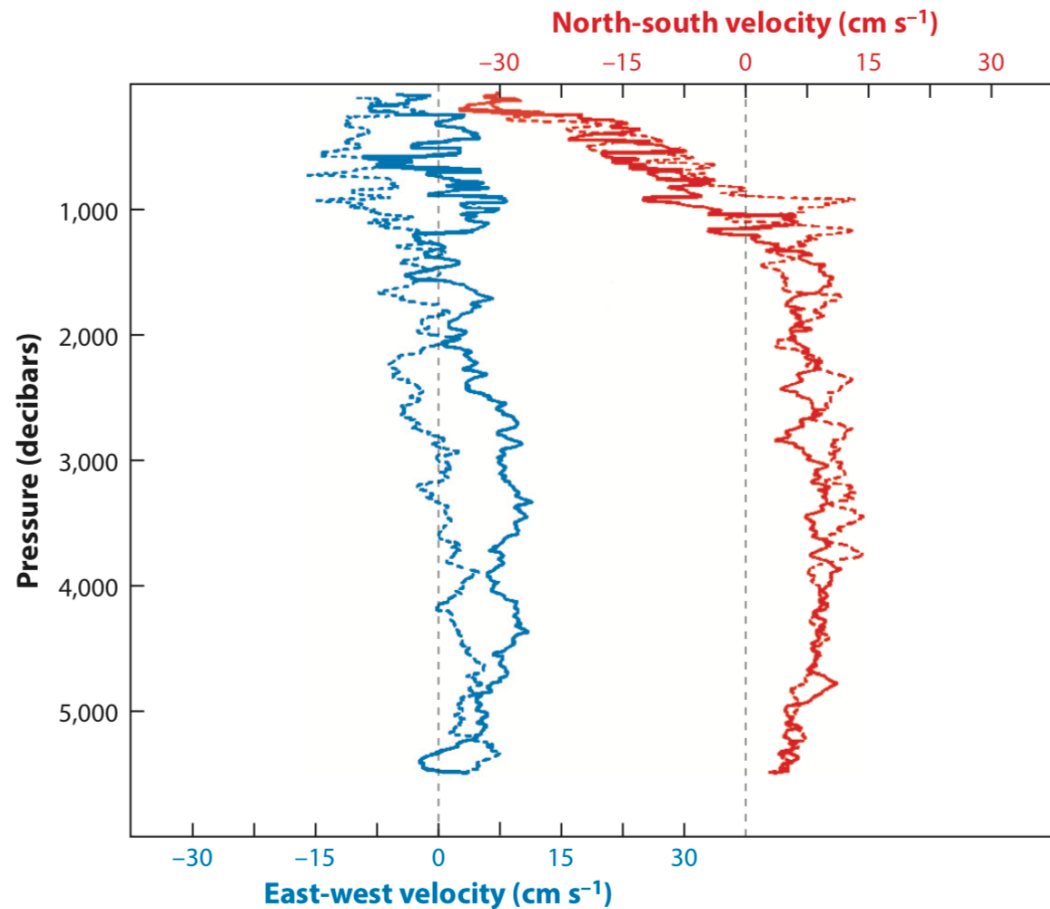
$$\omega^2 = \frac{N^2 k^2 + f^2 m^2}{X^2 + m^2}$$

- For hydrostatic NIW:

$$\omega^2 = f^2 + \frac{N^2 k^2}{m^2} \quad k \ll m$$

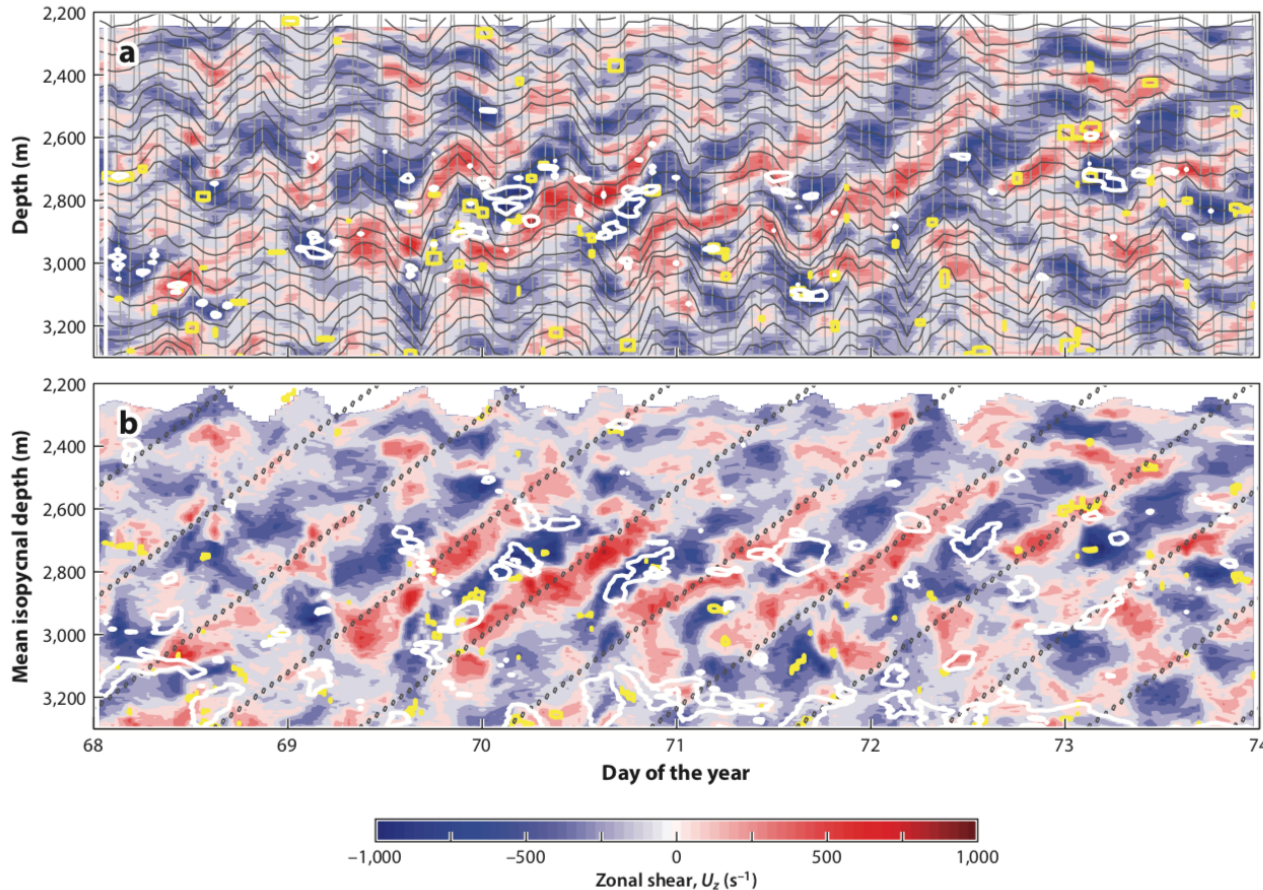
## 1.3. Generation of Near-Inertial waves (NIW)

- NIW are also recognizable by their a strong vertical shears



Two profiles (dashed and solid lines) of east-west (blue) and north-south (red) velocity taken at an interval of half an inertial period, showing high-wavenumber near-inertial motions. [Leaman & Sanford, 1975]

# 1.3. Generation of Near-Inertial waves (NIW)



For vertical wavelength of 350 m and  $\omega = 1.03f$ , the horizontal wavelength would be 80 km and the vertical group velocity  $10^{-3} \text{ m s}^{-1}$

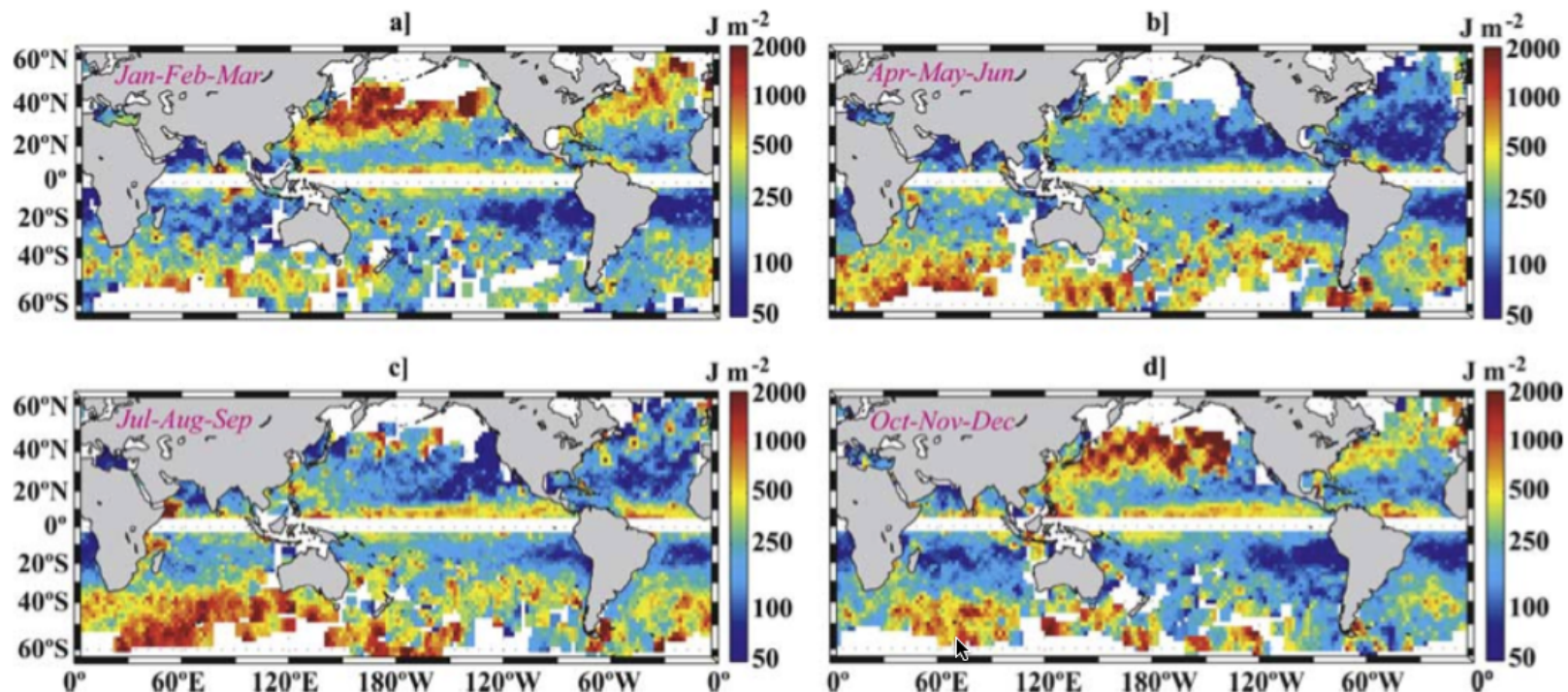
Zonal shear plotted versus (a) depth and (b) density (expressed as the mean depth of each isopycnal), showing the upward phase propagation of near-inertial shear layers. Shear layers are aligned with isopycnals (dark gray lines in panel a), which are heaved vertically by internal waves of other frequencies (primarily tidal; light gray lines); this heaving is removed in the isopycnal-following frame (panel b). The dissipation rate from overturns is contoured in yellow (contour value  $1.5 \times 10^{-8} \text{ W kg}^{-1}$ ); the Richardson number (white contours) drops below 0.8 once per wave period. In panel b, the dotted lines represent the wave phase for a signal with  $\omega = 1.03 f$  and  $\lambda = 350 \text{ m}$ .

## 1.3. Generation of Near-Inertial waves (NIW)

**The general characteristics of NIWs are as follows:**

- Clockwise and counterclockwise polarization in the Northern and Southern Hemispheres, respectively
- Frequency of  $1\text{--}1.2f$
- Vertical wavelength of  $100\text{--}400\text{ m}$
- Lateral scale of  $10\text{--}500\text{ km}$

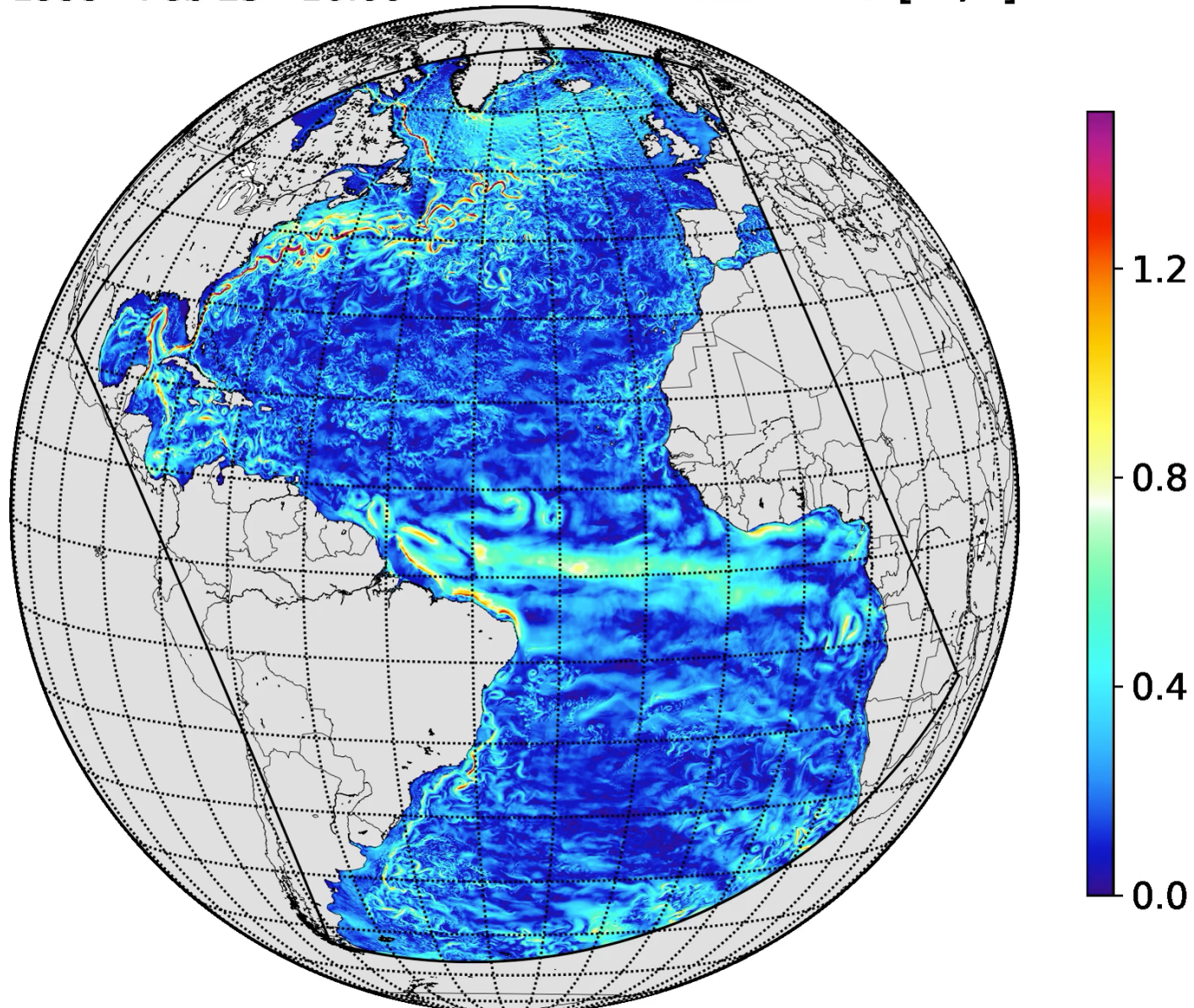
## 1.3. Generation of Near-Inertial waves (NIW)



Seasonal band-passed near-inertial energy density in the boundary layer is elevated under storm tracks. Results computed from surface drifter trajectories. **[Chaigneau et al., 2008]**

1999 - Feb 25 - 16:00

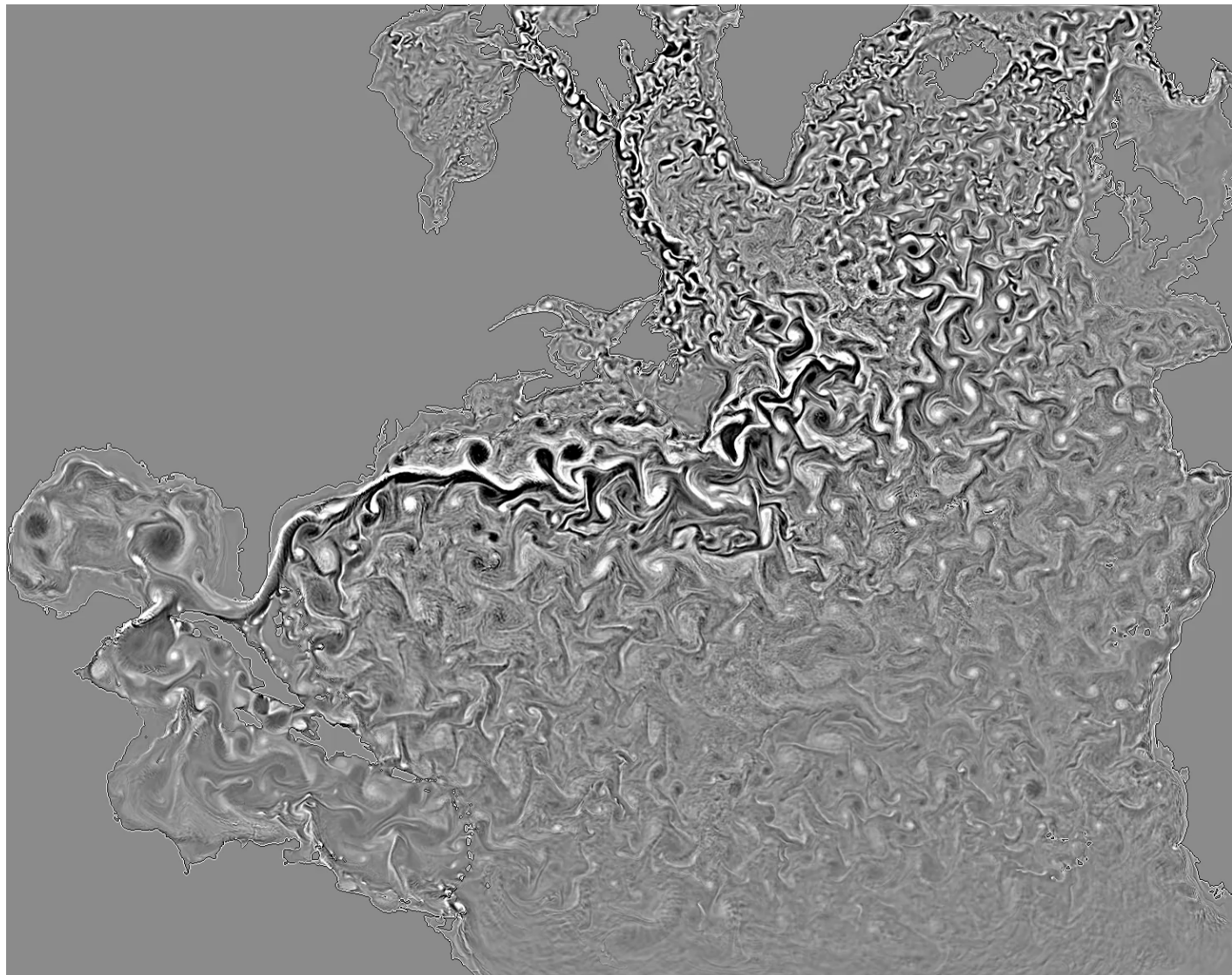
currents [m/s]



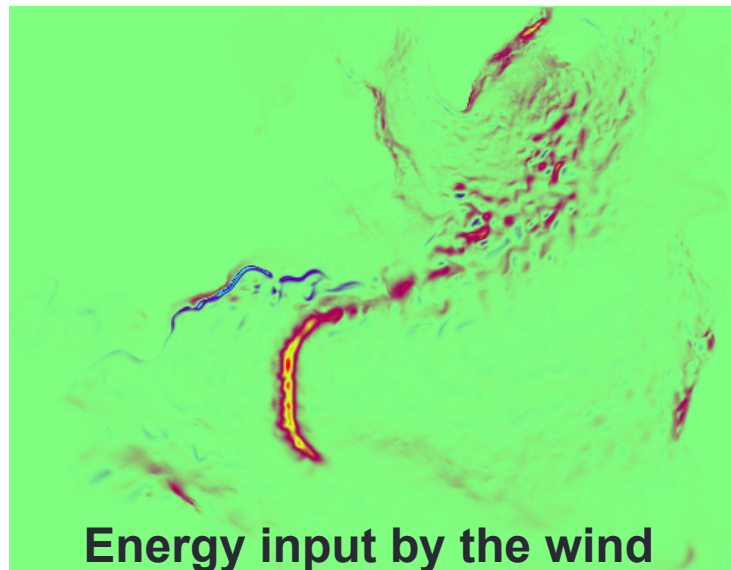
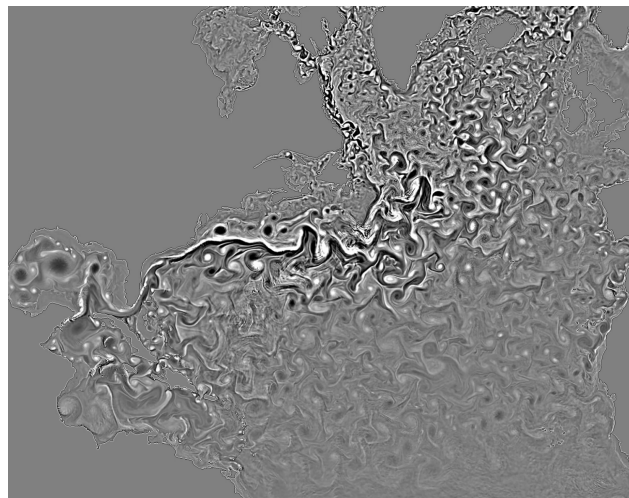
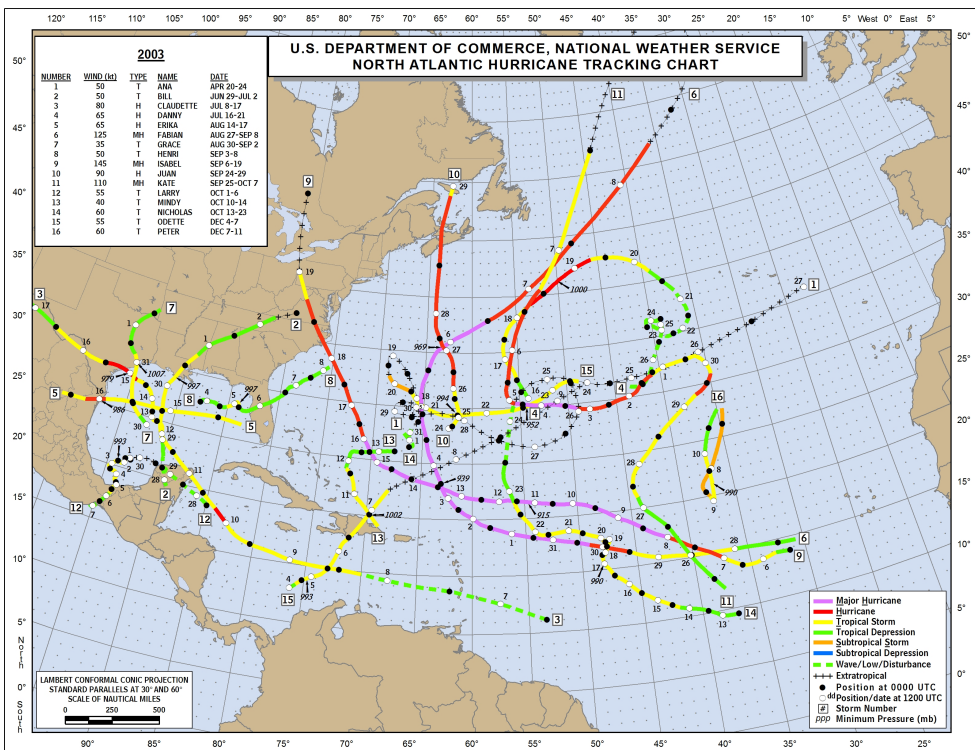
- High-frequency surface forcings (using hourly CFSR data and bulk flux formulae)

## 1.3. Generation of Near-Inertial waves (NIW)

- **High-frequency surface forcings**  
(using hourly CFSR data and bulk flux formulae)
- 

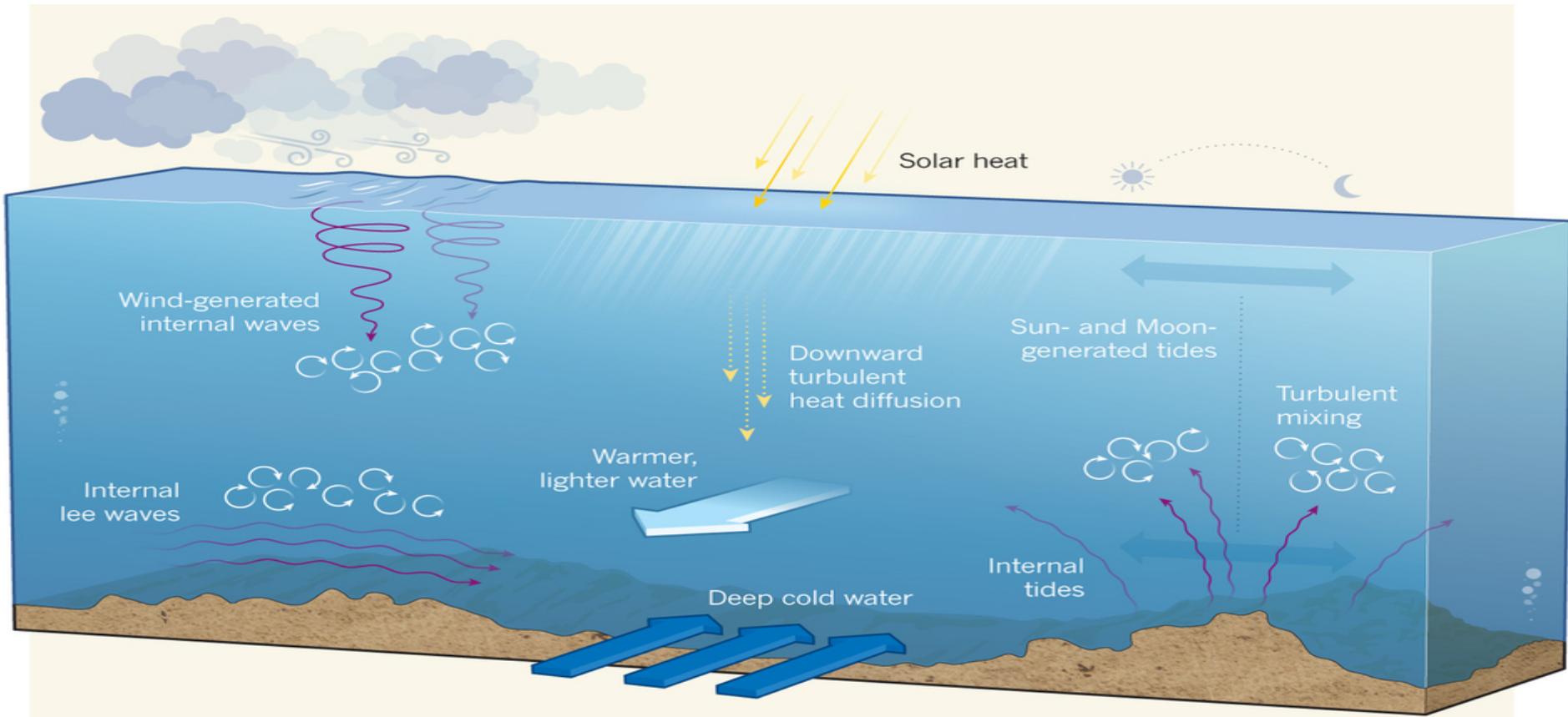


# 1.3. Generation of Near-Inertial waves (NIW)



# 1. Internal waves generation

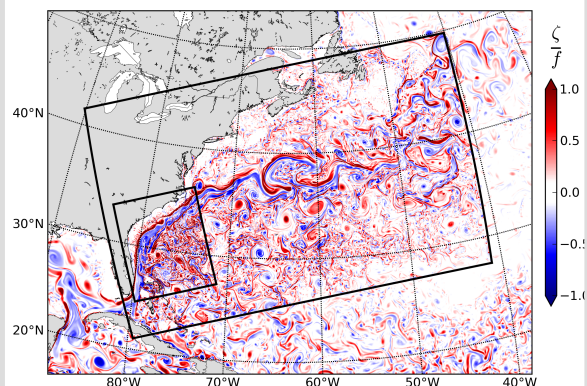
- Mechanisms:



From Mackinnon 2013

# Realistic modelling including tides and NIW

- Gulf Stream / Sargasso Sea**

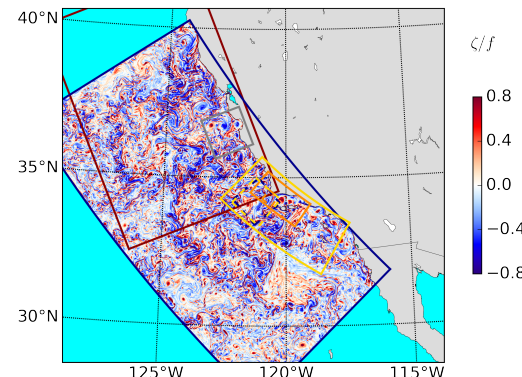


750 m res. forced with:

- Monthly winds
- Hourly winds
- Hourly winds + Tides

(+200 m with HF forcings )

- California Current**

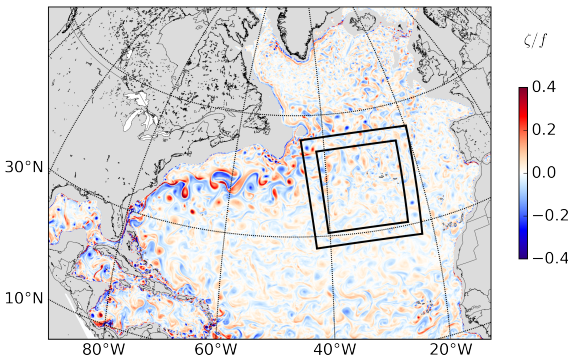


1 km res. forced with:

- Daily winds
- Hourly winds
- Hourly winds + Tides

(+300 m, 100 m with HF forcings and tides)

- Mid-Atlantic ridge**

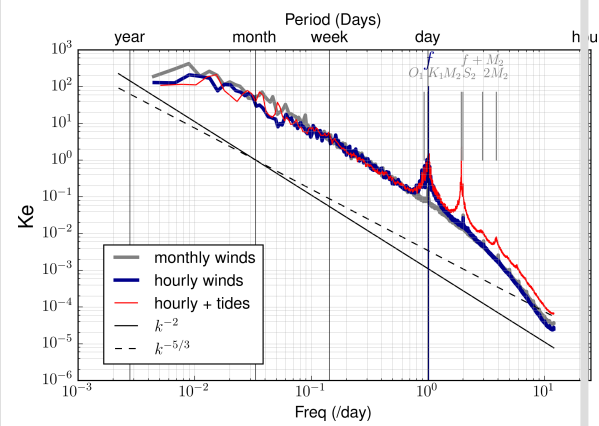
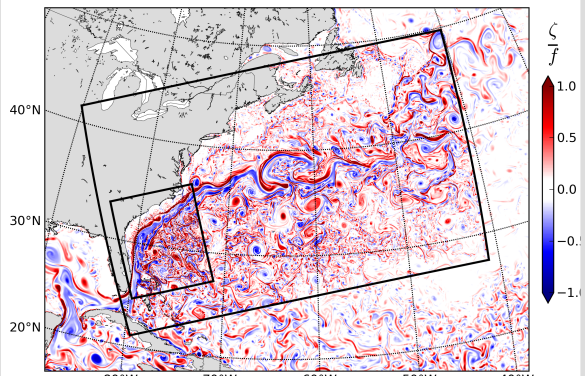


750 m res. forced with:

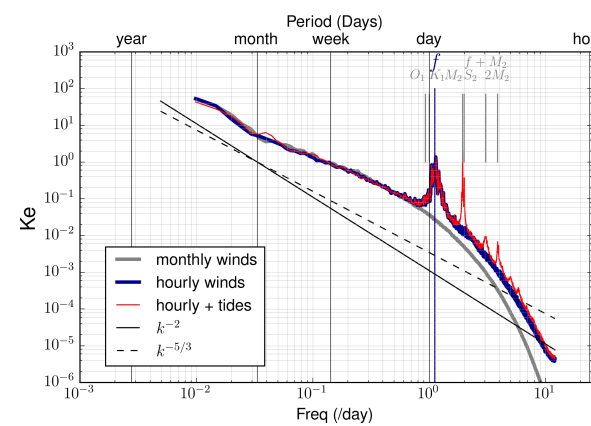
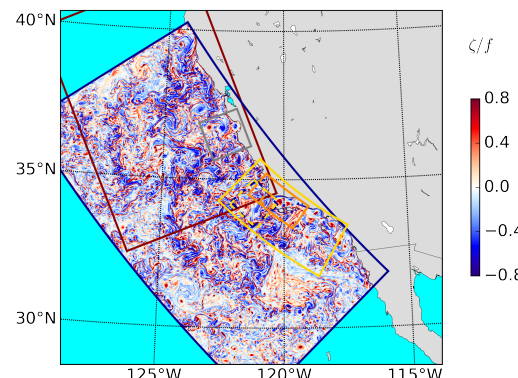
- daily winds
- daily winds + Tides
- Only tides

# Realistic modelling including tides and NIW

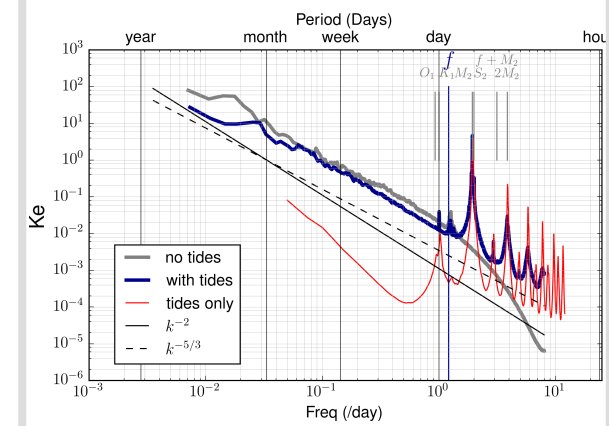
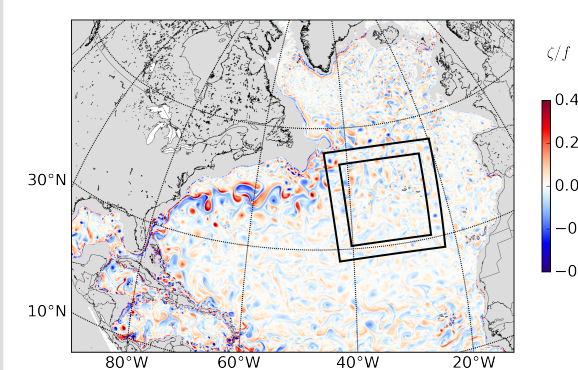
- Gulf Stream / Sargasso Sea**



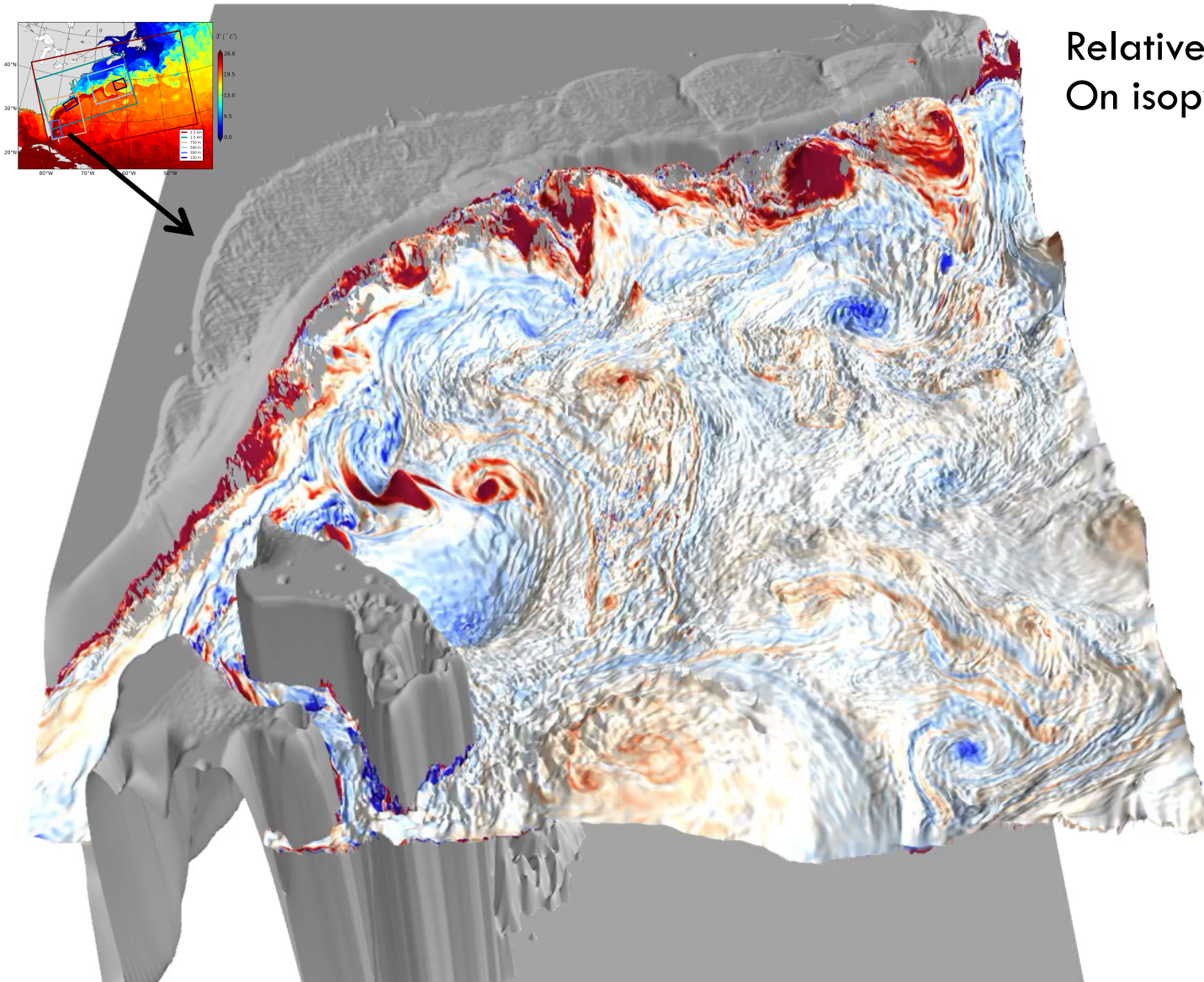
- California Current**



- Mid-Atlantic ridge**



# Method: Realistic modelling including tides

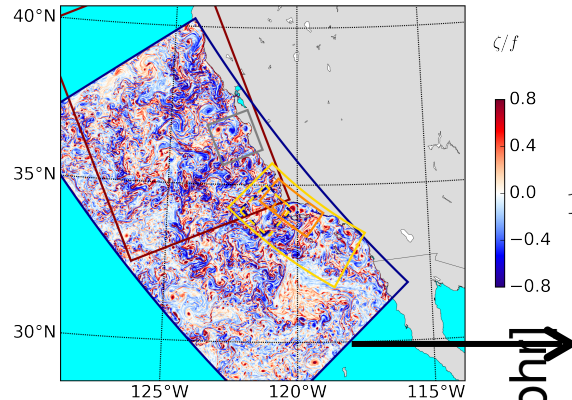


Relative vorticity  $(\pm f)$   
On isopycnal  $\sigma = 27 \text{ kg m}^{-3}$

$$\Delta x = 750 \text{ m}$$

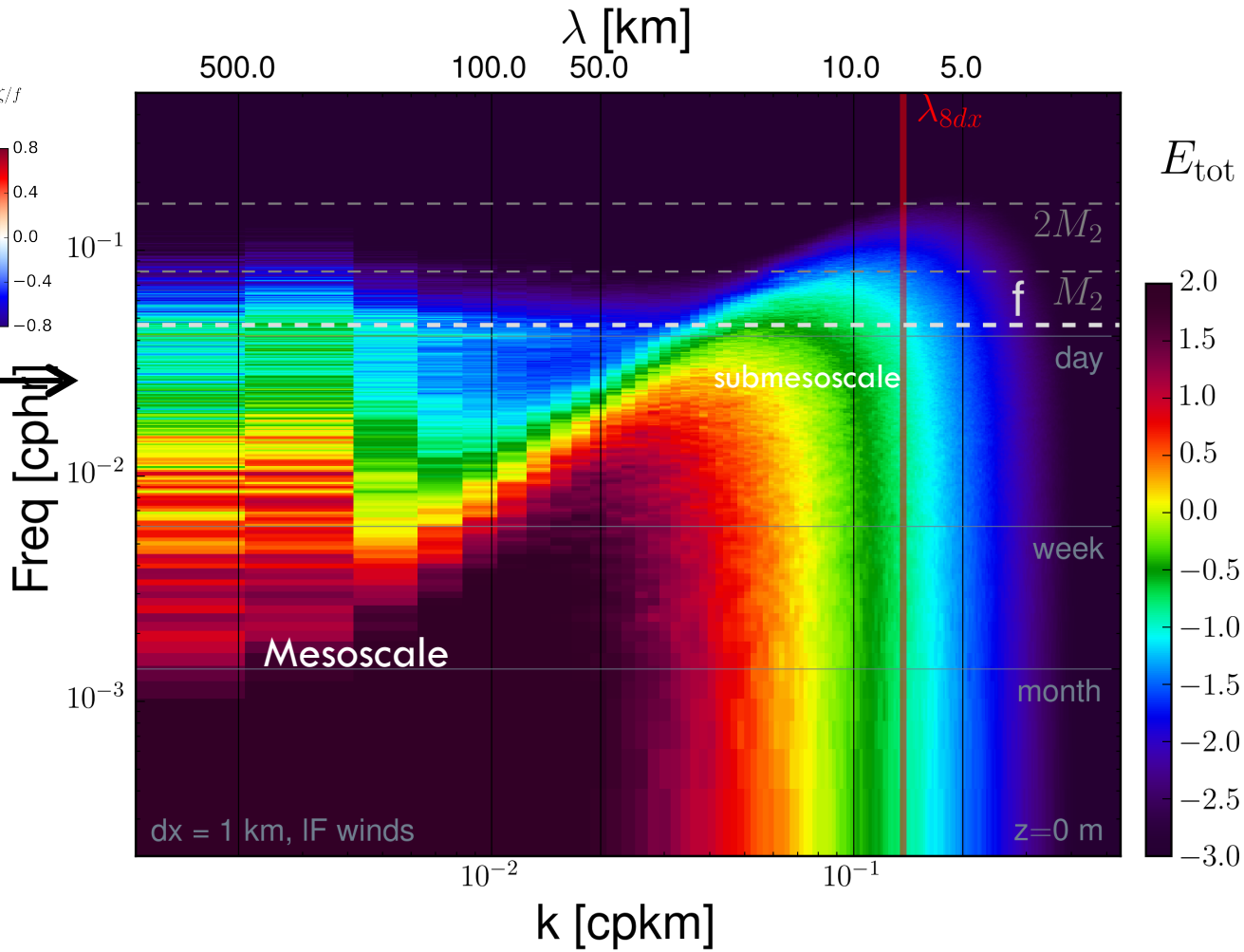
HF wind  
+  
Tides

# Realistic modelling including tides and NIW



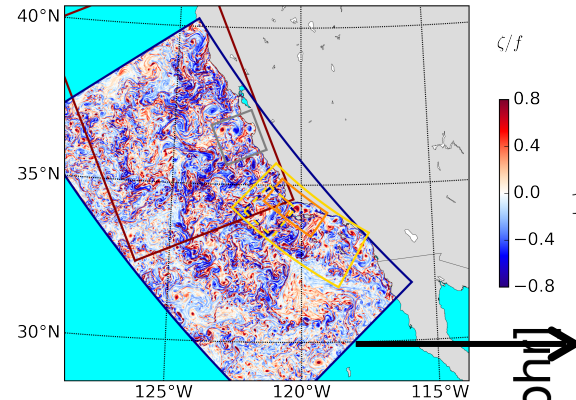
**Daily winds No tides**

= deficient in internal waves

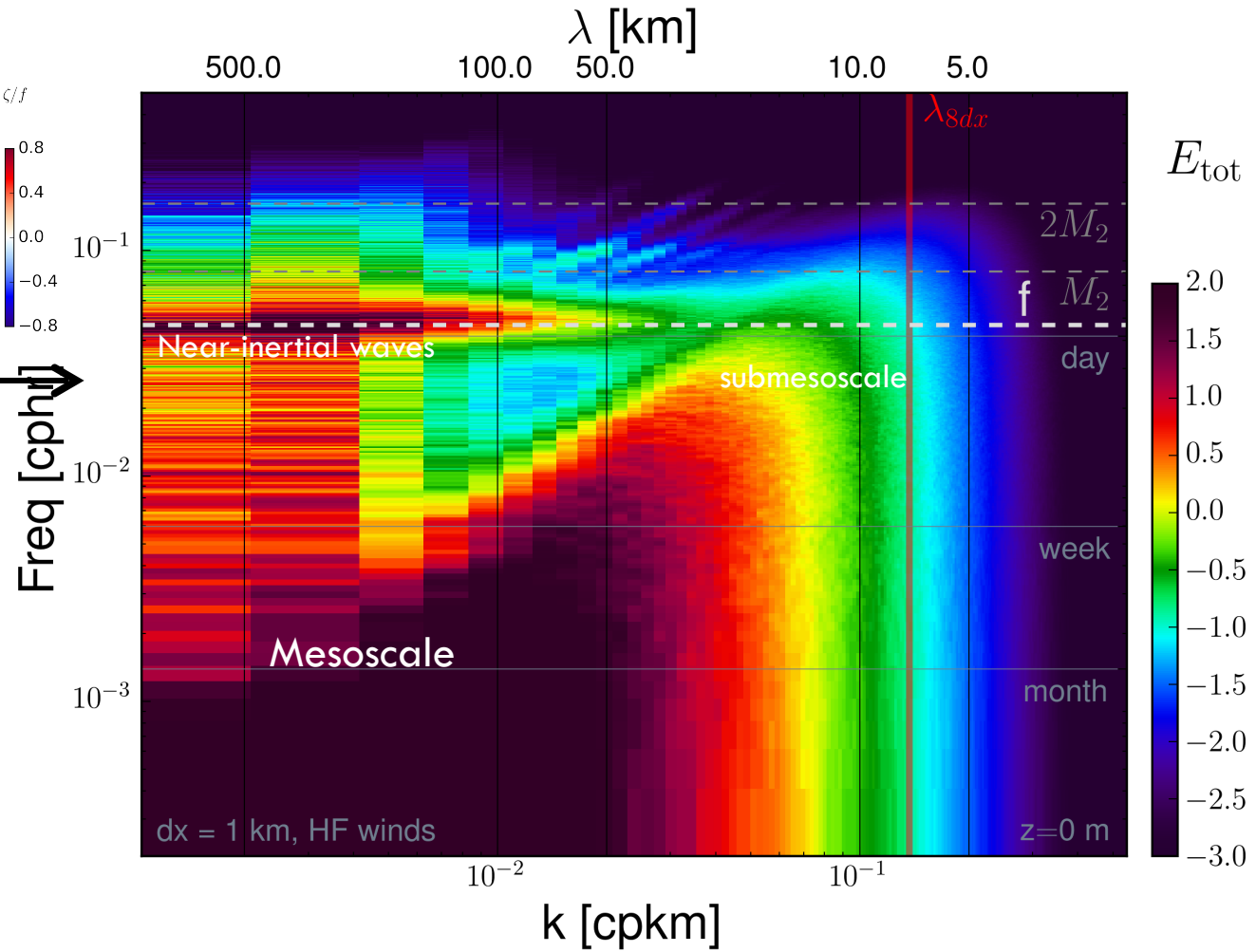


Azimuthally-averaged 2D frequency-wavenumber kinetic energy spectra in the California Current.

# Realistic modelling including tides and NIW

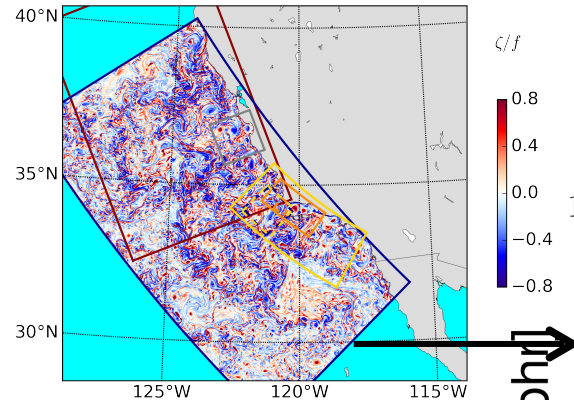


+ High frequency wind

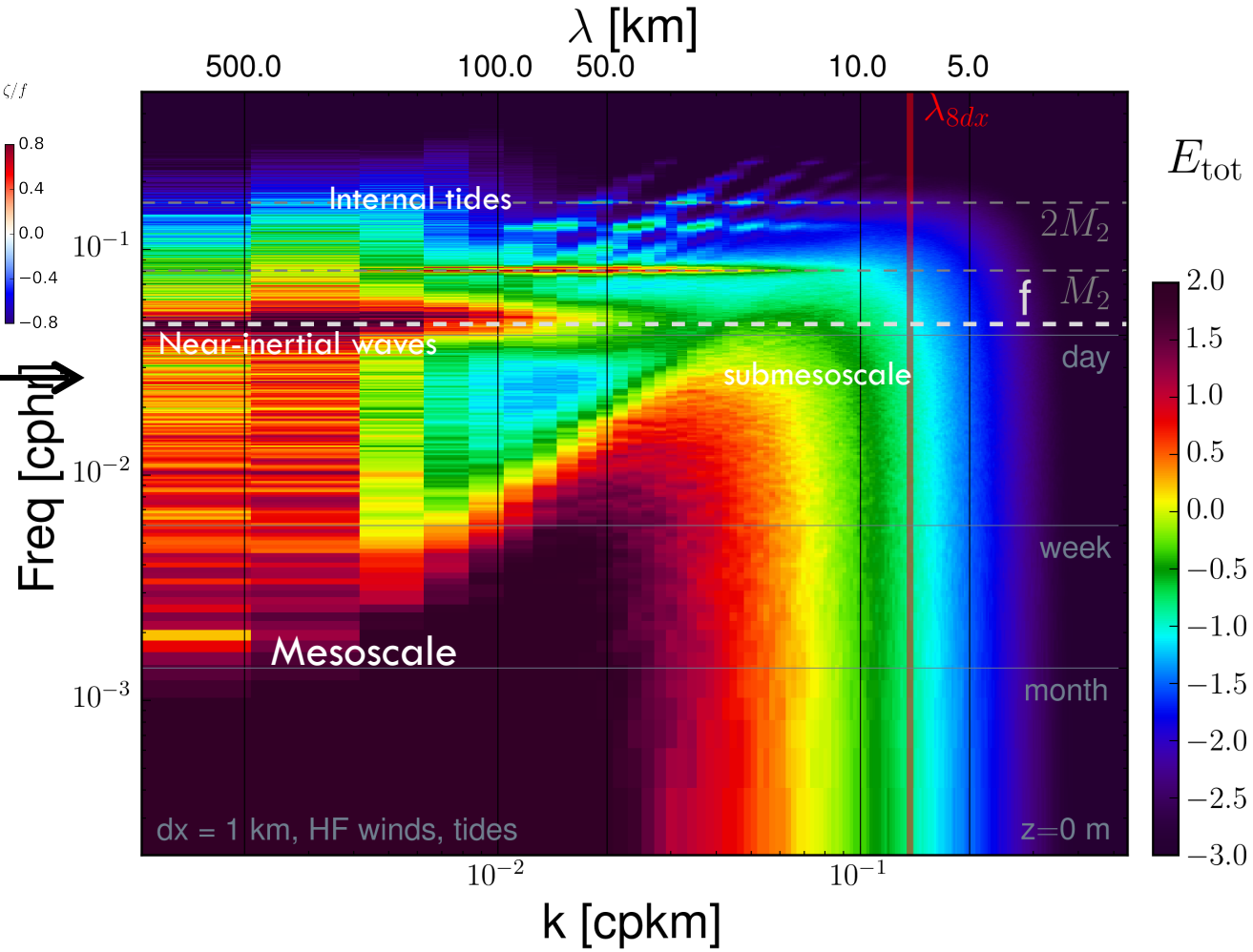


Azimuthally-averaged 2D frequency-wavenumber kinetic energy spectra in the California Current.

# Realistic modelling including tides and NIW

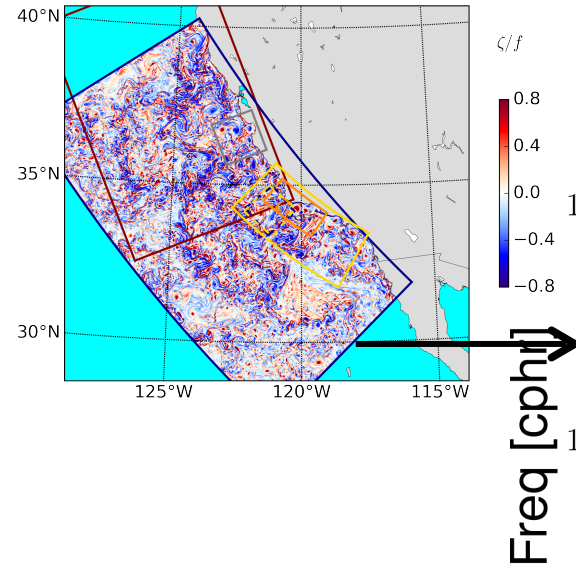


- + High frequency wind
- + Tidal forcings

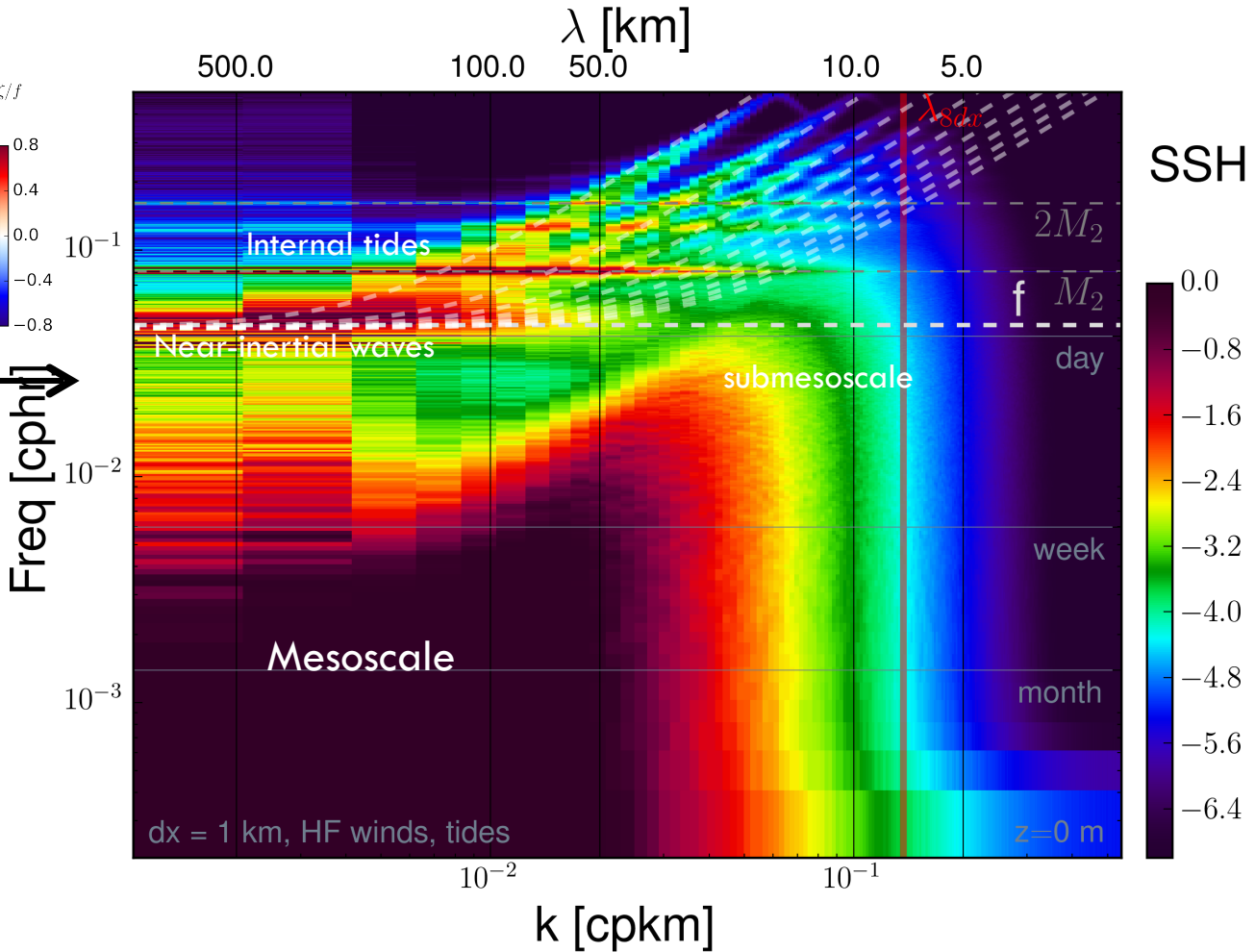


*Azimuthally-averaged 2D frequency-wavenumber kinetic energy spectra in the California Current.*

# Realistic modelling including tides and NIW



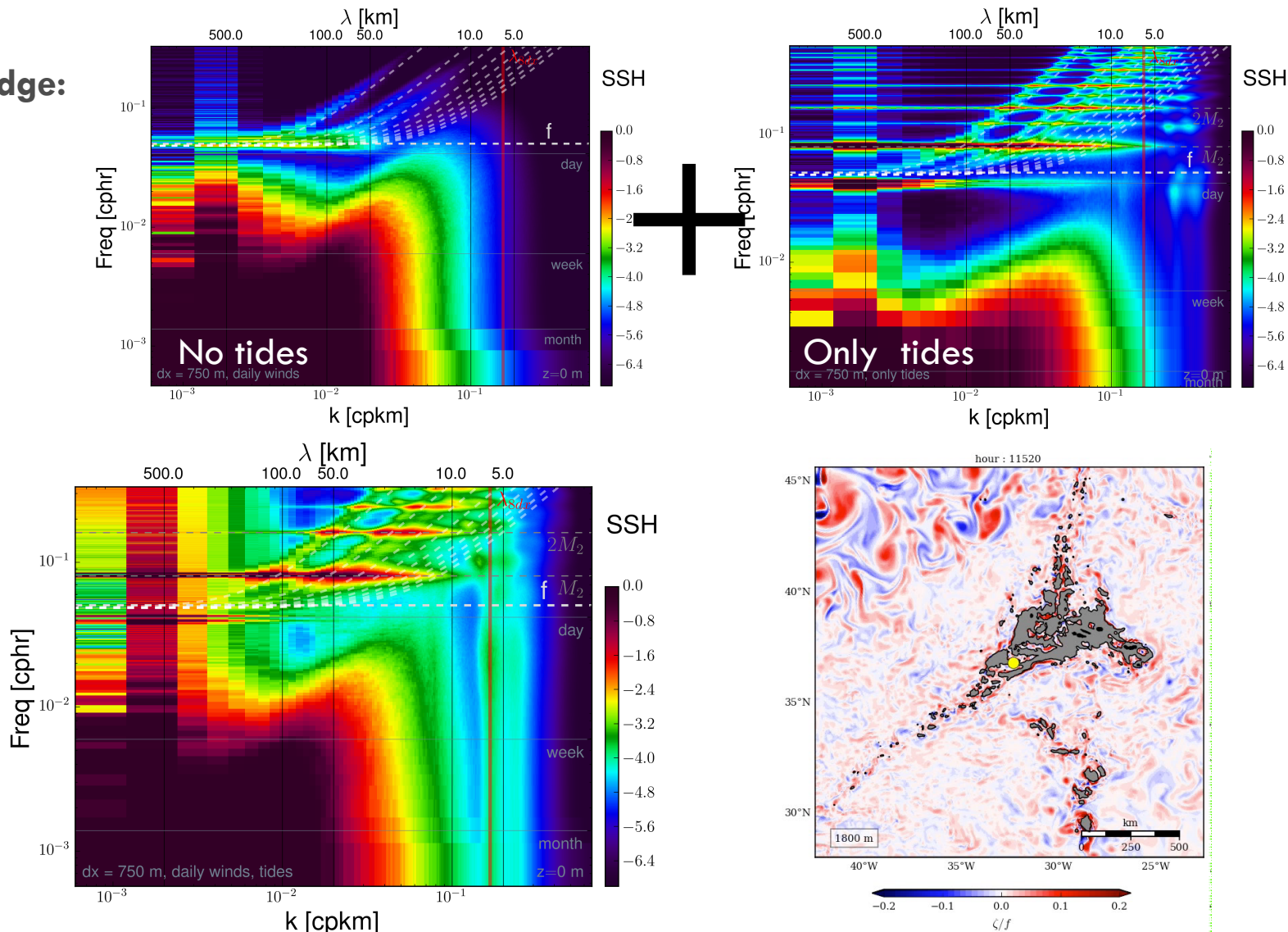
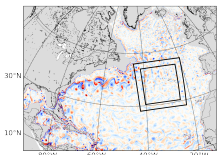
Signature of high-frequency internal waves are amplified on **Sea Surface Height**.



*Azimuthally-averaged 2D frequency-wavenumber spectra for SSH in California Current*

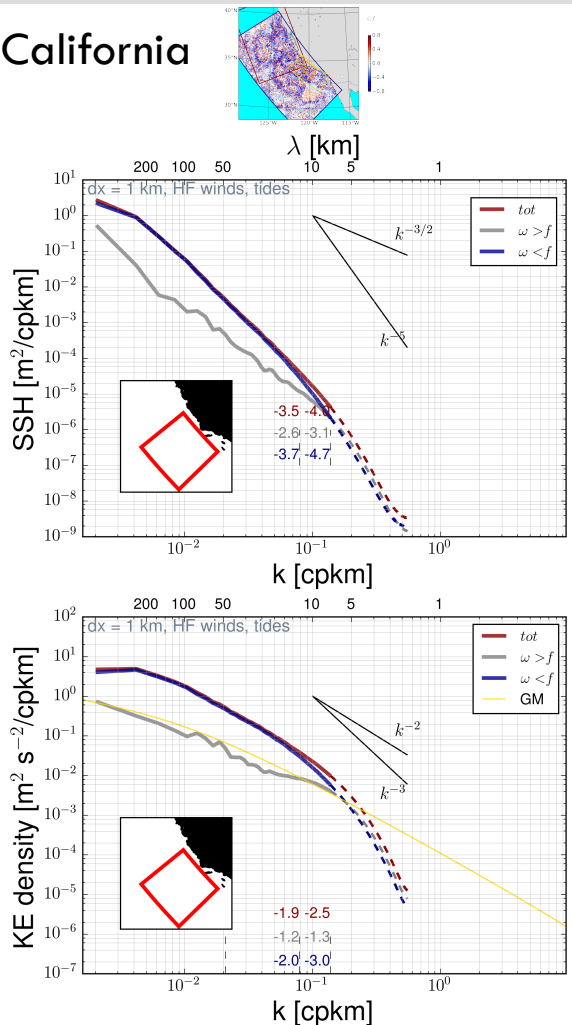
# Realistic modelling including tides and NIW

**Mid-Atlantic ridge:**

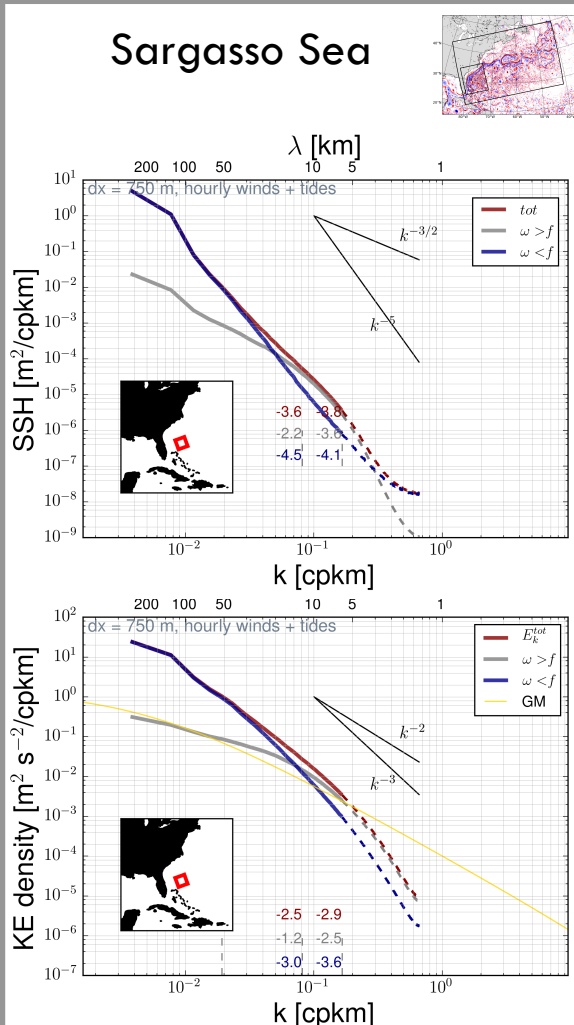


# Where is the flow balanced?

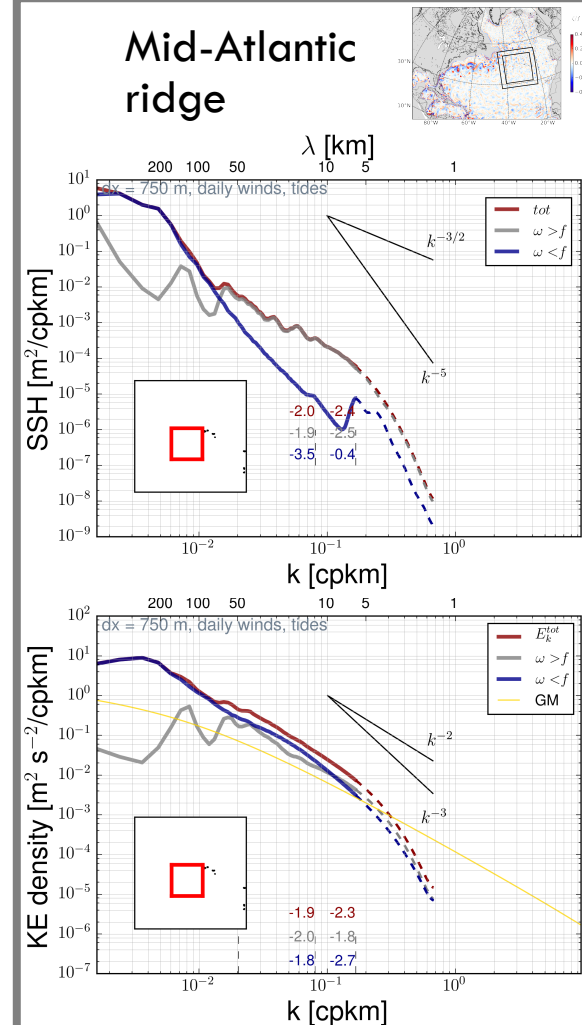
## California



## Sargasso Sea

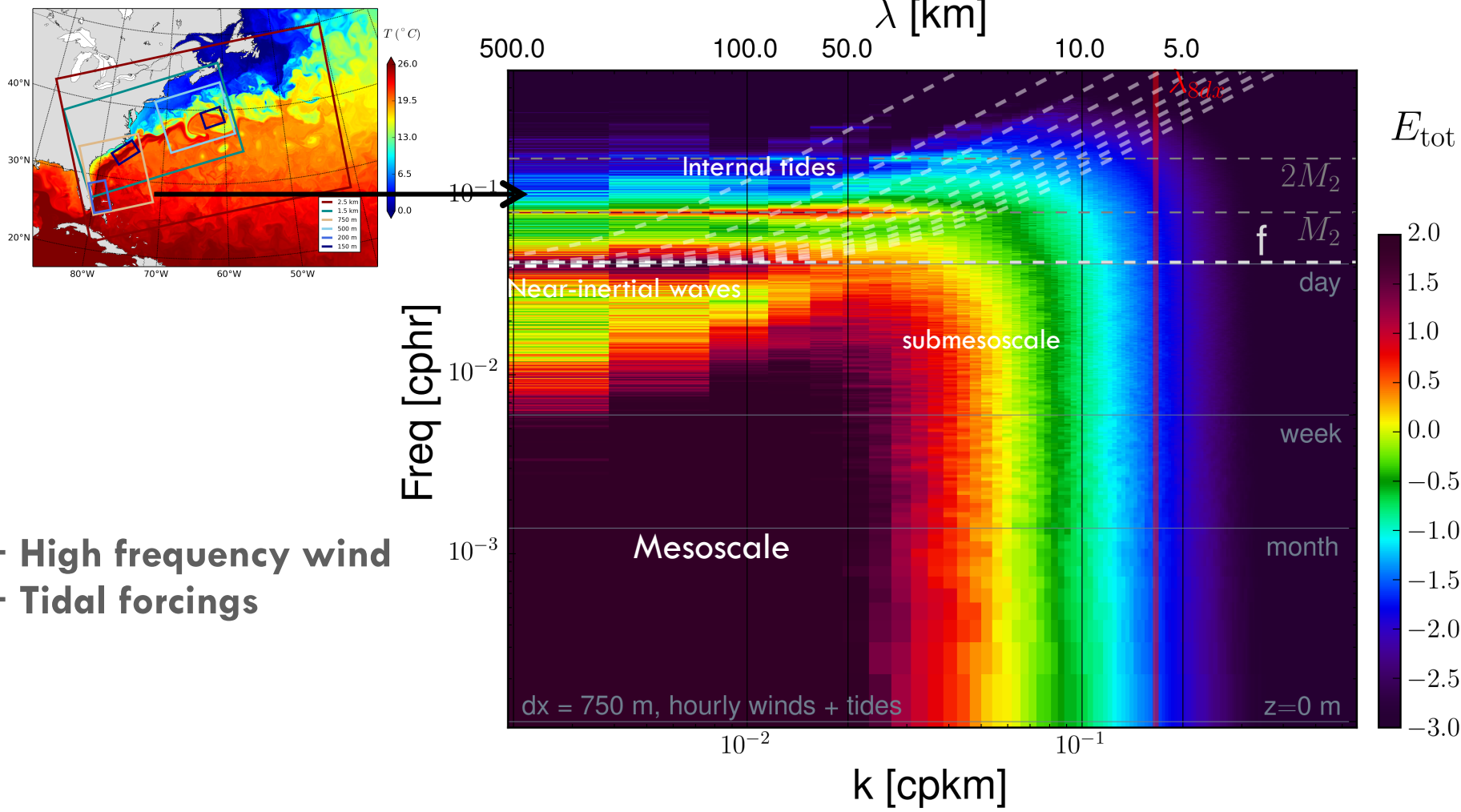


## Mid-Atlantic ridge



Signature of internal waves are amplified on **Sea Surface Height** – Leading to more dramatic breaks in slopes than in Kinetic energy.

# Where is the flow balanced?



- + High frequency wind
- + Tidal forcings

*Azimuthally-averaged 2D frequency-wavenumber kinetic energy spectra in the Sargasso Sea.*

# Where is the flow balanced?

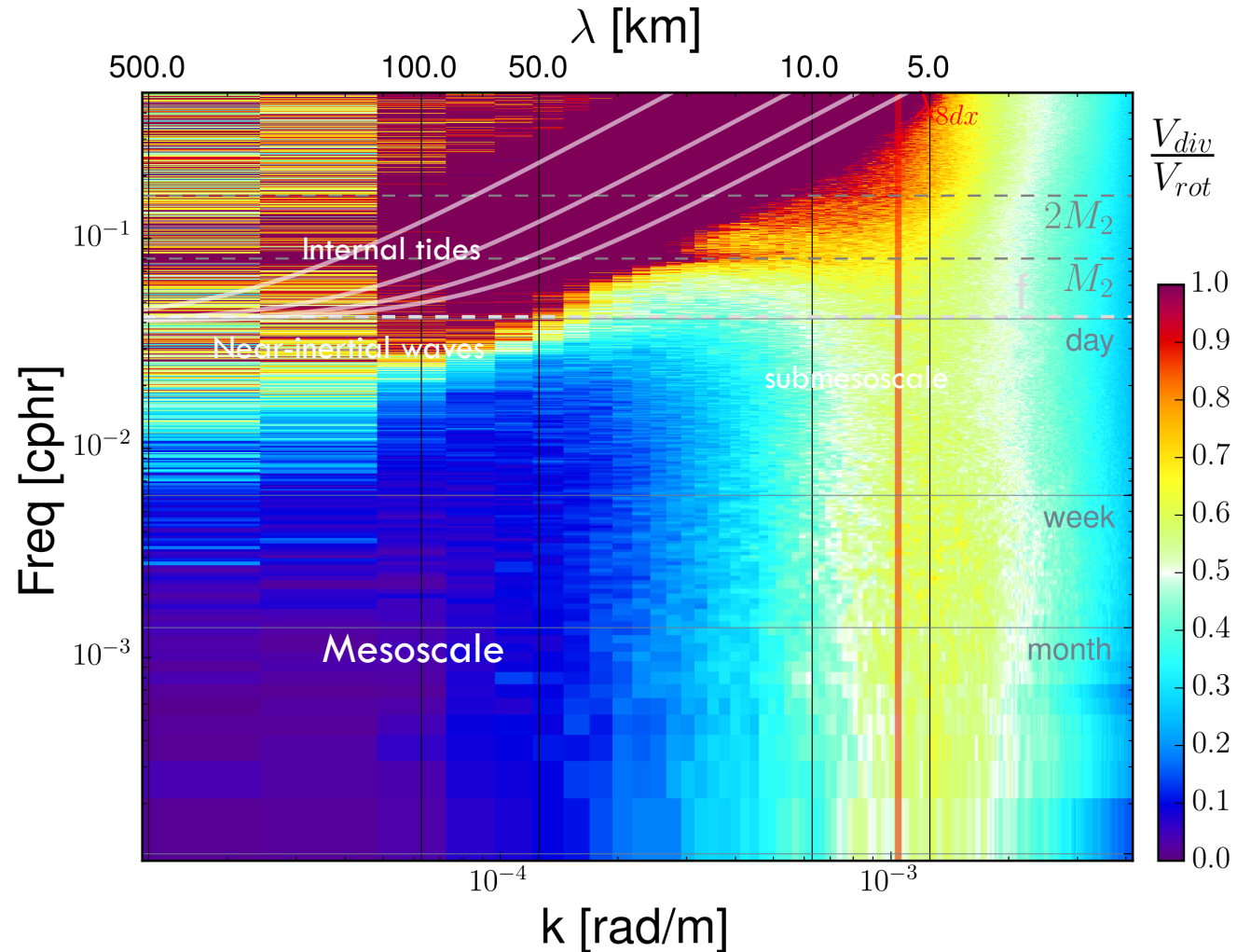
Ratio of divergent /  
rotational part of the  
kinetic energy

using Helmholtz  
decomposition of a 3d  
incompressible flow

$$\mathbf{u}_h = \mathbf{u}_r + \mathbf{u}_d ,$$

$$\nabla_h \cdot \mathbf{u}_r = 0$$

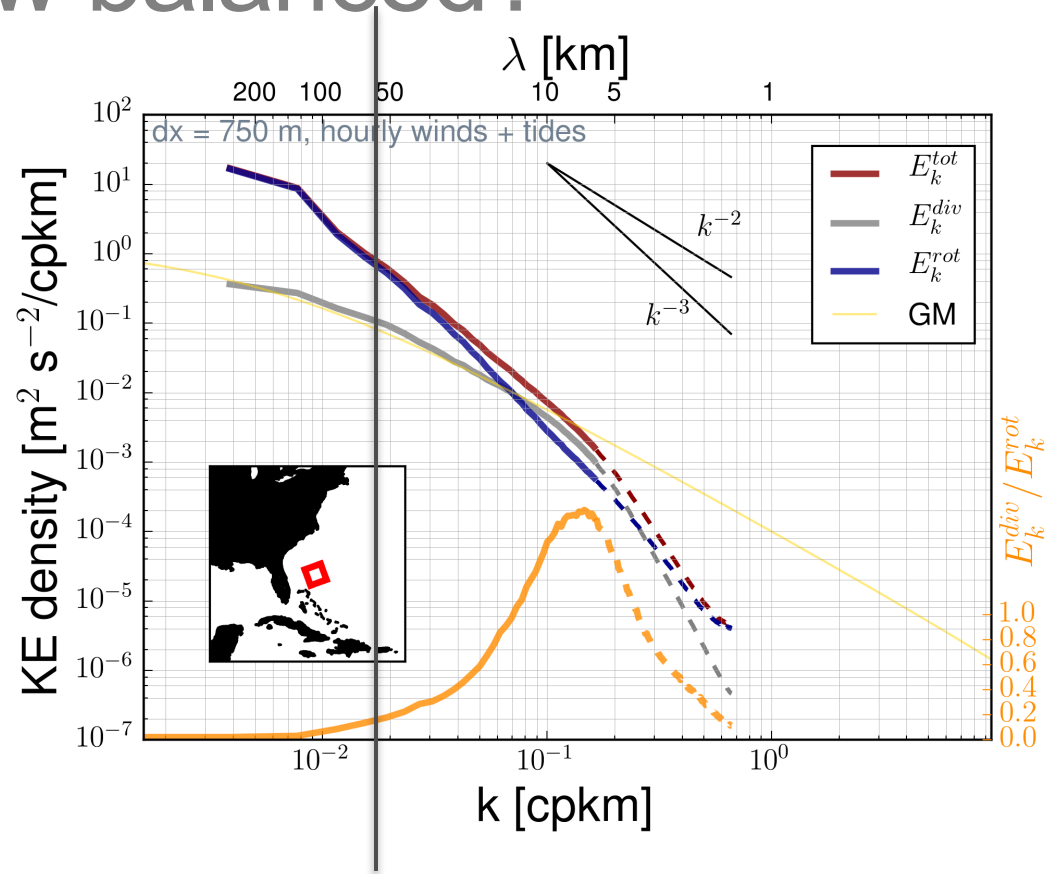
$$\hat{\mathbf{z}} \cdot \nabla_h \times \mathbf{u}_d = 0$$



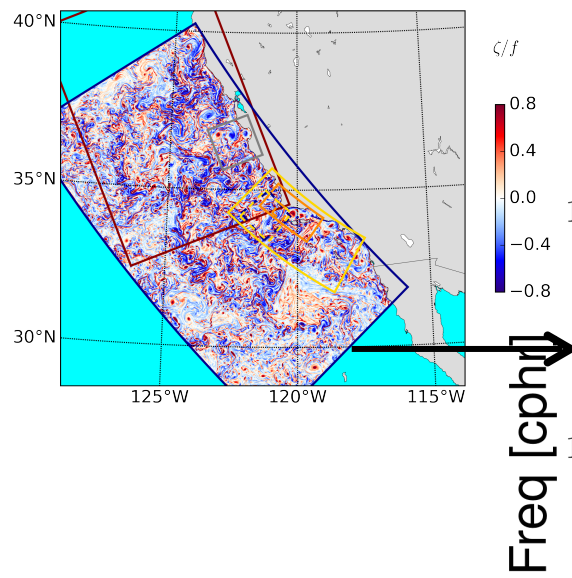
# Where is the flow balanced?

Transition between balanced and unbalanced at scales between 10 – 100 km depending on the dynamical regime (geographical region + season).

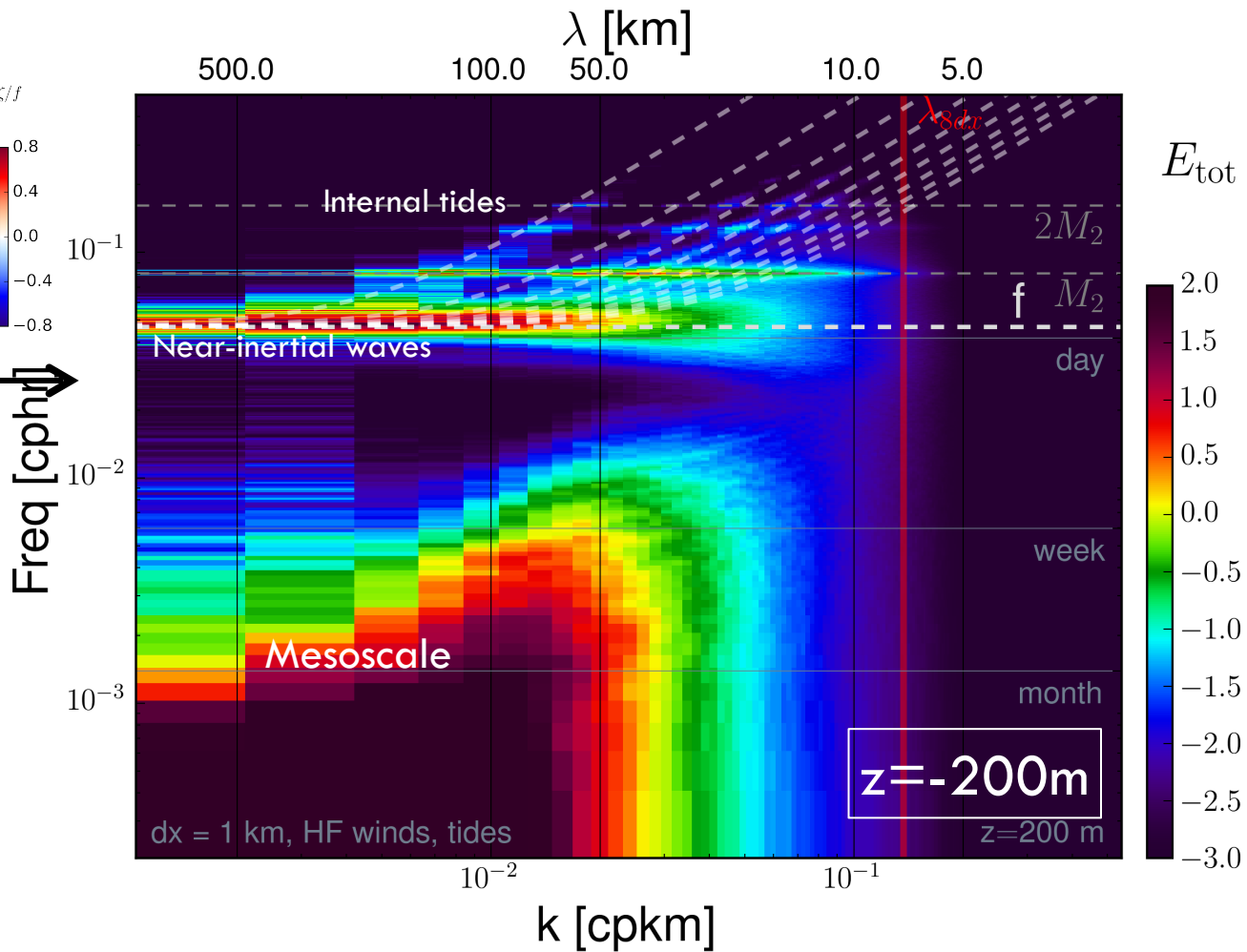
Qualitatively similar results for Northwestern Pacific [Rocha et al., 2016a; Qiu et al., 2017] or the Drake Passage [Rocha et al., 2016]. See global census in [Qiu et al., 2018].



# Can we separate waves from submesoscales?

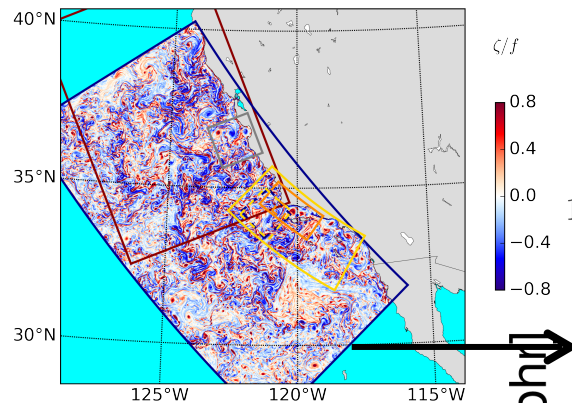


Below the mixed-layer, separation between internal waves and balanced dynamics is easy.

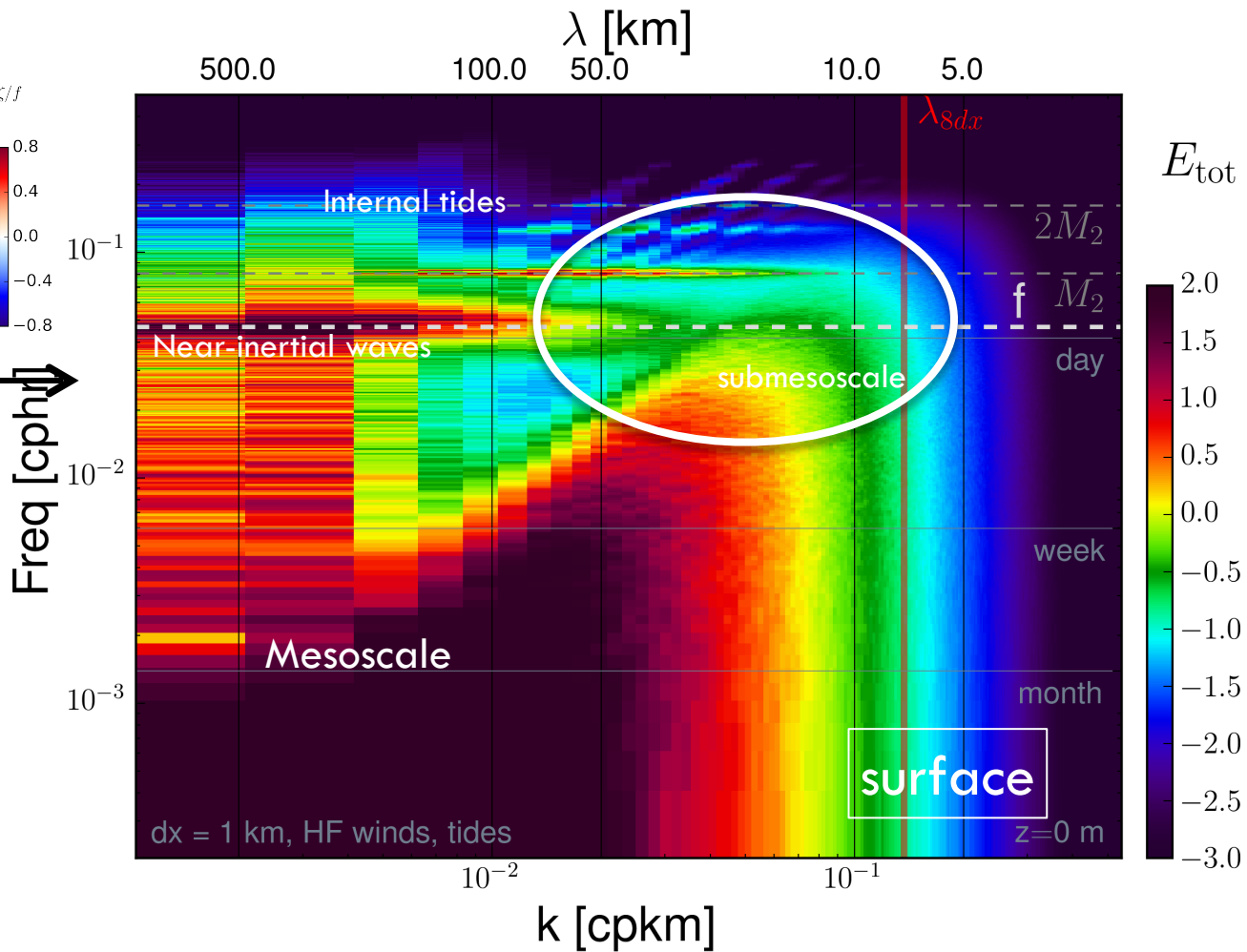


Azimuthally-averaged 2D frequency-wavenumber kinetic energy spectra in the California Current.

# Can we separate waves from submesoscales?



In the mixed-layer it is  
much more complicated



Azimuthally-averaged 2D frequency-wavenumber kinetic energy spectra in the California Current.